Neural crest development in a human embryonic stem cell-based model system

Dissertation

zur

Erlangung des Doktorgrades (Dr. rer. nat.)

der

Mathematisch-Naturwissenschaftlichen Fakultät

der

Rheinischen Friedrich-Wilhelms-Universität Bonn

vorgelegt von

Sabine Münst, geb. Schenk

aus Siegburg

Bonn 2012

Angefertigt mit Genehmigung der Mathematisch-Naturwissenschaftlichen Fakultät der Rheinischen Friedrich-Wilhelms-Universität Bonn

1. Gutachter: Prof. Dr. Oliver Brüstle

2. Gutachter: Prof. Dr. Michael Hoch

Tag der Promotion: 24.08.2012

Erscheinungsjahr: 2012

“the only interesting thing about vertebrates is the neural crest“

P. Thorogood, 1989

Table of content

Abbreviations

AA	ascorbic acid
APS	ammonium persulfate
BDNF	brain-derived neurotrophic factor
BMP	bone morphogenetic protein
BRN3A	brain-specific homeobox/POU domain protein 3A
cDNA	complementary deoxyribonucleic acid
CNS	central nervous system
DAPI	4′,6-Diamidino-2-phenylindol
dcAMP	dibutyl cyclic adenosine monophosphate
EMT	epithelial-to-mesenchymal transition
EBs	embryoid bodies
EGF	epidermal growth factor
ES	embryonic stem
FACS	fluorescence activated cell sorting
FCS	fetal calf serum
FGF	fibroblast growth factor
Fn	fibronectin
GDNF	glial-derived-neutrophic factor
GFAP	glial fibrillary acidic protein
HNK-1	human natural killer-1
HRP	horseradish peroxidase
hES	human embryonic stem
ICM	inner cell mass
iPS	induced pluripotent stem
L	liter
Ln	laminin
lt-hESNSCs	long term proliferated human embryonic stem cell-derived neural stem cells
MEF	murine embryonic fibroblasts
mL	milliliter
NC	neural crest
p75NTR	low affinity nerve growth factor receptor (p75NTR)
NGS	normal goat serum
NRG-1	neuregulin-1
PAX	paired box

PBS	phosphate buffered saline
PFA	paraformaldehyde
PNS	peripheral nervous system
PO	poly-L-ornithine
RA	retinoic acid
RNA	ribonucleic acid
rpm	rounds per minute
RT-PCR	reverse transcriptase-polymerase chain reaction
SDIA	stromal-derived-inducing-activity
SDS-PAGE	sodium dodecylsulfate polyacrylamide gel electrophoresis
SHH	sonic hedgehog
SMA	smooth muscle actin
SOX	SRY-related HMG-box
SSEA	stage-specific embryonic antigen
TGF	transforming growth factor
TH	tyrosine hydroxylase
TFAP2A	transcription factor activating enhancer binding protein 2 alpha
TRA	tumour recognition antigens
Wnt	wingless/Int

Summary

The neural crest is a transient embryonic cell population with outstanding characteristics. After their delamination from the closing neural tube, neural crest cells migrate extensively throughout the body and differentiate into highly diverse cell types, including peripheral neurons and glia, but also mesenchymal tissues of the head region. Neural crest development has been extensively studied in several animal models, however, the neural crest of primates, particularly of humans, remains largely inaccessible. The research on human embryonic stem (hES) cells offers a highly interesting possibility to study events of early embryonic development in an *in vitro* setting. In the thesis presented here, differentiating hES cells were used to study human neural crest development. Remarkably, the process of neural crest delamination is mimicked in the cell culture dish, thereby recapitulating early developmental processes. Cultivation of spontaneously differentiated embryoid bodies (EBs) in neural differentiation medium yielded prominent neural rosettes that, according to their morphology and marker expression, resembled a primitive form of the neural tube. Neural crest cells, identified by expression of the neural crest-associated markers p75NTR, HNK-1, SOX*E*, and AP2α, migrated from those neural tube-like structures over the fibroncetin-coated dish and formed distinct crescent-shaped aggregates at a defined distance. This process is accompanied by a characteristic cadherin switch, which is typical for an epithelial-to-mesenchymal transition, as it occurs in neural crest development *in vivo*. The aggregation of neural crest cells into clearly distinguishable clusters could be exploited to purify them from the heterogenous cell culture by manual picking. The level of purity, assessed by expression of p75NTR and SOXE, of the obtained cell population resembled cell populations isolated by Fluorescence Activated Cell Sorting for p75NTR (>95%). Comparison with a neural stem cell population obtained from the same parental hES cell line via microarray analysis confirmed upregulation of neural crest cell markers and distinct differences towards neural stem cells. The purified neural crest cell population could be differentiated into peripheral neurons and glia, as well as to smooth muscle cells, adipocytes, osteoblasts and chondrocytes.

The hES cell-based culture model presented here provides access to early human neural crest development and offers multiple possibilities to study the delamination, migration and differentiation of neural crest cells. Moreover, this model system provides potential for modeling of neural crest-associated diseases and pharmacology testing.

Zusammenfassung

Bei der Neuralleiste handelt es sich um eine transiente, embryonale Zellpopulation mit außergewöhnlichen Eigenschaften. Nach Verlassen des sich schließenden Neuralrohres migrieren die Neuralleistenzellen durch den Körper und differenzieren in verschiedenste Zelltypen. Zu ihren Nachkommen gehören periphere Neurone und Gliazellen, aber auch mesenchymales Gewebe aus der Kopfregion. Die Entwicklung der Neuralleiste wurde in verschiedenen Tiermodellen intensiv erforscht. Auf Grund ihrer Unzugänglichkeit ist über die Neuralleiste in Primaten, speziell im Menschen, jedoch nur wenig bekannt. Die Verwendung von humanen embryonalen Stammzellen bietet eine sehr interessante Möglichkeit die Vorgänge der frühen Embryonalentwicklung *in vitro* nachzuvollziehen. In dieser Arbeit wurden differenzierende humane embryonale Stammzellen verwendet, um die Entwicklung der Neuralleiste zu untersuchen. Tatsächlich konnte gezeigt werden, dass typische Vorgänge der Neuralleistenentwicklung in der Zellkulturschale abgebildet werden. Durch Kultivierung von spontan differenzierten Embryoid Körperchen in Medium, welches die neurale Differenzierung begünstigt, wurden neurale Rosettenstrukturen gewonnen, die in ihrer Morphologie und Markerexpression einer primitiven Form des Neuralrohres ähneln. Neuralleistenzellen, welche durch die Expression der Neuralleistenmarkern p75NTR, HNK-1, SOX*E*, and AP2α identifiziert wurden, migrierten von den Neuralrohr-ähnlichen Strukturen über die Fibronektinbeschichtete Schale, um schließlich in einem definierten Abstand halbmondförmige Aggregate zu bilden. Dieser Prozess wurde von einem charakteristischen Cadherin-Switch begleitet, welcher typisch für eine epithelial-mesenchymale Transition ist, die in der Neuralleistenentwicklung *in vivo* ebenfalls zu beobachten ist. Die Aggregation von Neuralleistenzellen zu klar abgegrenzten Clustern konnte dazu genutzt werden, sie durch manuelle Isolation aus der heterogenen Zellkultur aufzureinigen. Die auf diese Weise angereicherte homogene Zellpopulation exprimierte die Neuralleistenmarker p75NTR und SOX*E* auf vergleichbar hohem Niveau wie die Zellpopulationen, die durch Fluoresecence Acticated Cell Sorting auf p75NTR aufgereinigt wurden (>95%).

Eine Genexpressionsanalyse zeigte im Vergleich zu einer neuralen Stammzellpopulation, welche aus der selben humanen embryonalen Stammzelllinie gewonnen wurde, eine deutliche Hochregulierung von wichtigen Neuralleisten-assoziierten Genen, sowie klare Unterschiede zu neuralen Stammzellen. Die gewonnene Population von Neuralleistenzellen konnte erfolg-

reich in periphere Glia und Neurone sowie in die mesenchymalen Zelltypen Chondrozyten, Adipozyten, Osteoblasten und glatte Muskelzellen differenziert werden.

Das hier vorgestellte Zellkulturmodell ermöglicht Zugang zur frühen Entwicklung der humanen Neuralleiste und bietet dadurch zahlreiche Möglichkeiten um ihre Delamination, Migration und Differenzierung zu untersuchen. Dies eröffnet zudem das Potential, Neuralleisten-assozierte Krankheiten zu modellieren und pharmakologische Wirkstoffe zu testen.

1 Introduction

1.1 Pluripotent stem cells

Stem cells are defined as undifferentiated cells that self-renew and possess the ability to differentiate into progenitor cells that develop along specific pathways into mature cell fates. There are several types of stem cells, which differ in their origin and also in their differentiation potential. Adult stem cells persist in several tissues of the adult body, e.g. blood, skin, teeth and bone marrow. They have the function to repopulate or repair their resident tissue in response to injury. Some of them possess a powerful, far-ranging differentiation potential (Clarke et al., 2000; Krause et al., 2001). However, as they do not give rise to all cell type of the three germ layers, they are termed multipotent. Pluripotent stem cells on the other hand are cells that possess the ability to differentiate into any somatic cell type. Today, basically three types of pluripotent cells are known; embryonic stem (ES) cells, which are found in the inner cell mass (ICM) of the early blastocyst, induced pluripotent stem (iPS) cells, which are artificially generated by reprogramming somatic cells into an ES cell-like state via the introduction of reprogramming factors, and embryonic germ (EG) cells, which are derived from the testis. In the first part of the introduction human ES (hES) cells and iPS cells, as well as their therapeutic potential are discussed in detail (schematic overview in Fig.1).

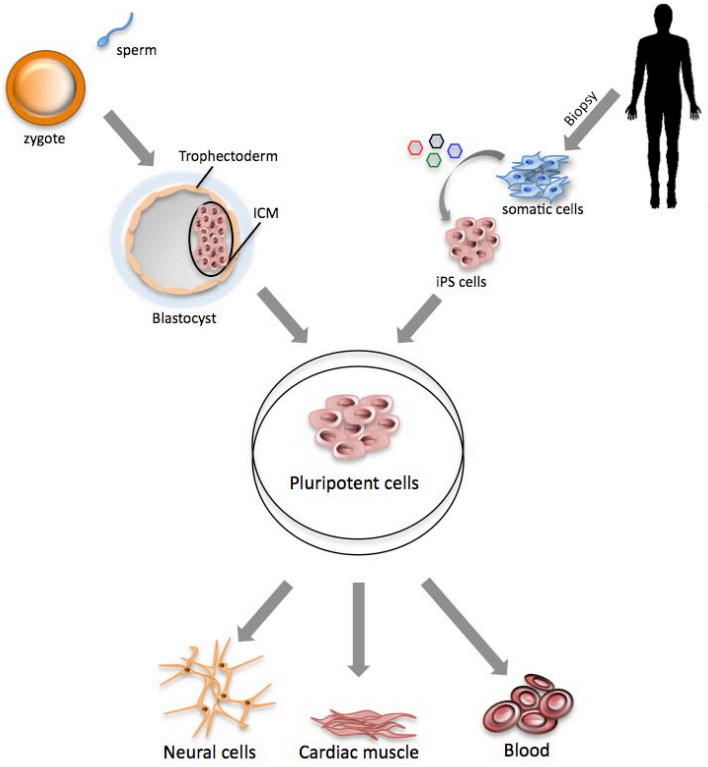

Figure 1: Schematic overview of the derivation of pluripotent stem cells. hES cells are derived from the inner cell mass of the blastocyst (upper lefthand side), while iPS cells are obtained by cellular reprogramming of somatic cells through the introduction of pluripotency factors (upper righthand side). Those pluripotent cells are able to give rise to tissues of all three germlayers (lower central part).

1.1.1 Human embryonic stem cells

In the early 80s, the first ES cells were isolated from the ICM of the mouse blastocyst and their unique properties of self-renewal and pluripotency were revealed (Evans and Kaufman, 1981; Martin, 1981). Research on mouse ES cells provided valuable knowledge about maintenance and differentiation of pluripotent cells. In 1998, Thomson et al. succeeded in the derivation of ES cells from the ICM of an 8-day-old human blastocyst. Just like their murine counterparts, hES cells exhibit pluripotency and self-renewal (Amit et al., 2000; Reubinoff et al., 2000; Thomson et al., 1998). They require different culture conditions compared to mouse ES cells though, as they cannot be cultivated under feeder-free conditions in the presence of leukemia inhibitor factor. Attempts have been made to cultivate hES cells on Matrigel, a growth factor containing substrate, with fibroblast-conditioned medium (Xu et al., 2001) or to supplement culture medium with fibroblast growth factor (FGF) and tumor growth factor-β (TGF-β; Amit et al., 2004). Importantly, in a clinical context, cells must not be cultivated with any source of animal-derived cells or substances. While in the beginning of hES cell research it was essential to co-cultivate hES cell lines with murine fibroblasts, more and more cell lines were established that have been cultured on human fibroblasts and therefore did not come into contact with animal substances of any kind during their generation (Inzunza et al., 2005). hES cells are identified by their typical marker expression of surface molecules such as stage-specific embryonic antigen-3 (SSEA-3) and SSEA-4, as well as tumour recognition antigens 1-60 (TRA1-60) and TRA1-80. Furthermore several transcription factors are associated with pluripotency, namely NANOG (Chambers et al., 2003; Mitsui et al., 2003), POU5F1, which is known as OCT4 (Nichols et al., 1998), and SOX2 (Avilion et al., 2003).

Obviously, the generation and culture of hES cells raises ethical concerns, as it implies the destruction of human embryos during blastocyst stage. For the preparation of hES cells, embryos that are surplus during *in vitro* fertilizations are used. Regulations differ according to the laws of the particular countries. In Germany, the key date regulation applies; meaning that research on hES cells is allowed if the cells have been generated before January 2005. However, the generation of hES cells is prohibited in Germany, so that hES cells have to be imported from other countries. The research on hES cells is supported as their unique features promise large benefit for mankind. Due to their enormous differentiation potential, hES cells might have a promising potential in cell replacement therapies. hES cells have been successfully differentiated into cells from heart (Kehat et al., 2001), liver (Lavon et al., 2004), the

blood (Kaufman et al., 2001) and nervous system (Reubinoff et al., 2001; Zhang et al., 2001). However, medical application faces some major obstacles. For transplantation purposes it is essential that the cell population to be transplanted is free of unwanted mature cell fates that have developed analogue to the cell type of interest. Furthermore the population has to be free of undifferentiated pluripotent cells to exclude tumor formation. Therefore, highly selective differentiation and isolation paradigms have to be used. In addition to the problem of tumor formation of transplanted undifferentiated stem cells, therapeutical applications of stem cells harbor the problem of immune rejection in the case of allogenic transplants.

Besides the potential of hES cells for advances in regenerative medicine, basic hES cell research enables the detailed investigation of human development. On the one hand, basic hES cell research forces the investigation of the factors that keep stem cells in their undifferentiated state. Recently, this knowledge led to the successful reprogramming of somatic cells to induced pluripotent stem (iPS) cells by introducing defined factors (Takahashi et al., 2007; Takahashi and Yamanaka, 2006; Yu et al., 2007). In addition, hES cells facilitate the study on differentiation processes leading to the formation of distinct mature cell types. Another utilization of hES cells and hES cell-derived somatic cells in medical research is the development of new drugs for therapeutic application as well as toxicity testing.

1.1.2 Induced pluripotent stem cells

IPS cells are derived from somatic cells, which are reprogrammed to an undifferentiated ES cell-like state. They are referred to as ES cell-like because they do not only exhibit a similar morphology, but are also pluripotent, as they have been shown to give rise to cells of all three germ layers. The first murine iPS cells were generated 2006 by Takahashi & Yamanaka, human iPS cells were generated shortly after (Takahashi et al., 2007; Takahashi and Yamanaka, 2006; Yu et al., 2007). In the first groundbreaking publications by Takahashi and colleagues, the four genes OCT4, KLF4, C-MYC, and SOX2, known to maintain pluripotency in ES cells, were introduced into embryonic fibroblasts by a viral approach, resulting in the generation of iPS cells that are able to generate cells of the three germ layers. The breakthrough in iPS cell research aroused enormous hope for medical applications. iPS cells may harbor the potential of autologues cell replacement therapies, which would overcome the problem of immune rejection. Another major application of iPS cell research is disease modeling by using patient-specific iPS cells. Since the seminal work by Takahashi and Yamanaka research-

ers are constantly modifying and improving the technique of cellular reprogramming. For the medical progress of iPS cell research, it is indispensable to discover other somatic cells as starting material for reprogramming, which are easy to access from patients by a tissue biopsy. In addition to embryonic foreskin fibroblasts, cord blood stem cells (Haase et al., 2009), adult skin fibroblasts (Park et al., 2008), keratinocytes (Aasen et al., 2008) and adipose stem cells (Sun et al., 2009) have been successfully used for reprogramming. Another approach to promote iPS cell research is to circumvent safety issues evoked by reprogramming. Using a retroviral or lentiviral vector for factor delivery genetically modifies the emerging iPS cells, as viral transduction leads to insertional mutagenesis of the host genome. Additionally, KLF4 and C-MYC are potent oncogenes, which could eventually lead to cancer if an iPS cell-derived transplant would be used in the clinic. Therefore studies aimed at alternative approaches, for example C-MYC and KLF4 were substituted with NANOG and LIN28 (Yu et al., 2007). Reprogramming was also achieved without C-MYC (Wernig et al., 2008) and even the introduction of only OCT4 was sufficient to reprogram neural stem cells (Kim et al., 2009). However, a recent publication shows that reduction of reprogramming factors leads to reduction of reprogramming efficiency and differentiation potential (Lohle et al., 2011). In 2010, Vierbuchen and colleagues showed that embryonic and postnatal fibroblasts could be directly converted into neurons by introducing three neural-lineage-specific transcription factors. Thereby a population of functional neurons was obtained without the intermediate step of tumorigenic pluripotent stem cells (Vierbuchen et al., 2010). For the diminishment of safety hazards, other delivery methods were explored, e.g. adenoviral vectors or even non-viral approaches like recombinant proteins or non-viral plasmid transfection as well as episomal vectors. Recently somatic cell reprogramming was successfully achieved by administration of synthetic modified mRNA (Warren et al., 2010). Interestingly mouse and human cells could also be efficiently reprogrammed to pluripotency by transfection of microRNA only (Anokye-Danso et al., 2011; Miyoshi et al., 2011). The potential of iPS cells in terms of disease modelling and drug testing became strikingly clear when the first patient specific iPS cells were generated from patients suffering from genetic diseases like muscular dystrophies, spinal muscular atrophy (Ebert et al., 2009), amyotrophic lateral sclerosis (Dimos et al., 2008), Parkinson’s disease (Soldner et al., 2009), Huntington's disease (Park et al., 2008), and Machado-Joseph disease (Koch et al., 2011). For review on recent advances in modelling neurological diseases, see Ming et al., 2011.

1.2 The neural crest

The neural crest is made up of a transient, highly migratory cell population found in all vertebrate embryos. Neural crest cells give rise to a wealth of derivatives found in virtually all tissues of the body and are therefore often considered as the "fourth germ layer". Neural crest cells originate at the interface of the dorsal part of the closing neural tube and the adjacent epidermis. After their emergence, they start to migrate along defined pathways. The differentiation potential of migrating neural crest cells is highly diverse. The cell fate of neural crest cells depends on the very region from which they emerge and on the migration pathway they choose. According to their axial level, they can be roughly subdivided into cranial, trunk, vagal (from the neck region) and sacral (from the tail region) neural crest cells. Cranial neural crest cells migrate into the pharyngeal arches and build up the facial cartilage and bone, neurons and glia of the cranial ganglia, as well as melanocytes. A subpopulation of cranial neural crest cells is made up of cardiac neural crest cells, which differentiate into smooth muscle of the cardiovascular system, pericytes, and cardiac sympathetic and parasympathetic neurons.

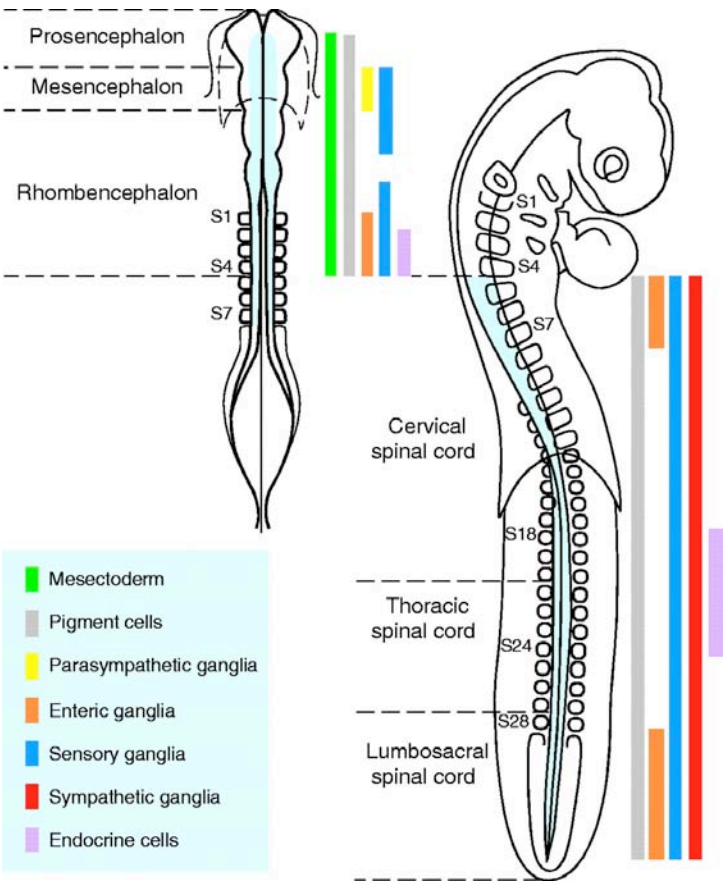

Figure 2: Fates of the neural crest. Neural crest derivatives are shown exemplary in the chick embryo at 7 somite stage (left side) and and 28 somite stage (right side). Pigment cells and sensory ganglia are derived from virtually every region. Mesoectoderm is exclusively derived from cranial NC cells, sympathetic ganglia exclusively from trunk NC cells. The vagal and sacral NC cells give rise to enteric ganglia, vagal NC cells also to endocrine cells. A subset of trunk NC cells also gives rise to endocrine cells. (Adapted from Le Douarin et al., 2004).

Trunk neural crest cells differentiate into neurons and glia of the peripheral nervous system, melanocytes, as well as the medullary part of the adrenal gland (Le Douarin and Kalcheim, 1999). Vagal and sacral neural crest cells populate the gut forming the enteric neurons and glia (Burns and Douarin, 1998) as well as endocrine cells (Fig. 2).

1.2.1 Neurulation and neural crest specification

The hour of birth of the central and peripheral nervous system (CNS; PNS) is the neurulation, as the neural plate lifts to form the neural tube. Neurulation and the induction of neural crest cells are provoked by the concerted action of bone morphogenetic proteins (BMPs), members of the Wnt family, fibroblast growth factors (FGFs), Notch and retinoic acid (RA). BMP, a member of the TGF-β protein family, is expressed in the non-neural epithelium. In the lifting neural plate BMP is repressed by the BMP antagonist sonic hedgehog (SHH), which is segregated by the underlying notochord. As the neural tube is built by fusion of the neural folds, the neural plate border forms the dorsal organization of the neural tube, the roof plate of the later spinal cord, which expresses BMP. At the same time the ventral part of the neural tube, the developing floor plate, is ventralized by SHH expressed by the notochord. Thereby a gradient of dorsal-ventral agents is established, at which neural crest cells will emerge from the BMP-rich dorsal part of the neural tube (Fig. 3). In addition to the dorsal-ventral gradient, the patterning of the anterior-posterior axis is crucial for neural crest induction. Candidates for this purpose are the posteriorizing signaling agents Wnt, FGF and RA, which are expressed in the non-neural ectoderm and the dorsal neural tube during neural crest emergence (Dickinson et al., 1995). Knock-out studies in mice depleting Wnt1 and Wnt3A resulted in neural crest defects, demonstrating the key role of these signaling molecules in neural crest induction (Ikeya et al., 1997). Experiments with *Xenopus* have shown that a dominant negative form of the FGF receptor 1 suppresses the neural crest inducing activity of the paraxial mesoderm (Monsoro-Burq et al., 2003), and temporally-regulated RA depletion resulted in specific neural crest abnormalities (Dickman et al., 1997). In addition, Notch signaling has an impact on neural crest induction. It has been shown that overexpression, as well as downregulation of Notch resulted in reduction of neural crest cells (Coffman et al., 1993; Endo et al., 2002). This effect is either mediated by Notch signaling controlling the inducing activity of BMP during neural crest development or by the fact that Notch signaling represses neurogenesis. Notch

therefore can also be regarded as a rheostat governing neural crest induction just like Sox2 or Nanog act as rheostats regulating stemness properties in ES cells (Rizzino, 2008).

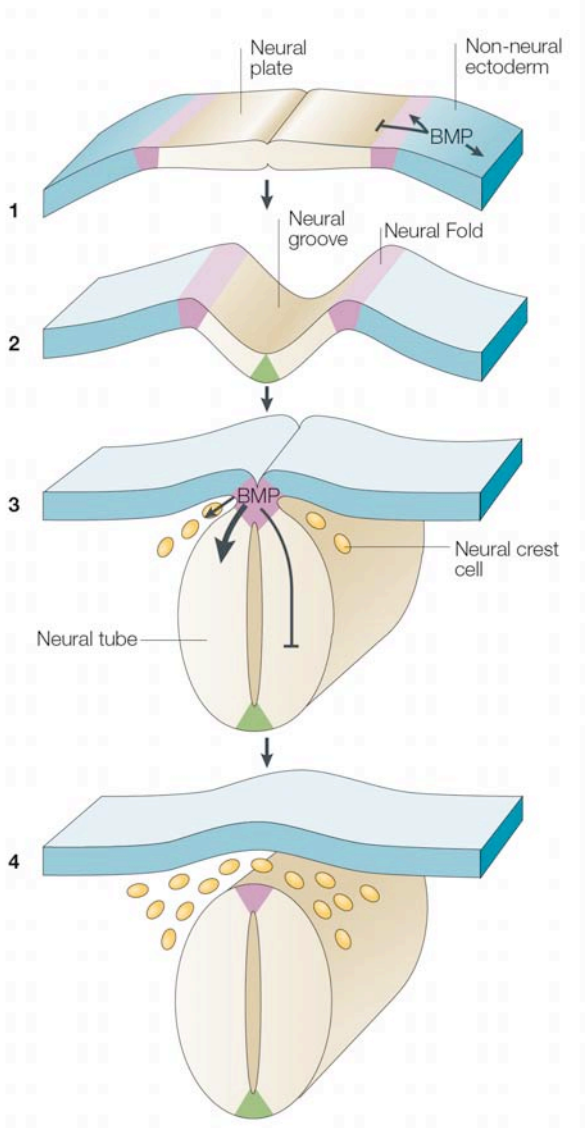

Figure 3: Neurulation and emergence of neural crest cells. BMP is expressed in the non-neural ectoderm, but is repressed in the folding neural plate (1+2). As the neural folds fuse to form the neural tube, and the neural tube separates, it gets organized into the dorsal part (3+4; shown in purple), expressing BMP, and the ventral part (shown in green) expressing SHH. Thereby a descending BMP gradient is established (indicated in 3, right half). NC cells emerge from the dorsal part of the neural tube (3+4; shown in yellow). (Adapted from Liu and Niswander, 2005).

The complex gene network regulating the specification of first neural plate border cells and later neural crest cells has been widely studied in chicken, mice, lamprey, *xenopus*, and zebrafish by using knock-out animals or morpholinos and has shown some epistatic relationships. Msx1/2, as well as Pax3/7, have been identified as important neural plate border specifiers induced by dorsal BMP expression. They are expressed in the neural folds, and subsequently, as the neural folds fuse, in the dorsal part of the neural tube. Cells that are already specified as neural crest cells show additionally expression of the transcription factors Snai1, Snai2, Foxd3, Sox9, cMyc, AP2, and members of the Id family. As neural crest cells

leave the neural tube and start their migration, throughout the body they express the low affinity nerve growth factor receptor p75NTR and the carbohydrate epitope HNK-1 on their surfaces, as well as the transcription factor Sox10 (Sauka-Spengler and Bronner-Fraser, 2008). The changes in the gene expression lead to a series of drastic cellular changes that evoke an epithelial-to-mesenchymal transition (EMT) of neural crest cells. Thereby neural crest cells change their epithelial characteristics to gain a migrating, mesenchymal phenotype (Duband et al., 1995). Switching cadherin expressions mediate one important cellular change during EMT. In the neural plate, the columnar epithelia cells express E-cadherin (Thiery et al., 1984). During neural tube closure E-cadherin expression is replaced by N-cadherin and NCAM, causing the neural folds to recognize each other and to fuse. As neural crest cells undergo EMT, they downregulate these cell adhesion molecules of strongly contacted cells and upregulate the type II Cadherins -6b, -7 and -11, which allow them to detach from the neuroepithelium, gain their mesenchymal morphology and start their migration (Hatta et al., 1987; Nakagawa and Takeichi, 1995; Nakagawa and Takeichi, 1998). Another cellular event is the switch from tight junctions, e.g. Occludin and Claudins, to gap junctions, like Connexin43 (Ikenouchi et al., 2003; Lo et al., 1997). As neural crest cells are guided by external cues on their migration pathways, upregulation of receptors for guidance molecules, like ephrin receptors (Krull et al., 1997), Slit/Robo (Jia et al., 2005) and Neuropilin-l (Gammill et al., 2006; McLennan and Kulesa, 2007) is necessary. The junctions between neural crest cells and extracellular matrix are increased by an upregulation of integrins (Lallier and Bronner-Fraser, 1993). At the time when neural crest cell migration ceases, cellular changes occur in a reverse manner to the onset of migration, e.g. N-cadherin is upregulated and expression of integrins decreases (Akitaya and Bronner-Fraser, 1992; Kasemeier-Kulesa et al., 2006).

1.2.2 Fate of cranial neural crest cells

In former times it was thought that all mesenchymal tissues, in the trunk as well as in the head are derived from the mesoderm. So it was a revolutionary time, as at the turn of the 19th century the first scientists discovered an alternative origin of the mesenchymal tissues in the head, namely the neural crest. Many decades they were disbelieved due to the deadlocked opinion of the community and real attention was not paid until cell-labeling techniques were established, first in the avian (Johnston, 1966; Le Lievre and Le Douarin, 1975) and later in the mouse (Osumi-Yamashita et al., 1994).

The fate of cranial neural crest cells is determined by their spatial identity and the onset of migration. While early-migrating cranial neural crest cells form the mesenchymal derivatives, late-migrating neural crest cells predominantly stay close to the neural tube and form the cranial ganglia (Kulesa et al., 2010). Neural crest cells from the diencephalon, the posterior part of the forebrain, in concert with the mesoderm, give rise to the frontal and parietal bones (Jiang et al., 2002). Neural crest cells arising from the mesencephalon and the rhombomeres populate the different pharyngeal arches, i.e. the anlage for the mesodermal tissues of the head (Fig. 4).

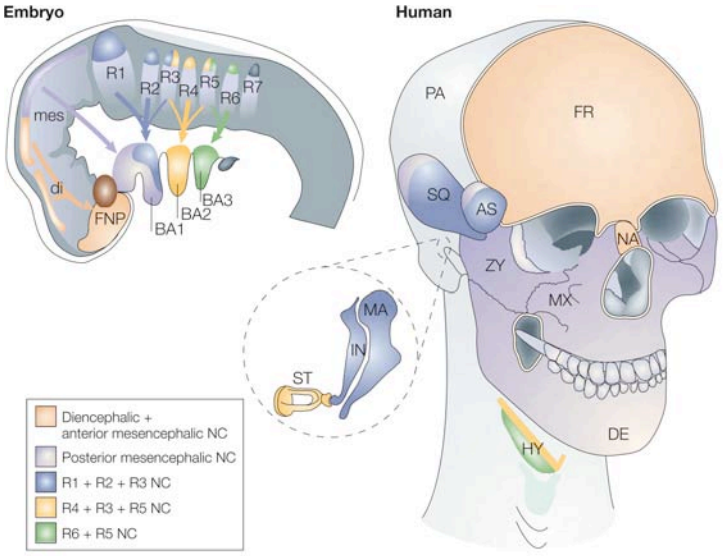

Figure 4: Contribution of cranial neural crest cells to the facial skeleton. On the left side the migration pathways of cranial neural crest cells in the embryo are depicted. The color code gives evidence about the origin of the facial bones of the adult skull shown on the right. Neural crest cells from the diencephalon and the anterior mesencephalon migrate between the eyes, to form the frontonasal plate (orange). Neural crest cells from the mesencephalon migrate to the first pharyngeal arch, where they will form the jaw (purple). From the rhombomeres (R) Neural crest cells migrate in three major streams, cells from R1+R2 migrate to the first pharyngeal arch (blue), cells from R4 to the second pharyngeal arch (yellow) and cells from R6 to the third pharyngeal arch (green). Neural crest cells from R3 and 5 migrate rostrally or caudally to join the main streams. Abbreviations: AS, alisphenoid bone; BA: Branchial arch (another term for pharyngeal arch commonly used in fish and amphibian); DE, dentary bone; di, diencephalon; FNP, frontonasal process; FR, frontal bone; HY: hyoid bone; IN, incus; MA, malleus; mes: mesencephalon; MX, maxillary bone; NA, nasal bone; PA: parietal bone; R: rhombomere; SQ, squamosal bone; ST, stapes; ZY, zygomatic bone. (From Santagati and Rijli, 2003).

Neural crest cells from the mesencephalon and first and second rhombomere migrate between the eyes to form the palatal shelves and the upper jaw, and also populate the first pharyngeal arch, also called mandibular arch, which will give rise to the lower jaw and the neurons of the trigeminal ganglion. Cranial neural crest cells from rhombomere 4 populate the second arch, also called hyoid arch, which gives rise to the hyoid skeleton and the neurons of the facial

nerve. Cells migrating from rhombomere 6 and 7 will populate the posterior arches, giving rise to skeletal elements like thymus, thyroid and epiglottic cartilage (Lumsden et al., 1991; Schilling and Kimmel, 1994). The neural crest cells from rhombomeres 3 and 5 deviate rostrally or caudally to join the migrating streams of the even numbered rhombomeres (Sechrist et al., 1993). Besides the mesenchymal components, each pharyngeal arch also contains a cranial nerve, whose sensory part is build up by the respective neural crest cells. The first arch gives rise to the sensory part of the trigeminal nerve (V), the second to the facial nerve (VII), and the third to the glossopharyngeal nerve (IX).

The more caudal cranial neural crest cells (from rhombomere 7 to somite 3) contribute to the mesenchym-derived heart and are therefore termed cardiac neural crest cells. They are involved in the complex development of the aorticopulmonary septum and the conotruncal cushions and form the smooth muscle linings of the blood vessels (Kirby et al., 1983).

Hindbrain segmentation, establishment, and maintenance are accompanied by expression of members from different gene families, of which the HOX gene code has been identified as a key player. In vertebrates, four HOX gene clusters are found, named a-d, and associated 13 paralogue groups. The HOX code of the neural tube can only be partly transferred to the neural crest cells migrating from it. HOX2A is the most anteriorly expressed HOX gene, in the neural tube it is expressed caudally at the boundary of rhombomere 1 and 2. However, neural crest cells migrating from those rhombomeres, forming the first pharyngeal arch, do not express any HOX genes (Fig. 5).

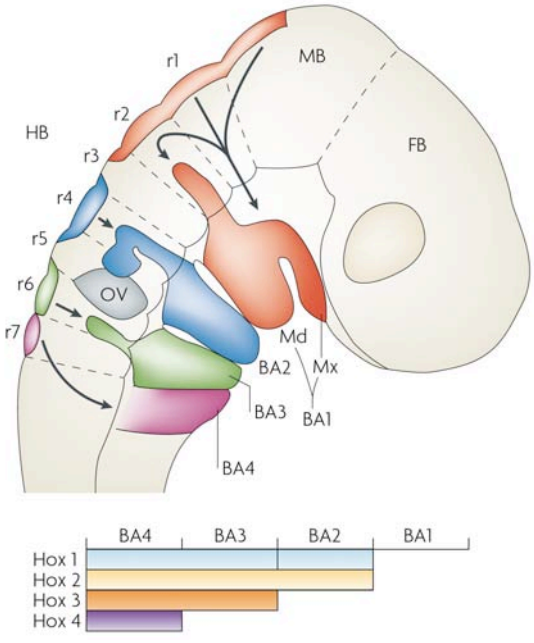

Figure 5: Migration pathways of NC cells to the pharyngeal arches and associated HOX gene expression. Schematic demonstration based on experiments in chick and mouse embryos. The first pharyngeal arch is devoid of HOX expression (red), while the more caudal arches express the first four paralogues in ascending order. Abbreviations: BA, branchial (pharyngeal) arch; FB, forebrain; HB, hindbrain; MB, midbrain; Md, mandibular part of BA1; Mx, maxillar part of BA1; OV, otic vesicle r, rhombomere. (Adapted from Guthrie, 2007).

HOX2A expression is restricted to neural crest cells migrating to the second pharyngeal arch, namely from rhombomere 4 and the caudally and rostrally migrating neural crest cells from rhombomere 3 and 5. It has been shown that HOX gene expression is directly linked with skeletogenic potential. While the HOX negative neural crest cells of the first pharyngeal arch give rise to the most skeletal elements of the head, the neural crest cells expressing only HOX2A and HOX2B in the second pharyngeal arch give rise to only the middle ear and the lesser horn of the hyoid bone. The neural crest cells of the third and fourth pharyngeal arch, expressing additionally HOX3 and 4 genes, give rise to the greater horn of the hyoid bone, thymus, parathyroid and thyroid glands. In the trunk, where the neural crest cells express a higher number of HOX genes, no skeletal elements are formed (Trainor, 2003).

For the guidance of neural crest migration, several models exist but yet the underlying mechanisms remain to be clarified. Those include population pressure and contact inhibition of movement, cell nudging, polarized cell movement and cell chemotaxis. Population pressure and contact inhibition of locomotion means cells migrate away from densely populated areas where new cells are born constantly, as it has been described for *Xenopus* neural crest cells (Carmona-Fontaine et al., 2008). The term cell nudging has been established to describe that the contact with neighboring cells leads to a forward movement, induced by membrane blebbing on the opposite side of the cell-to-cell contact. Cell nudging has been first described in 1976 (Tickle and Trinkaus, 1976), the work of Jesuthasan suggests a similar phenomenon for zebrafish trunk neural crest cells, as the cells adhere to each other and even show a thickening of pertrusion after contact. The same work also shows that contact to the somites results in thinning of pertrusion and a rapid stop of motility (Jesuthasan, 1996). Another work on zebrafish neural crest cells showed that cells adapt a polarized morphology after their emergence from the neural tube and start directed migration. This observed polarized cell movement is contradictory to another publication where it has been shown that neural crest cells can reverse direction (Kulesa et al., 2000; Kulesa et al., 2005). Besides the cellular forces accompanying cell-to-cell contacts and morphology, cell chemotaxis has been demonstrated as powerful neural crest guide. Neural crest cells react on excitatory and inhibitory signals from their environment. Here differences exist between cranial and trunk neural crest cells, as cranial neural crest cells migrate into the pharyngeal arches and trunk neural crest cells migrate along the somite region. In the head, signaling is needed that mediates the boundaries of the different streams. The crest-free spaces at R3 and R5 are mediated by the expression of

chemorepellents in the mesenchyme. Neural crest cells express Eph receptors and ephrin ligands that act with Eph/ephrins in the mesenchyme in a repulsive manner. Here also semaphorin-3A and -3F are expressed, which repel neural crest cells due to their expression of neuropilin-1 and -2 receptor. Mutations of ErbB4, a neuregulin receptor expressed in R3 and R5, also results in abnormal neural crest cell invasions. Neural crest cells are attracted into the arches via C-X-C chemokine receptor type 4 (CXCR4) signaling. While the receptor CXCR4 is expressed in migrating neural crest cells, its ligand, the stromal cell derived factor (SDF-1), is expressed on the migratory path of neural crest cells and in the pharyngeal arch region (Olesnicky Killian et al., 2009). The neuropilin-1 receptor not only has a function in the repellence of neural crest cells from the mesoderm, but in their attraction and homing as well, as its ligand, the vascular endothelial growth factor (VEGF) expressed in the ectoderm of the pharyngeal arch, has shown to have a strong attracting effect on neural crest cells (McLennan et al., 2010).

1.2.3 Fate of trunk neural crest cells

Trunk neural crest cells migrate in two major waves. The first neural crest cells that leave the neural tube migrate medio-ventral between the somites and the neural tube to either form the dorsal root ganglia close to the neural tube, or continue their migration ventrally to populate the sympathetic ganglia and adrenal chromaffin cells. The neural crest cells of the second wave migrate dorso-lateral between ectoderm and somites. These neural crest cells will contribute to the melanocyte lineage (Fig. 6A). Vagal neural crest cells, which migrate from the neural tube close to the somites 1-7, and sacral neural crest, which migrate caudal to the 24th somite, populate the gut to form the enteric nervous system and smooth muscle (Fig. 6B).

Concerning guiding cues for trunk neural crest cells partly the same chemokines are involved as in cranial neural crest cell migration, however, the presence of the somites results in a different anatomic scene. Additionally, slit/Robo signaling has been identified as important guidance mechanism. Neural crest cells express Robo-1 and Robo-2 and avoid cells expressing the slit ligands (Jia et al., 2005). In the head, however, migrating neural crest cells express slit-1, whereas placode cells express Robo-2, thereby regulating interactions during cranial nerve generation. The first wave of neural crest cells is guided on the ventral route, as they are repelled laterally by ephrin expression and ventrally attracted by SDF-1/CXCR4 signaling, as well as thrombospondin, which promotes neural crest migration and adhesion (Belmadani et

al., 2005; Santiago and Erickson, 2002; Tucker et al., 1999). However, as migration occurs only through the rostral half of the somite, neural crest cells on the caudal half are repelled by Semaphorin-3A (from the dermomyotome) and -3F (from the caudal sclerotome), ephrins, and F-spondin (Debby-Brafman et al., 1999; Krull et al., 1997; Schwarz et al., 2009). Some neural crest cells accumulate within the somites and cluster to build the dorsal root ganglia later on. For the segmental dorsal root ganglia arrangement Neuropilin-1/Semaphorin-3A and Neuropilin-2/Semaphorin-3F are required. Neuropilin-1/Semaphorin-3A repulse neural crest cells from the intersomitic space and facilitates segmentation of dorsal root gangliogenesis, while Neuropilin-2/Semaphorin-3F guides neural crest migration (Roffers-Agarwal and Gammill, 2009).

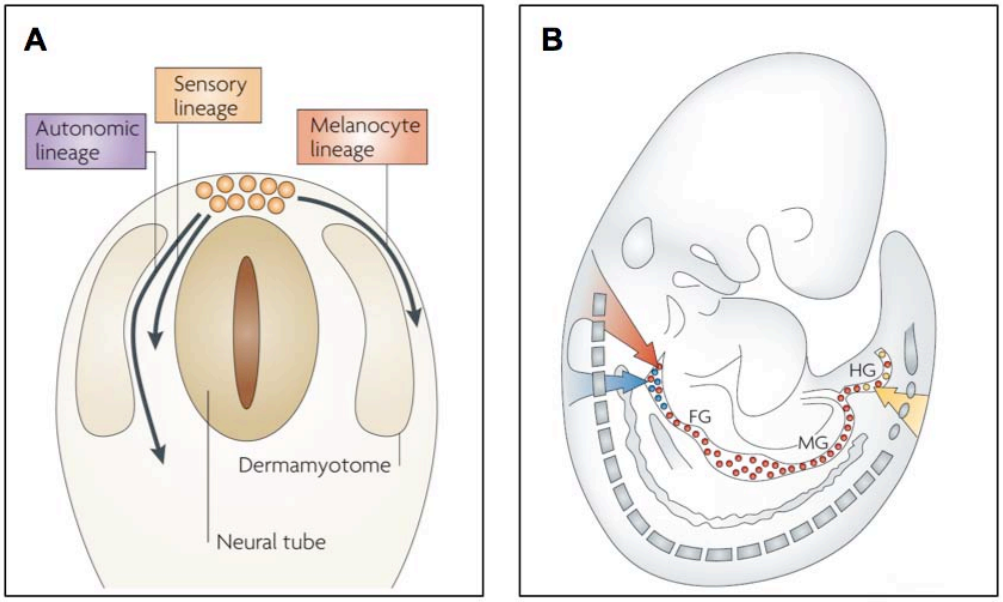

Figure 6: Migration pathways of trunk neural crest cells and migration of vagal and sacral neural crest cells towards the gut. (A): The first wave of migrating neural crest cells (left arrows) takes the medio-ventral route and migrates between the somites and the neural tube. Those cells will form the dorsal root ganglia, and, the cells that migrate further, also the autonomic ganglia. The second neural crest cells to leave the neural tube migrate dorsolateral and form the pigment cells of the skin. (Adapted from Marmigere and Ernfors, 2007). (B): neural crest cells from the vagal and sacral region populate the enteric gut and form the enteric ganglia as well as enteric smooth muscle. FG: foregut; MG: midgut; HG: hindgut. (Adapted from Heanue and Pachnis, 2007).

Neural crest cells that passed the somites are guided towards the aorta, where they will form the sympathetic ganglia. This is facilitated by neuregulin secreted by the mesenchyme around the dorsal aorta, which attracts ErbB2/B3 expressing neural crest cells and the vascular-derived neurotrophic factor artemin from peripheral blood vessels, which attracts sympathetic precursors expressing the glial-derived neutrophic factor (GDNF) family receptor GFRα

(Britsch et al., 1998; Honma et al., 2002). Semaphorin-3a prevents lateral migration to the limb and medial migration to the aorta (Kawasaki et al., 2002). Slit-2 repels neural crest cells from ventral migration to the endoderm.

Later the migration pattern of neural crest cells situated at the dorsal part of the neural tube changes, as ephrin expression turns from a repellent into an attractant for EphB3 expressing melanoblasts and cells migrate laterally through the dermis in order to follow the melanocyte lineage (Santiago and Erickson, 2002). In addition, neural crest cells are now inhibited in their ventral migration through the somites by Neuropilin-1/Semaphorin 3a signaling (Roffers-Agarwal and Gammill, 2009).

As neural crest cells express integrins, which are receptors for fibronectin and laminin (Kil et al., 1998; Monier-Gavelle and Duband, 1997) it is not surprising that on all neural crest migration routes extracellular matrix proteins are found, which are essential for neural crest migration without directly guiding them. Particularly those include fibronectin, laminin and collagen (Duband and Thiery, 1987; Newgreen and Thiery, 1980).

1.2.4 Environmental cues for *in vitro* neural crest cell differentiation

In vitro neural crest differentiation has been extensively studied on mouse cells, by dissecting the neural tube, plating it on an appropriate substrate and allowing neural crest cells to delaminate and migrate. Using these *in vitro* neural crest cultures, researchers were able to perform extensive studies on identifying cues for directed differentiation of isolated neural crest cells. In order to do this, it is important to internalize the events leading to neural crest differentiation during *in vivo* embryonic development. Neural crest cells staying close to the neural tube form the dorsal root ganglia. *In vitro* differentiation showed that neural crest cells require the presence of the neural tube to enter the sensory neuron lineage. However, researchers were able to substitute the presence of the neural tube by application of Wnt to gain sensory neurons. The differentiation towards autonomic neurons could be facilitated by application of BMP4, which is segregated *in vivo* by the dorsal aorta to which the sympathetic neuron precursors migrate towards (Reissmann et al., 1996; Schneider et al., 1999; Shah et al., 1996). For the differentiation towards the peripheral glia type Schwann cells NRG-1 was identified as a powerful glial instructor (Leimeroth et al., 2002; Meyer et al., 1997; Shah et al., 1994). For mesenchymal differentiation of neural crest cells commonly the differentiating effect of

fetal calf serum (FCS) is used. It has been shown that smooth muscle differentiation is additionally enhanced by application of TGF-β (Shah et al., 1996; Trainor et al., 2002). Moreover cranial neural crest cells give rise to cartilage, bone, as well as to fat cells of the face, but also of the trunk. Even though *in vivo* trunk neural crest cells do not give rise to mesenchymal derivatives, they could be differentiated into skeletogenic phenotypes when cultured in the appropriate conditions, thereby exhibiting plasticity (McGonnell and Graham, 2002). Concerning the differentiation of pigment cells, it has been shown that stem cell factor (SCF; also called steel factor) supports survival, proliferation and also final differentiation of melanocytes *in vivo* (Kunisada et al., 1998). Furthermore it has been shown that the interaction of endothelin-3 with the endothelin-B receptor is essential for the development of melanocytes. Those factors have already been used to generate melanocytes from murine ES cells (Fang et al., 2006; Motohashi et al., 2007; Yamane et al., 1999) and hES cells (Fang et al., 2006).

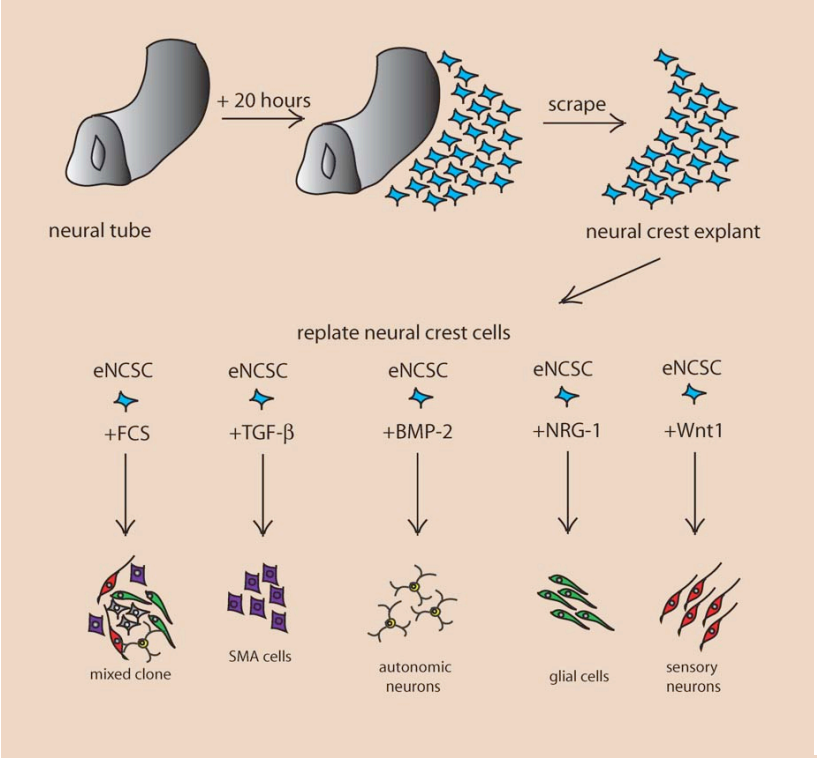

Figure 7: Differentiation potential of primary neural crest cells from the mouse. Murine primary neural crest cells are obtained by plating of the explanted embryonic neural tube on fibronectin, after 20 hours neural crest cells migrate out of the neural tube, which is than removed by scraping. Clonal plated neural crest cells give rise to smooth muscle upon TGF-β treatment, autonomic neurons are derived by application of BMP2, treatment with NRG-1 yields peripheral glia cells, and sensory neurons are obtained by application of Wnt1. Treatment with FCS leads to development of a mixed clone. (Adapted from Shakhova and Sommer, 2010).

1.2.5 Differentiation of neural rosettes and neural crest cells from pluripotent stem cells

Pluripotent stem cells have been extensively used for the study of CNS development. Neural differentiation of hES cells as well as iPS cells is efficiently achieved by an intermediate neural rosette step. Neural rosettes are made of radial arranged columnar cells that show similar properties to the neural tube, and are therefore often considered as neural tube-like structures (Elkabetz et al., 2008; Li et al., 2005). When isolated, they give rise to rosette-type neural stem cells (Elkabetz et al., 2008; Koch et al., 2009; Zhang et al., 2001). Those neural stem cells show high proliferation rates and are tripotent as they differentiate into neurons, astrocytes and oligodendrocytes.

Typically, either an embryoid body (EB) step or a stromal co-cultivation is used to initiate neural differentiation and to gain neural rosettes. The neural inducing effect of stromal cells, so called stromal-derived-inducing-activity (SDIA) is largely unexplored. As the cultivation of hES cells in stromal cell conditioned medium leads to an inducing effect, it is likely that secreted factors are responsible for the phenomenon (Vazin et al., 2008). The application of BMP suppresses the neural inducing effect of stromal cells on mouse ESCs, indicating that inhibition of BMP is relevant for the SDIA. However, it is shown in the same publication that also the co-cultivation of fixed stromal cells can induce neural differentiation, so probably surface bound components are also of importance (Kawasaki et al., 2000). Due to the unidentified underlying mechanism and the fact that they are animal-derived, stromal cells are, despite their strong neuralizing effect, unfeasible in a therapeutic context.

EBs are formed by aggregation of free-floating pluripotent stem cells and withdrawal of pluripotency-sustaining extrinsic factors. The differentiation of this paradigm is undirected, so that all three germ layers are generated. Growth factor application in order to direct differentiation is difficult, as the proper dispersal in the aggregate is not granted. Furthermore EBs are inapplicable for long term cultivation, as they loose shape and build vacuoles. Many protocols therefore use the initial differentiation to EBs, but then switch to an adherent culture by plating the aggregates (Zhang et al., 2001).

As neural rosettes and the neural stem cells derived thereof display *in vitro* properties of the neural tube, it is obvious that neural crest cells are found in close relation to this mimicked developmental step. SDIA-based protocols have been used to generate neural crest cells, ei-

ther through an intermediate rosette step (Lee et al., 2007) or direct differentiation on the stromal cell layer (Hotta et al., 2009; Pomp et al., 2005b). Two protocols also use EB-based differentiation paradigms to either FACSort neural crest cells directly from the EB (Jiang et al., 2009) or derive them from isolated neural rosettes obtained by plating of EBs (Colleoni et al., 2010).

1.2.6 Therapeutic potential of pluripotent stem cell-derived neural crest cells

Due to the unavailability of human embryonic tissues, the research on human neural crest development was largely restricted so far. Few data exist on primary human neural crest (Betters et al., 2010; O'Rahilly and Muller, 2007; Thomas et al., 2008). Recently, hES cells have been discovered as source for neural crest cells. Due to their ability to self-renew, they offer an inexhaustible pool of parental cells. Basic research on neural crest development helps us to understand the early events of embryonic development in the healthy human, but also the aberrations occurring in neural crest-related disorders, termed neurocristopathies. Among those are the neural crest related cancers, like Neuroblastoma, Schwannoma, and Melanoma, which are the most aggressive cancer cell types. Neural crest EMT and migration resembles a programmed version of the unprogrammed invasion occurring during metastasis. Therefore, the study on this highly proliferative cell population is of high interest in cancer research. Due to the complex impact of neural crest cells on the development of vertebrates, numerous diseases are known that are related to neural crest malfunction. Examples are Hirschsprung's disease and Charcot-Marie-Tooth disease, affecting primarily the peripheral nervous system, DiGeorge and CHARGE syndrome, which result from cranial and cardiac neural crest dysfunction. In the future cell culture models might be used to generate and test medical treatment. The possibility to derive large cell numbers of human neural crest derivatives offers vast prospects for high throughput screening of compounds. For example, *in vitro* cultivated sensory neurons could be of great value in the development of pain medication. Additionally, the generation of patient-specific iPS cells may lead to exciting disease models for neurocristopathies. First attempts in this direction have shown that patient-specific iPS cell-derived neural crest cells can serve as disease model for the neural crest-related disorder familiar dysautonomia (Lee et al., 2009).

1.3 Aim of the project

The neural crest is a transient embryonic cell population that contributes to a vast amount of different cell types of the vertebrate body. Its emergence, migration and differentiation have been studied extensively in animal models, but many aspects of this versatile population remain unrevealed. Due to the inaccessibility of human embryonic primary tissue, the studies on neural crest development are highly limited. This project aimed at the investigation of human neural crest development using hES cells as inexhaustible cell source. Whereas the occurrence of neural rosettes in differentiating hES cell cultures is a well-known phenomenon, less is known about the co-appearance of neural crest cells. The aim of this work was to assess whether hES cell-derived neural rosettes exhibit dorsal-ventral organization and thereby resemble a primitive form of the neural tube. It should be investigated whether neural crest cells emerge from these neural tube-like structures. After successful characterization of potential neural crest cells on mRNA and protein level, a purified human neural crest cell population should be established, which multipotency should be proven by successful differentiation into multiple neural crest derivatives. Having established a stable cell culture model, a further aim was to show the prospects to what extend this model could be used to investigate human neural crest development. Therefore the shifting expression of cadherins, as observed during EMT *in vivo*, should be investigated during the *in vitro* delamination process of human neural crest cells.

2 Materials and Methods

2.1 Materials

Tab. 1: List of equipment

Equipment	Article	Manufacturer	Registered Office
Chemiluminescence detection	Chemidoc XRS	Bio-rad Laboratories	Munich
Electrophoresis	Agagel Mini	Biometra	Göttingen
	Agagel Midi-Wide	Biometra	Göttingen
	ProteanIII MiniGel System	Bio-rad Laboratories	Munich
Thermocycler	T3 Thermocycler	Biometra	Göttingen
Incubators for cell culture	Heracell	Biometra	Göttingen
Microscopes	Axiovert 40C Axiovert 200M Stemi 2000-C	Carl Zeiss	Jena
Microscope camera	AxioCam MRm	Carl Zeiss	Jena
pH-Meter	CG840	Schott	Mainz
Photometer	NanoDrop	Peqlab	Erlangen
Power supply for electrophoresis	Standard PowerPack P25	Biometra	Göttingen
	PowerPack 200	Bio-rad Laboratories	Munich
Sterile workbenches	Herasafe	Heraeus	Hanau

Tab. 2: List of laboratory plastic ware

Laboratory plastic ware	Cat. No.	Manufacturer	Registered Office
4-well culture dishes	179820	Nunc	Wiesbaden
6-well culture dishes	140685	Nunc	Wiesbaden
12-well culture dishes	150682	Nunc	Wiesbaden
Cellstar ^{TM} 175 cm^2 flasks	660175	Greiner Bio-One	Solingen
Culture dishes ∅ 3,5 cm	353001	BD Biosciences	Heidelberg
Culture dishes ∅ 6 cm	353004	BD Biosciences	Heidelberg

Culture dishes ∅ 10 cm	353003	BD Biosciences	Heidelberg
Culture dishes ∅ 15 cm	93150	MIDSCI	St. Louis, USA
EB culture dishes ∅ 6 cm	083878	Nunc	Wiesbaden
Nitrocellulose membranes	4684.1	Carl Roth GmbH	Karlsruhe
PCR strip tubes - 0.2 mL	81-38440	PEQLAB	Erlangen
Round bottom tubes - 12x75mm	352054	BD Biosciences	Heidelberg
Serological pipettes (25, 10, and 5 mL)	356525 356551 356543	BD Biosciences	Heidelberg
Syringes - 20 mL	300296	BD Biosciences	Heidelberg
Syringe filter - 0.2 μm	PN 4612	PALL	Dreieich
Tubes - 0.5 mL	667204	Greiner Bio-One	Solingen
Tubes - 1.5 mL	616201	Greiner Bio-One	Solingen
Tubes - 15 mL	227261	Greiner Bio-One	Solingen
Tubes - 50 mL	188271	Greiner Bio-One	Solingen
Cryovials - 1 mL	375353	Nunc	Wiesbaden
Cryovials - 1.8 mL	375418	Nunc	Wiesbaden

Tab. 3: List of chemicals, media and supplements

Chemicals, media and supplements	**Cat. No.**	**Manufacturer**	**Registered Office**
2-Mercaptoethanol	13256	Invitrogen	Karlsruhe
2-Phospho-L-ascorbic acid trisodium salt	49752	Sigma-Aldrich	München
3-Isobutyl-1-methylxanthine	I5879	Sigma-Aldrich	München
Agarose	35-1020	PEQLAB	Erlangen
Alcian Blue	236551	Sigma-Aldrich	München
Alizarin red	A5533	Sigma-Aldrich	München
Ascorbic acid	A4403	Sigma-Aldrich	München
B-27 supplement	17504	Invitrogen	Karlsruhe
B-27 supplement minus Vitamin A	12587	Invitrogen	Karlsruhe
BDNF	248-BD	R&D systems	Wiesbaden
Bromphenol blue	B0126	Sigma-Aldrich	München
BSA	A8806	Sigma-Aldrich	München

dcAMP	D0627	Sigma-Aldrich	München
Collagenase type IV	17104	Invitrogen	Karlsruhe
Cytocon™ buffer II	Cy01-01-H07-01-01	Evotec	Hamburg
DABCO	0718.2	Carl Roth GmbH	Karlsruhe
Dexamtehasone	D1756	Sigma-Aldrich	München
DNA ladder (100bp)	SM0241	Fermentas	Leon-Rot
dNTPs	20-2012	PEQLAB	Erlangen
DMEM/F12 (1:1)	11320	Invitrogen	Karlsruhe
DMEM high glucose	41965	Invitrogen	Karlsruhe
DMSO	D2650	Sigma-Aldrich	München
D-PBS	14190	Invitrogen	Karlsruhe
EDTA	E6511	Sigma-Aldrich	München
EGF	236-EG-01M	R&D systems	Wiesbaden
Ethanol	UN 1170	Merk	Darmstadt
Ethidium bromide	2218.1	Carl Roth GmbH	Karlsruhe
FGF2 (hES cell medium)	13256	Invitrogen	Karlsruhe
FGF2 (neural differentiation)	233-FB	R&D systems	Wiesbaden
FCS	10270	Invitrogen	Karlsruhe
Fibronectin	33010	Invitrogen	Karlsruhe
Forskolin	F6886	Sigma-Aldrich	München
Gelatine	G-1890	Invitrogen	Karlsruhe
Glacial acetic acid	1.00063.10011	Merk	Darmstadt
Glucose	49150	Sigma-Aldrich	München
Glycerol	G8773	Sigma	München
β-Glycerol phosphate disodium salt pentahydrate	50020	Sigma-Aldrich	München
Glycine	G7126	Sigma-Aldrich	München
Goat serum donor herd	G6767	Sigma-Aldrich	München
Halt™ Protease Inhibitor Single-Use Cocktail	78430	Thermo Scientific/ Pierce Biotechnology	Rockford, USA
Horse serum	H1270	Sigma-Aldrich	München
Hydrocortisone	H0888	Sigma-Aldrich	München
Indomethacin	I7378	Sigma-Aldrich	München
Insulin	I6634	Sigma-Aldrich	München

Insulin-transferrin-selenium medium supplement	I3146	Sigma-Aldrich	München
Knockout-DMEM	10829	Invitrogen	Karlsruhe
Laminin	L2020	Sigma-Aldrich	München
L-Glutamine	25030	Invitrogen	Karslruhe
Linoleic Acid-Albumin from BSA	L9530	Sigma-Aldrich	München
Matrigel	E1270	BD Biosciences	Heidelberg
Methanol	4627.6	Carl Roth GmbH	Karlsruhe
Mowiol	475904	Merck	Darmstadt
N2-supplement	17502	Invitrogen	Karlsruhe
$NaHCO_3$	S5761	Sigma-Aldrich	München
Neuregulin-1	396-HB	R&D systems	Wiesbaden
Neurobasal™	21103	Invitrogen	Karlsruhe
NGF	256-GF	R&D systems	Wiesbaden
Non-essential amino acids	11140	Invitrogen	Karlsruhe
Oil red	O0625	Sigma-Aldrich	München
Paraformaldehyde	P6148	Sigma-Aldrich	München
Penicillin-Streptomycin	15140	Invitrogen	Karlsruhe
Poly-L-ornithin	P2533	Sigma-Aldrich	München
Protein Assay Dye Reagent	500-0006	Bio-Rad	Hercules, USA
Sodium azide	S2002	Sigma-Aldrich	München
Sodium pyruvate	11360	Invitrogen	Karlsruhe
Serum replacement	10828	Invitrogen	Karlsruhe
SuperSignal West Femto Maximum Sensitivity Substrate	34095	Thermo Scientific/ Pierce Biotechnology	Rockford, USA
GoTaq® Flexi DNA Polymerase	M8305	Promega	Madison, USA
Transferrin	4452-01	Millipore	Billerica, USA
Tris	1.08382.1000	Merck	Darmstadt
Triton-X100	T8787	Sigma-Aldrich	München
TrypLE™ Express	12604	Invitrogen	Karlsruhe
Trypan blue	15250	Invitrogen	Karlsruhe
Trypsin-EDTA (10x)	15400	Invitrogen	Karlsruhe

2.1.1 Cell lines

CD1 primary embryonic fibroblasts derived from the mouse strain CD1

H9.2 hES cell line, Haifa, Israel (Amit et al., 2000)

I3 hES cell line, Haifa, Israel (Amit et al., 2000)

2.1.2 Cell culture media

Mouse embryonic fibroblast (MEF) medium

90%	DMEM high glucose
10%	FCS, heat inactivated
2 mM	L-glutamine
1 mM	Sodium pyruvate
0.1 mM	Non-essential amino acids

MEF freezing medium

70%	DMEM high glucose
20%	FCS, heat inactivated
10%	DMSO

Human embryonic stem (hES) cell medium

80%	Knockout-DMEM
20%	Serum replacement
1 mM	L-glutamine
0.1 mM	Non-essential amino acids
0.1 mM	β-Mercaptoethanol
4 ng/mL	FGF2

Embryoid body (EB) medium

80%	Knockout-DMEM
20%	Serum replacement
1 mM	L-glutamine
0.1 mM	Non-essential amino acids

N2 medium

99%	DMEM/F12 1:1
1%	N2 supplement
1.6 g/L	D(+)-Glucose
20 μg/mL	Insulin
0.1 mg/mL	Transferrin

Neural differentiation medium

50%	N2 medium
49%	Neurobasal medium
1%	B27 supplement
100 ng/mL	dcAMP

Chondrocyte medium

MEF medium

10 μM	Forskolin
10 ng/mL	FGF2
100 μM	Ascorbic acid

Osteocyte medium (Fang et al., 2005)

90%	DMEM/F12 1:1
10%	FCS
1x	Insulin-transferrin-selenium medium supplement
1mg/mL	Linoleic acid BSA
0.1 μmol/L	Dexamethasone
0.05 mmol/L	L-ascorbic acid-2-phosphate
10 mmol/L	β-glycerophosphate

Adipocyte medium (Fang et al., 2005)

90%	DMEM high Glucose
10%	Horse serum
1x	Insulin-transferrin-selenium medium supplement
1 mg/mL	Linoleic acid BSA
1 μM/L	Hydrocortisone
0.5 mM/L	Isobutylmethylxanthine
60 μM/L	Indomethacin

2.1.3 Coating materials

Poly-L-ornithine (PO)
0.015 mg/mL in H_2O
Dishes were incubated over night and washed twice with PBS before further treated.

Fibronectin (Fn)
2 µg/mL in PBS
Applied on PO-coated dishes.

Laminin (Ln)
2 µg/mL in PBS
Applied on PO-coated dishes.

2.1.4 Buffers, solutions and gels for immunological detection methods

Mounting medium (Mowiol)

6 mL	H_2O
4.8 mL	Glycerol
2.4 g	Mowiol

→ stirred overnight, followed by addition of

12 mL	0.2 M Tris pH 8.5

→ incubated at 50°C till solved, followed by addition of

45 mg	DABCO

→ cleared from solid matter by centrifugation for 15 min at 5000 rpm.

4% Paraformaldehyde (PFA, 500 mL)

20 g	PFA
450 mL	PBS
3-4	NaOH pellets

→ stirred under the fume hood till dissolved
→ pH adjustment to 7.4
→ filled up to 500 mL

4 x Tris/SDS buffer pH 8.8

1.5M	Tris-Cl, pH 8.8
0.4%	SDS

4 x Tris/SDS buffer pH 6.8

0.5M	Tris-Cl, pH 6.8
0.4%	SDS

SDS-PAGE stacking gel for 5 mL

2.85 mL	H_2O
0.83 mL	30%/0.8% acrylamide/bis-acrylamide
1.25 mL	4x Tris/SDS buffer, pH 6.8
0.075 mL	10% APS
0.0015 mL	TEMED

SDS-PAGE separating gel (10%) for 10 mL

4.1 mL	H_2O
3.33 mL	30%/0.8% acrylamide/bis-acrylamide
2.5 mL	4x Tris/SDS buffer, pH 8.8
0.075 mL	10% APS
0.0015 mL	TEMED

Immunoblot (wet) transfer buffer

25 mM	Tris
192 mM	Glycine
20%	Methanol

10x SDS-PAGE electrophoresis buffer

250 mM	Tris
1.92 M	Glycine
1%	SDS

TBS-T

50 mM	Tris-Cl, pH 7.4
150mM	NaCl
0.1%	Tween 20

5x SDS loading buffer

250 mM	Tris-Cl, pH 6.8
10%	SDS
50%	Glycerol
0.02%	Bromophenol blue

→ 10% 2-Mercaptoethanol added before use

50xTAE buffer

2 M	Tris
50 mM	EDTA, pH 8.0
1 M	glacial acetic acid

2.2 Methods

2.2.1 Cell culture and cell separation

Cells were cultured in humid incubators at 37°C and 5% CO_2 at any time. As long as not differently stated, cell centrifugation was carried out at 1000 rpm for 5 min.

2.2.1.1 Expansion and inactivation of fibroblasts used in co-culture to maintain hES cells

To maintain the unique features of hES cells, they were cultured on a layer of murine embryonic fibroblasts (MEFs), also called feeder cells, which provide nutritional and cellular support to the pluripotent cells. Prior to co-cultivation, MEFs had to be expanded and irradiated in order to mitotically inactivate them. Fibroblasts were isolated from CD1 mouse embryos (E13.5-E14.5), mycoplasma tested, and cryopreserved for storage. For expansion, fibroblasts were thawed in a 37°C water bath. The cell suspension was transferred to 10 mL of MEF medium. The cryovial was rinsed with 1 mL of medium. After centrifugation the cell pellet was resuspended and cells were plated on three 15 cm dishes in a volume of 20 mL MEF medium each and transferred to the incubator. As soon as the cells were grown to confluency and showed a compact morphology (after 4-5 days), the dishes were washed with 10 mL of PBS. Afterwards 5 mL of Trypsin-EDTA was added to each dish, followed by a short incubation time at 37°C until the cells started to detach from the dish when tapped (app. 3 min). The Trypsin-EDTA solution was inactivated by adding 5 mL of 10% FCS/DMEM. The cell sus-

pension was transferred to a 50 mL tube, and the dishes were rinsed with 10% FCS/DMEM. After centrifugation the cell pellet was resuspended and cells were replated on new 15 cm dishes at a ratio of 1:3. The fibroblasts were cultivated until passage 3 before they were prepared for irradiation. For that purpose, cells were trypsinized and collected as previously described, resuspended in 30 mL of MEF medium and transferred into a 175 cm^2 cell culture flask. The cells were irradiated using the RS 2000 X-Ray biological irradiator (Rad Source). Fibroblasts were irradiated with a single-dose of 15 Gy. Following irradiation the cell suspension was transferred to a 50 mL tube, and the flask was rinsed with 5 mL MEF medium. After centrifugation cells were resuspended in MEF medium and the total cell number was determined. For this purpose 10 µL of cell suspension were mixed 1:1 with trypan blue, in order to exclude dead and therefore blue stained cells from the count. Cells were counted in a Fuchs-Rosenthal counting chamber. The cell number was calculated as follows:

Average cell count per square x 5 x 2 x 10^4 = cells/mL

→ *5 squares resemble 1 µL*

→ *2 is the dilution factor caused by dilution with trypan blue*

According to the determined cell number, cells were diluted and frozen in MEF freezing medium at a final concentration of 2.4 x 10^6 cells/mL. The cryovials were embedded in Styrofoam boxes and stored at -80°C for 1-2 days before transferring them to liquid nitrogen for long-term storage.

2.2.1.2 Cultivation of hES cells

One day prior to thawing of hES cells, irradiated MEFs were thawed in MEF medium at a density of 1.2 x 10^6 cells/mL per 6-well dish, which were pre-coated with 0,1% Gelatine (solved in H_2O) for 20 min. hES cells were thawed in a 37°C water bath. The cell suspension was transferred to 5 mL of hES cell medium and the cryovial was rinsed with 1 mL of medium before the cell suspension was centrifuged at 800 rpm for 3 min. Cells were frozen at a density of two wells per cryovial and were therefore also seeded on two wells of a MEF 6-well dish in 2 mL hES cell medium per well. The medium was changed every day. Every 4-5 days, when the hES cell colonies exceeded in size, cells were splitted on new feeder cells at a ratio of 1:2 – 1:5, depending on density of colonies. hES cell colonies were enzymatically detached by incubation with 1 mL/well collagenase (1 mg/mL) for 1 hour. Using this method,

the hES cell colonies detach from the feeder layer, while the feeder cells largely remain on the culture dish. 1 mL of hES cell medium was used to carefully rinse the colonies from the well. The cell suspension was centrifuged at 800 rpm for 3 min. Afterwards the cell pellet was gently resuspended in 1 mL of hES cell medium using the tip of a 1000 µL pipette to disassociate the colonies. This is a crucial step of the protocol, as the colonies differentiate when they are too large and do not re-plate when they are too small.

For feeder-free cultivation of hES cells, as it was done prior to RNA isolation, hES cells were splitted as described above and re-plated feeder-free on matrigel-coated dishes in fibroblast conditioned medium supplemented with 4 ng/mL FGF2. Conditioned medium was prepared beforehand by cultivation of fibroblasts in hES cell medium, which was preserved with the daily medium change. hES cells were cultivated 4-5 days with a daily medium change before they were harvested for RNA isolation.

2.2.1.3 Establishment of the neural crest delamination model

hES cells were forced into spontaneous differentiation by aggregation to free floating EBs. For this purpose, cells were enzymatically treated as described above, but here the disassociation of the colonies was avoided. After centrifugation at 800 rpm for 3 min, colonies were resuspended in EB medium and seeded on 10 cm cell culture dishes. One 6-well plate yielded one 10 cm dish. EBs were cultivated in 8 mL of EB medium per dish. The next day the medium containing the free-floating aggregates was collected in a tube, aggregates were allowed to settle by gravity, and the supernatant was discarded and replenished with fresh EB medium. Aggregates were transferred on 10 cm Petri dishes, which prevent attachment of aggregates. The first day of pre-cultivation on cell culture dishes will remove remaining fibroblasts from the culture, which were previously inadvertently detached by collagenase treatment. The EB medium was replenished every other day. After 5 days of culture, EBs were plated on PO/Fn-coated cell culture dishes. One EB containing Petri dish was plated on two 10 cm cell culture dishes. The next day, when EBs attached to the dish, medium was changed to N2 medium containing 20 ng/mL FGF2 and 2.5 µg/mL Fn. Medium was replenished every other day. Cell cultures were processed for analysis or neural crest cell isolation after 7-9 days of cultivation in N2 medium.

2.2.1.4 Isolation of neural crest cells by FACS

One approach to isolate the p75NTR-positive cell population from the heterogenous cultures of plated EBs is immuno-based FACSorting. Therefore cells were detached with TrypLE™ Express, which is less harsh than Trypsin-EDTA, centrifuged and exposed to blocking buffer (Cytocon + 0.1% BSA) for 15 minutes. Cells were centrifuged and subsequently exposed to anti-p75NTR (DAKO) diluted 1:500 in blocking buffer for 15 minutes. The tube was filled with 10 mL PBS, centrifuged and exposed to the secondary antibody Cy5 (Dianova) diluted 1:500 in blocking buffer for 15 minutes. After one washing step with PBS the cells were centrifuged and subsequently diluted in Cytocon buffer+0.02% DNAse to gain a cell density of approximately $5x10^6$/mL. Additionally an unstained control was prepared, as well a secondary antibody control. Just before sorting the cells were filtered through a 40 µm nylon mesh in a 12x75 mm round bottom tube. 0.2 mg/mL of propidium iodide was added to stain for dead cells. The cell sorting was done in cooperation with the Flowcytometry Core Facility of the Institute of Molecular Medicine and Experimental Immunology, University of Bonn. Sorting was performed using the FACS Vantage SE with FACSDiVa option (BD Biosciences). Sorted cells were replated on PO/Fn/Ln-coated cell culture dishes in N2 medium containing 20 ng/mL FGF, 20 ng/mL EGF, 0.1% B27, 100 U Penicillin and 100 µg Streptomycin.

2.2.1.5 Isolation of neural crest cells by manual picking

Crescent-shaped aggregates were identified and picked using a stereomicroscope (STEMI 2000C, Carl Zeiss) in the sterile environment of a horizontal lamina flow hood. Aggregates were encircled using a sterile cannula and gathered with a pipette tip. The free-floating aggregates were transferred to a PO/Fn-coated cell culture dish containing N2 medium supplemented with 20 ng/mL FGF, 20 ng/mL EGF and 0.1% B27 and cultivated for 24 hours. The replated aggregates, as well as the cells migrating thereof, were detached by treatment with TrypLE™ Express, gently trituated with a glass pipette and replated as monolayer on PO/Fn-coated cell culture dishes. Cells were passaged using TrypLE™ Express every 3-4 days in a 1:3 ratio.

2.2.1.6 Differentiation of manually isolated neural crest cells

For differentiation, manually isolated neural crest cells not older than passage 3 were used.

Peripheral neurons

For neuronal differentiation cells were plated on PO/Fn/Ln-coated dishes and cultivated in neural differentiation medium supplemented with 20 ng/mL nerve growth factor (NGF), 10 ng/mL brain-derived neutrophic factor (BDNF) and 100 μM ascorbic acid. Cells were fixed or harvested for RNA isolation after three weeks of differentiation.

Schwann cells

For differentiation towards Schwann cells, cells were plated on PO/Ln/Fn-coated dishes and cultivated in N2 medium containing 1% B27, 10 ng/mL FGF2, 5 μM Forskolin and 20 ng/mL neuregulin-1 (NRG-1). After 2 weeks in this Schwann cell promoting proliferation medium, FGF2 was withdrawn to induce terminal differentiation. Cells were fixed or harvested for RNA isolation after additional two weeks of terminal differentiation.

Mesenchymal cell types

Cells were differentiated into smooth muscle, chondrocytes, osteoblasts and adipocytes. For all differentiation paradigms, cells were cultivated on Matrigel-coated dishes. Cells were cultivated either in mesenchymal medium, chondrocyte medium, adipocyte medium or osteoblast medium for at least 3 weeks prior to fixation or processing for RNA isolation.

2.2.2 Electrophysiological recordings

All measurements were carried out in collaboration with Jaideep Kesavan. Neural crest-derived neurons differentiated for 6-8 weeks *in vitro* were selected for experiments. Whole cell current-clamp and voltage-clamp recording was carried out with Axopatch- 200B amplifier (Molecular Devices, USA) that was interfaced by an A/D-converter (Digidata 1440, Molecular Devices, USA) to a PC running PClamp software (Version 10, Molecular Devices). Pipette electrodes (GB150F-8P, Science products, Germany) were fabricated using a vertical puller (Narishige PC-10, Japan) and fire-polished (final tip resistances 2–4 MΩ). All recordings were performed at room temperature in a bath solution containing (in mM): 140 NaCl, 5 KCl, 2 $CaCl_2$, 0.8 $MgCl_2$, 10 Hepes and 10 glucose (pH 7.2; osmolality 310–320 mOsm). For most recordings of membrane potential or current, the patch pipette contained the following

(in mM): 120 potassium gluconate ($C_6H_{11}O_7K$), 20 KCl, 10 NaCl, 10 EGTA, 1 $CaCl_2$, 4 Mg ATP, and 0.4 Na GTP, 10 Hepes and 0.2% biocytin (pH 7.2, osmolality 280–290 mOsm). For some voltage-clamp recording, another pipette filling solution was used (in mM): 120 potassium fluoride, 20 KCl, 10 NaCl, 10 EGTA, 1 $CaCl_2$, 4 Mg ATP, and 0.4 Na GTP, 10 Hepes and 0.2% biocytin (pH 7.2, osmolality 280–290 mOsm). After measurements, cells were fixed in 4% PFA and prepared for immunofluorescence analysis. Biocytin-filled neurons were identified via application of Texas Red Avidin D. For details on staining procedures see 2.2.4.

2.2.3 Time-lapse imaging

In order to visualize the dynamic processes of the developmental events, a plated EB and an isolated crescent-shaped delaminate were monitored for several hours using time-lapse imaging. Time-lapse imaging was conducted using the inverse microscope Axiovert 200M (Carl Zeiss). The climate in the incubation chamber was adjusted to 37°C and 5% CO_2. The Openlab™ software from Improvision® was programmed to issue a command to the camera (Axiocam MRM, Carl Zeiss) every five minutes. In this way the objects were monitored for 72 hours. The resulting pictures were merged to time-lapse movies using Quicktime™ 7.6.4. Subsequently to the recording of pictures, cells were fixed in 4% PFA and prepared for immunofluorescence analysis. For details on staining procedures see 2.2.4.

2.2.4 Immunocytochemical analysis

Cells were fixed with 4% PFA for 10 minutes. Afterwards cells were washed three times with PBS and subsequently incubated in blocking solution (5% NGS in PBS) for 15 minutes, followed by incubation with primary antibody for at least 2 hours (details are given in Table 4, diluted in blocking solution). Cells were then washed three times with PBS and incubated with the appropriate secondary antibody for 45 minutes (details are given in Table 5, diluted in PBS). Cell nuclei were counter-stained applying DAPI staining solution (details are given Table 5, diluted in H_2O) for 1 minute. After washing with PBS cells were covered using Moviol and a cover slip for microscopic analysis.

Tab. 4: List of primary antibodies used for immunofluorescence analysis

Antibody	Dilution	Cat. No.	Manufacturer	Registered Office
Mouse anti-AP2α	1:10	5E4 Supernatant	Developmental Studies Hybridoma Bank	Iowa, USA
Mouse anti-Brn3a	1:50	MAB1585	Millipore	Billerica, USA
Mouse anti-HNK1	1:20	Kind gift from B. Schmitz		
Mouse anti-p75NTR (p75)	1:100	M3507	DAKO	Hamburg
Mouse anti-PAX3	1:300	Pax3 Concentrate	Developmental Studies Hybridoma Bank	Iowa, USA
Mouse anti-PAX7	1:300	Pax7 Concentrate	Developmental Studies Hybridoma Bank	Iowa, USA
Mouse anti-SHH	1:25	5E1	Developmental Studies Hybridoma Bank	Iowa, USA
Mouse anti-SMA	1:125	IS611	DAKO	Hamburg
Mouse anti-SOX*E*	1:50	Kind gift of M. Wegner (Schmidt et al., 2003)		
Mouse anti-TH	1:1,000	T1299	Sigma-Aldrich	München
Rabbit anti-GFAP	1:1,000	IS524	DAKO	Hamburg
Rabbit anti-L1CAM	1:300	Kind gift from M. Schachner		
Rabbit anti-N-cadherin	1:200	BTA7	R&D systems	Wiesbaden
Rabbit anti-Peripherin	1:300	AB1530	Millipore	Billerica, USA

Tab. 5: List of secondary antibodies and fluorochromes used for immunofluorescence analysis

Secondary antibody/Fluorochrome	Final concentration	Cat. No.	Manufacturer	Registered Office
Alexa Fluor® 555 goat anti-mouse IgG (H+L)	2 µg/mL	A21424	Invitrogen	Karlsruhe
Alexa Fluor® 488 goat anti-rabbit IgG (H+L)	2 µg/mL	A11008	Invitrogen	Karlsruhe
DAPI staining solution	2 µg/mL	D9542	Sigma-Aldrich	München
Texas Red® Avidin D	10 µg/mL	A2006	Vector Laboratories	Burlingame, USA

2.2.5 Histological stains

For the identification of adipocytes, chondrocytes, and osteoblasts histological staining methods were used. Oil red staining was done by exposing fixed cells to Oil red O solution (0.5% Oil red O in 60% Isopropanol/dH_2O) for 15 minutes. Alizarin red staining solution (2% alizarin red in dH_2O, pH4.1) was applied for 5 minutes and alcian blue (1% alcian blue in 0.5% acetic acid/dH_2O, pH3.1) for 5 minutes. See Table 3 for information on suppliers of dyes. Before and after application of the staining solutions, cells were washed with dH_2O.

2.2.6 Molecular analysis

RNA was extracted from cell pellets using RNeasy® Mini Kit including a DNase digestion step with RNase-Free DNase Set (both Quiagen) according to the instructions given by the manufacturer. RNA quality and quantity was measured using the UV-Vis spectrophotometer NanoDrop ND-1000 (PEQLAB).

2.2.6.1 Reverse transcriptase- polymerase chain reaction

For reverse transcriptase-polymerase chain reaction (RT-PCR) transcription to cDNA was performed using iScript™ cDNA Synthesis Kit (Bio-Rad Laboratories). The instructions provided by the manufacturers were obeyed. According to the obtained quantity, the cDNA was diluted with nuclease-free H_2O to yield a concentration of 100 ng/µL. PCR was conducted by using GoTaq® green flexi (Promega). Sequences, product sizes and annealing temperatures of used primer pairs are given in Table 6. Primer sequences were either obtained from the publications cited or designed from sequences available at the NCBI GenBank database by using the primer Blast. Primers were synthesized by Invitrogen. PCR reactions were prepared as described in Table 7. The GoTaq polymerase was added just before starting the PCR reaction. PCR parameters used for amplification are shown in Table 8. For each primer pair a negative control (without template) and an appropriate positive control (Table 9) were conducted. PCR products were analyzed for their sizes using agarose gel electrophoresis.

Tab. 6: Details of used primer pairs

Primer	Sequence	Product size [bp]	Annealing Temperature [°C]
ACAN (Aggrecan)	s- CACTGTTACCGCCACTTCCC as- ACCAGCGGAAGTCCCCTTCG (Lee et al., 2007)	184	56
ACTA2 (SMAα)	s- CTGTTTTCCCATCCATTGTGG as- GCAACACGAAGCTCATTGTAG (Lee et al., 2007)	205	54
ACTG2 (SMAγ)	s- ACCCTCGGTGCTCCAGTCCC as-CACGGCCAGCCAAGTCCAGG	596	65
ASCL1	s- CGGCCAACAAGAAGATGAGT as- TGGAGTAGTTGGGGGAGATG	150	60
B3GAT1 (HNK1)	s- GCAAGAAGGGCTTCACTGAC as- GCCCCCAGAATAGAAAGGAG (Jiang et al., 2009)	165	56
CNP	s- GGCAGAGGAGTACGCTCAAC as- GTTGCTGCTCGCTTAACTCC	128	60
COL2A1 (Collagen type II α 1)	s- ATGATTCGCCTCGGGGCTCC as- CATTACTGGGAACTGGGCGC (Lee et al., 2007)	390	58
EGR2 (KROX20)	s- TTGACCAGATGAACGGAGTG as- CAGAGACGGGAGCAAAGC	108	60
FOXG1	s- CCCTCCCATTTCTGTACGTTT as- CTGGCGGCTCTTAGAGAT	204	60
GAPDH	s- ACGACCCCTTCATTGACCTCAACT as- ATATTTCTCGTGGTTCACACCCAT	320	60
GBX2	s- CTCGCTGCTCGCCTTCTC as- GCCAGTCAGATTGTCATCCG	169	60
HAND2	s- AGAAGACCGACGTGAAAGAGGAGA as-ACACGGGAGTGTCCTCTTCGTATT (Pomp et al., 2005b)	400	60
HOXA2	s- TTCAGCAAAATGCCCTCTCT as- TAGGCCAGCTCCACAGTTCT	176	60
HOXB2	s- TTTAGCCGTTCGCTTAGAGG as- CGGATAGCTGGAGACAGGAG	173	60

L1CAM	s- GAGAGTGACAACGAGGAG as- GCCAATGAACGAACCATC	144	60
MNX1 *(HB9)*	s- GGTGACCATGAGCGAGGTG as- CCTAAGATGCCCGACTTCAAC	174	60
NGFR *(p75NTR)*	s- CCCCCTTCTCCCACACTGCTA as- GAACCCCAAACCTGACTCCAT (Pomp et al., 2005a)	591	60
NKX2-2	s- TCTACGACAGCAGCGACAAC as- TTGTCATTGTCCGGTGACTC	154	60
NTRK1 *(TrkA)*	s- CCCTGCTCATGGTCTTTGA as- GGTGCACAAAATGCAGACC	195	60
NTRK2 *(TrkB)*	s- AAGGTGTTGGCCCAGCCTCCGTTAT as-GTCAGTTCCGTGGGCGGGTT	559	60
NTRK3 *(TrkC)*	s- AGCACTGCATCGAGTTTGTG as- AGTGGGTTTTTGGCAATGAG (Jiang et al., 2009)	199	60
OTX2	s- TGCAGGGGTTCTTCTGTGAT as- AGGGTCAGAGCAATTGACCA	234	60
PAX3	s- GAACACGTTCGACAAAAGCA as- GCACACAAGCAAATGGAATG (Koch et al., 2009)	160	60
PAX7	s- AAGATTCTTTGCCGCTACCA as- CACAGTGCTTCGGTCACAGT (Koch et al., 2009)	192	60
PHOX2B	s- AGTCCTGTATGGCTGGGATG as- GTACGGACTGCTCTGGTGGT	191	60
POU4F1 *(BRN3A)*	s- ACTCAGCCAGAGCACCATCT as- CAGAGAATGGGTGGAGGAAA	508	60
PRPH *(Peripherin)*	s- TTGAGTTCCTCAAGAAGCTGCACG as- CACCTCAGGCACAGTCGTCTTTAT (Pomp et al., 2005a)	605	60
SHH	s-GCTGATGACTCAGAGGTGTAAGGACAA as-TCGCGGTCAGACGTGGTGAT	174	62
SNAI1	s- ACCCCACATCCTTCTCACTG as- TACAAAAACCCACGCAGACA	217	60

SNAI2	s- GCGATGCCCAGTCTAGAAAA as- GCAGTGAGGGCAAGAAAAAG	203	60
SOX10	s- AGCCCAGGTGAAGACAGAGA as- AGGAGAAGGCCGAGTAGAGG	201	60
TFAP2A (AP2α)	s- TCCCTGTCCAAGTCCAACAGCAAT as- AAATTCGGTTTCGCACACGTACCC (Pomp et al., 2005a)	396	60
TH	s- CAGTTCTCGCAGGACATTG as- CGTCTGGTCTTGGTAGGG	243	60

Tab. 7: PCR reaction mix

Ingredient	**Final concentration**	**Volume [µL] in 25 µL reaction volume**
cDNA	100 ng	1
GoTaq® PCR buffer (10x)	1x	2.5
$MgCl_2$ (50 mM)	1.5 mM	0.75
dNTPs (dGTP, dATP, dTTP, dCTP; 100 mM)	0.4 mM	0.1
Primer mix (forward and reverse, each 10 µM)	0.4 µM	2
GoTaq® DNA polymerase	1 unit	0.1
H_2O		18.55

Tab. 8: PCR reaction steps

Process	**Temperature [C°]**	**Time [min]**
Initial denaturation	94	5
Denaturation	94	1
Annealing	Depended on primer (Tab.8)	0.5
Elongation	72	2
Final elongation	72	10

Tab. 9: List of RNA used as template for positive controls for RT-PCRs

RNA	Cat. No.	Manufacturer	Registered Office
Human adult brain total RNA	540005	Agilent Technologies	Santa Clara, USA
Human fetal brain total RNA	540157	Agilent Technologies	Santa Clara, USA
Human fetal colon total RNA	540161	Agilent Technologies	Santa Clara, USA
Human whole bone tissue total RNA	pM007-r	DV Biologics	Costa Mesa, USA
Human Schwannoma biopsy	Kind gift from T. Pietsch		

2.2.6.2 Agarose gel electrophoresis

In order to identify the fragment sizes of the obtained RT-PCR products, agarose gel electrophoresis was performed. This method is based on the characteristic of DNA to move from the negative to the positive pole in an electric current due to the negative charge of its sugar-phosphate backbone. For this purpose an agarose solution containing 1.5% agarose in 1xTAE buffer was prepared. Solubility of agarose was achieved by heating the solution. After cooling ethidium bromide was added to the agarose solution at a concentration of 1µg/mL. Ethidium bromide intercalates between the double strands of DNA and changes its absorption spectra. Therefore it can be visualized with UV light, which exhibits a wavelength of 254 nm. The agarose solution was poured into the gel chamber and a comb was added. After solidifying of the agarose gel, 15µL of PCR product was added into each slot. The GoTaq® green flexi buffer already contains an agarose gel loading buffer. Additionally a DNA ladder was applied on each gel, which served as migration standard. An electric current of 80V was applied. After 20-30 minutes the gel was analyzed using the Gel doc system (Bio-rad Laboratories).

2.2.6.3 Illumina analysis

The gene expression analysis was performed in cooperation with Dr. Michael Alexander from the Institute of Human Genetics, University of Bonn. hES cell-derived neural crest cells at passage 1 were compared to long term propagated neural stem cells derived from hES cells (lt-hESNSCs; Koch et al., 2009). Isolated total RNA (see 4.2.4) of cells (lt-hESNSCs and isolated delaminates) was checked for degradation via gel electrophoresis in a BioAnalyzer 2100 (Agilent Technologies, Waldbronn, Germany) with RNA 6000 nano lab chips following the instructions of the manufacturers' protocol. All used RNA samples showed intact 28S and

18S ribosomal RNA signals and a RNA integrity number (RIN) of >9.5. 100 ng of total RNA was reverse transcribed into cRNA and biotin-UTP labelled using the Illumina TotalPrep 96-RNA Amplification Kit (Ambion/Applied Biosystems, Darmstadt, Germany). Labelled cRNA was hybridized to Illumina human HT-12 Expression BeadChips v3 using standard protocols (Illumina, San Diego, USA). Duplicate analyses were performed for each sample. Fluorescence was detected with Illumina iScan (Illumina, San Diego, USA).

Human HT-12 microarrays interrogate for more than 99.99% of all known human genes (approx. 25,000 annotated RefSeq and UniGene genes) containing more than 48,000 probes. All expression profiles were extracted and average normalized using GenomeStudio software (Illumina, San Diego, USA).

2.2.7 Immunoblot analysis

Cells were either harvested on ice with a cell scraper (plated EBs) or manually isolated under the horizontal laminar flow bench (neural crest aggregates and neural tube-like structures) and subsequently lysed in RIPA (Radio Immuno Precipitation Assay) buffer supplemented with HALT protease inhibitor at 4°C for 30 min. After centrifugation of the lysates at 15.000 rpm at 4°C, the supernatant was collected and the protein concentration was measured via Bradford assay. For this purpose, a BSA standard series ranging from 0 to 12 µg was prepared. 4 µL of sample were diluted with 200 µL PBS. 50 µL of each standard and sample was applied in triplicate on a 96 well plate. Protein Assay Dye Reagent (Bio-rad Laboratories) was diluted 1:4 with PBS and 150 µL of the solution was added to each well. Following approx. 10 minutes of incubation, the plate was analyzed at 595 nm using an ELISA plate reader. According to their protein concentration, samples were aliquoted to gain a concentration of 50 µg and according to the obtained volume diluted with 5x SDS loading buffer Lämmli. Samples were either directly used for electrophoresis or stored at -20°C.

The gel chamber was assembled following manufacturers' instructions (Mini-PROTEAN® 3 Electrophoresis Cell, Bio-rad Laboratories). First, the separating gel was poured between the glass plates and covered with isopropanol. After polymerization (20-30 minutes), the isopropanol was removed and the stacking gel was poured on top of the separating gel. The comb was set in the stacking gel. After polymerization (20-30 minutes) the comb was removed, wells were washed once with ddH_2O and the gel was then placed into the electrophoresis

chamber. The chamber was filled with 1x running buffer and the samples were heated to 95°C for 5 minutes and thereafter centrifuged shortly before the samples were subjected to sodium dodecyl sulfate polyacrylamide gel electrophoresis (SDS-PAGE). 50 µg of total protein was loaded per lane of a SDS-PAGE. Additionally, 10 µL of marker containing different proteins of defined molecular weight was loaded on one lane. Subsequently, setting a constant voltage of 200 V started electrophoresis. The current amounted to 60-70 mA and declined to approx. 20 mA during the run. SDS-PAGE ran app. 45 minutes.

Proteins were blotted onto Nitrocellulose membranes applying wet blot technique. For this purpose membrane (0.45 micron), filter papers (both Carl Roth GmBH), sponges and the gel were soaked in 1x transfer buffer. The blotting chamber (Mini Trans-Blot Transfer Cell, Bio-rad Laboratories) was assembled following manufacturer's instructions. Briefly, membrane and gel were applied on top of each other and embedded into 2 layers of filter paper and sponges on each side. The clip was transferred into the chamber, which was filled with cold 1x transfer buffer and supplied with a cooling unit. A constant voltage of 100 V was applied. The current inclines during the blotting procedure from approx. 250 mA to 350 mA. Blotting ran for 1 hour. Subsequently the membrane was dismantled and transferred to TBS-T before the staining procedure was continued. Blocking of the membrane with 5% milk powder in TBS-T was followed by incubation with primary antibodies according to Table 10 and corresponding secondary antibody as indicated in Table 11. Proteins were detected using Super Signal West Femto Substrate in a Chemidoc XRS system (Bio-rad Laboratories).

Tab. 10: List of primary antibodies used for immunoblotting

Primary antibody	Dilution	Cat. No.	Manufacturer	Registered Office
Mouse anti-E-cadherin	1:1000	ALX-804-201-C100	Enzo Life Sciences	Farmingdale, USA
Rabbit anti-N-cadherin	1:500	BTA7	R&D systems	Wiesbaden
Rabbit anti-Cadherin-7	1:200	sc-68422	Santa Cruz Biotechnology, INC.	Santa Cruz, USA
Goat anti-Cadherin-11	1:100	AF1790	R&D systems	Wiesbaden
Goat anti-Sox10	1:200	AF2864	R&D systems	Wiesbaden
Mouse anti-p75NTR (p75)-Biotin	1:200	130-091-883	Miltenyi Biotec	Bergisch Gladbach
Mouse anti-actin	1:2000	MAB1501	Millipore	Billerica, USA

Tab. 11: List of secondary antibodies used for immunoblotting

Secondary antibody	Dilution	Cat. No.	Manufacturer	Registered Office
HRP-conjugated anti-goat IgG	1:500	AP106P	Millipore	Billerica, USA
HRP-conjugated anti-mouse IgG	1:1000	7076	Cell Signaling Technology	Frankfurt
HRP-conjugated anti-rabbit IgG	1:500	7074	Cell Signaling Technology	Frankfurt
Streptavidin-HRP	1:1000	P0397	DAKO	Hamburg

3 Results

3.1 Formation of neural tube-like structures in plated embryoid bodies

A well-known phenomenon during neural differentiation of hES cells is the formation of neural rosettes, which have been well characterized in many publications, and are, due to their resemblance to the developing neural tube, often referred to as neural tube-like structures. They are one source of hES cell-derived neural stem cells. As *in vivo* neural crest cells delaminate from the developing neural tube, the first step of this thesis aimed at the closer investigation of hES cell-derived neural tube-like structures (Zhang et al., 2007).

For the differentiation paradigm hES cells were cultivated and proliferated on a fibroblast layer. The cells formed compact colonies with defined borders, a typical morphology of pluripotent stem cells colonies (Fig. 8A). Spontaneous differentiation of hES cells was induced by cultivation in non-adherent cell culture dishes. After 5 days a population of EBs was obtained, which exhibited distinct spherical shapes with clear borders (Fig. 8B). The EBs were readily plated on Fn-coated cell culture dishes. Following 3 days of cultivation of plated EBs in neural induction medium containing FGF2 and Fn, first neural rosettes formed in the centre of the plated EBs. The structures became more prominent over an additional time period of 5 days in culture and displayed typical epithelial morphology with radial arranged columnar cells (Fig. 8C). Those prominent structures are in the following termed neural tube like-structures. After 6-7 days in neural induction medium, crescent-shaped aggregates formed in the periphery of the plated EBs, which contained the neural tube-like structures in their centers (Fig. 8D).

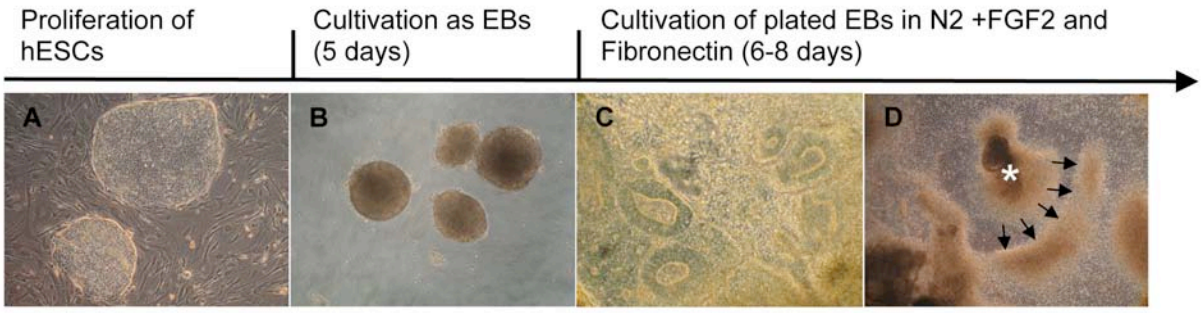

Figure 8: Outline of cell culture protocol. HES cells were maintained on fibroblast layer **(A)**. Withdrawal of fibroblasts and cultivation on uncoated Petri dishes led to formation of EBs **(B)**, which were cultivated for 5 days before plating on PO/Fn-coated cell culture dishes. Starting at day 3, neural rosette formation was observed in the center of plated EBs, which became more prominent during additional 5 days of culture and were termed neural tube like-structures **(C)**. Approx. day 8 after plating crescent-shaped aggregates became apparent in the periphery of the EBs, which contained the NTLS in their centers **(D,** asterisk marks the NTLS-containing centre of the EB**)**. NTLS: Neural tube-like structures.

3.2 Human embryonic stem cell-derived neural tube-like structures display a dorsal-ventral patterning

Neural crest cells delaminate and migrate from the dorsal part of the developing neural tube, where the neural folds meet and fuse to form the neural tube. The dorsal-ventral organization of the neural tube is accompanied by the expression of distinct transcription factors. Two important transcription factors that are expressed in the dorsal part of the neural tube are *PAX3* and *PAX7*. With the aim to investigate whether hES cell-derived neural tube-like structures express markers associated with the dorsal neural tube, 6-days-old neural tube-like structures were isolated by manual picking and processed in order to isolate RNA. RT-PCR showed that hES cell-derived neural tube-like structures strongly express the transcription factors *PAX3* and *PAX7* (Fig. 9A). Also, isolated neural tube-like structures expressed *SHH*. *In vivo*, SHH is secreted by the notochord and from the ventral part of the neural tube, the neural floor plate. These RT-PCR data show that markers associated with dorsal-ventral patterning of the neural tube can also be found in hES cell-derived neural tube-like structures.

Next, it should be assessed whether dorsal markers are expressed in certain regions of the hES cell-derived neural tube-like structures. Therefore, whole EB cultures were fixed at day 3 and day 6 after plating and exposed to specific antibodies. The analysis showed a difference between young neural rosettes (day 3) and mature neural rosettes (neural tube-like structures, from day 6). Young neural rosettes were found to diffusely express both neural plate border specifiers PAX3 and PAX7 in the whole structure (Fig. 9B+C). Neural tube-like structures on the other hand showed specific staining for PAX3 and PAX7 at the outer edges (Fig. 9D+E and magnifications). Also, the ventral marker SHH was found augmented in the lumen of some of the neural tube-like structures (Fig. 9F).

These staining patterns suggest that neural tube-like structures acquire a dorsal-ventral patterning with prolonged time in culture, expressing the dorsal markers PAX3 and PAX7 at their outer edges. This data indicates that these primitive *in vitro* structures indeed resemble the neural tube regarding their expression of dorsal markers. Therefore, when aiming at the differentiation of neural crest cells from hES cell cultures, these primitive neural tube-like structures are a promising source and were consequently further investigated in the next step of this thesis.

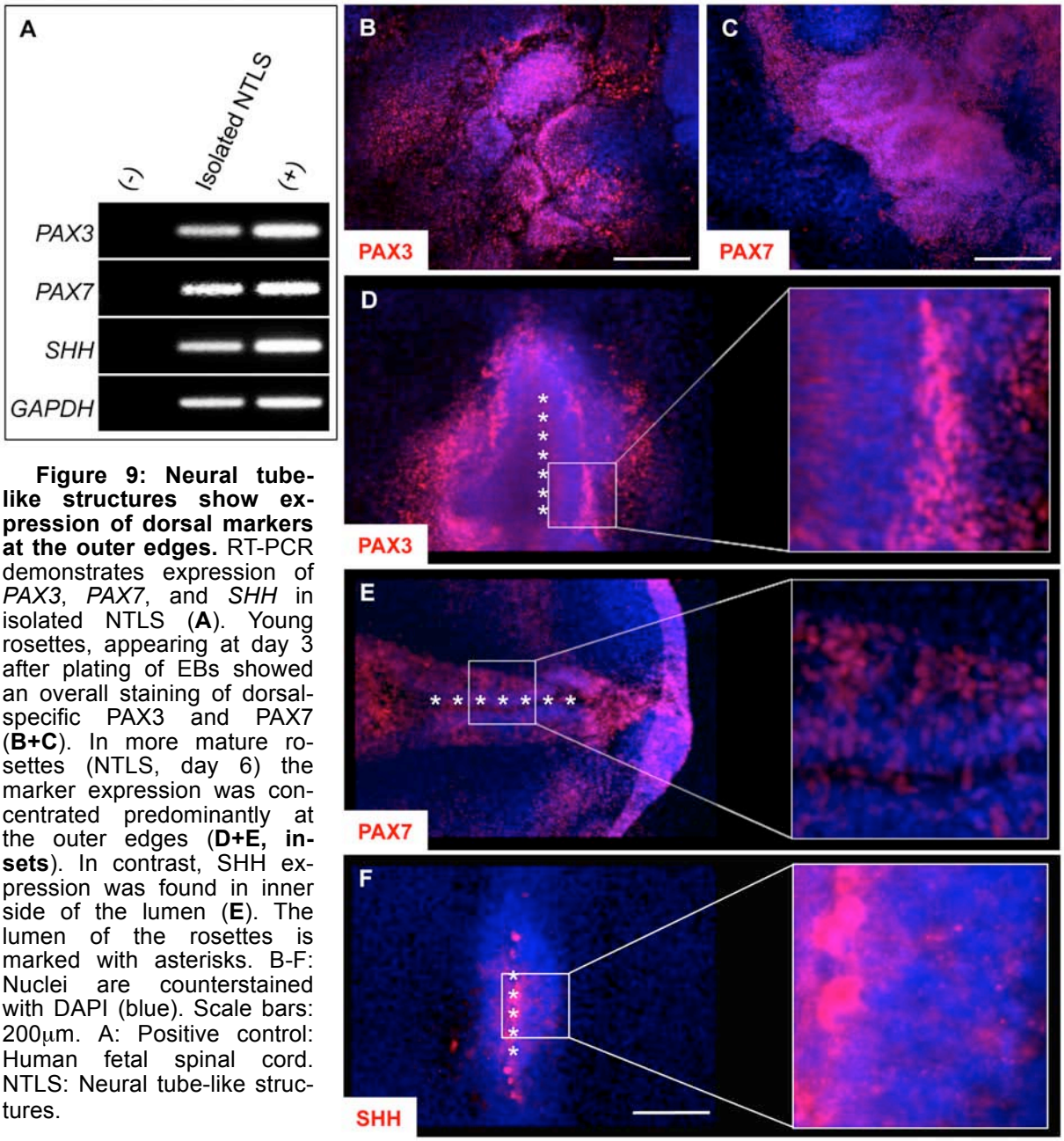

Figure 9: Neural tube-like structures show expression of dorsal markers at the outer edges. RT-PCR demonstrates expression of *PAX3*, *PAX7*, and *SHH* in isolated NTLS (**A**). Young rosettes, appearing at day 3 after plating of EBs showed an overall staining of dorsal-specific PAX3 and PAX7 (**B+C**). In more mature rosettes (NTLS, day 6) the marker expression was concentrated predominantly at the outer edges (**D+E, insets**). In contrast, SHH expression was found in inner side of the lumen (**E**). The lumen of the rosettes is marked with asterisks. B-F: Nuclei are counterstained with DAPI (blue). Scale bars: 200µm. A: Positive control: Human fetal spinal cord. NTLS: Neural tube-like structures.

3.3 Neural crest cells accumulate in distinct aggregates in the periphery of plated embryoid bodies

Taking into consideration the fact that neural crest cells migrate from the dorsal neural tube and with the knowledge that hES cell-derived neural tube-like structures express the dorsal markers PAX3 and PAX7, the question came up whether neural crest cells can be found in their periphery. During cultivation of plated EBs, it was observed that crescent-shaped aggregates formed in the periphery of plated EBs, which contained the neural tube-like structures in

their centers. Those crescent-shaped aggregates (in the following also referred to as delaminates) were even macroscopically detectable (Fig. 10A, arrows). Using the low magnification of a binocular microscope the self-organization of the plated EB becomes strikingly visible. While neural tube-like structures have formed in the centers of the plated EBs, crescent-shaped aggregates formed in their periphery (Fig. 10B, arrows). The aggregates formed reliably in a distance of 500-600 µm to the center of the plated EBs.

When examining the plated EB cultures for the expression of SOX*E*, TFAP2A, HNK-1 and p75NTR, it was found that those neural crest associated markers were increasingly expressed in the crescent-shaped aggregates. For the detection of SOX*E*, an antibody was used that recognizes SOX8, 9 and 10. SOX*E* transcription factors are important regulators of the neural crest. In the crescent-shaped aggregates strong expression of SOX*E* was detected (Fig. 10C+D). Another transcription factor associated with neural crest development is TFAP2A (also called AP2α). Expression of TFAP2A could also be detected in the delaminates (Fig. 10C). In addition, cells in the aggregates expressed the carbohydrate epitope HNK-1 (Fig. 10F) and the low affinity nerve growth factor p75NTR (Fig. 10G), proteins that are expressed on the surface of neural crest cells.

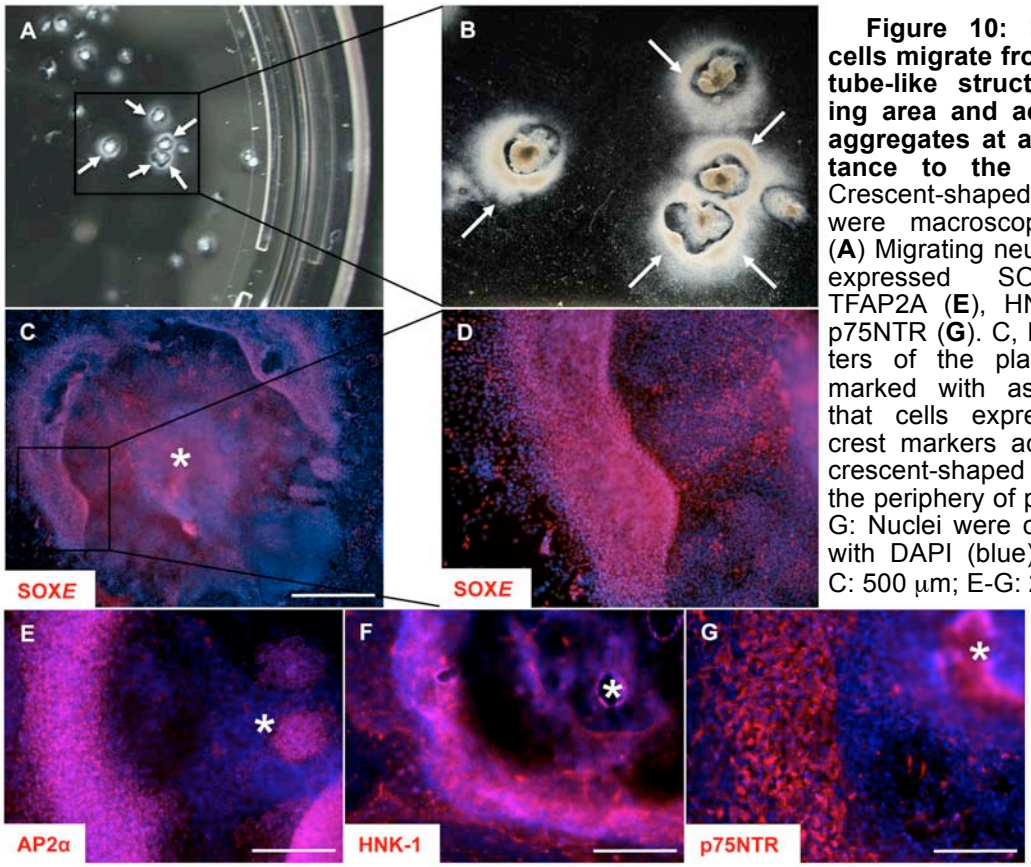

Figure 10: Neural crest cells migrate from the neural tube-like structure containing area and accumulate to aggregates at a distinct distance to the plated EBs. Crescent-shaped aggregates were macroscopically visible (**A**) Migrating neural crest cells expressed SOX*E* (**C+D**), TFAP2A (**E**), HNK-1 (**F**) and p75NTR (**G**). C, E-G: The centers of the plated EBs are marked with asterisks. Note that cells expressing neural crest markers accumulated in crescent-shaped aggregates in the periphery of plated EBs. C-G: Nuclei were counterstained with DAPI (blue). Scale bars: C: 500 µm; E-G: 200 µm.

To visualize the dynamic process of neural crest cells leaving the plated EB, time-lapse imaging of a plated EB was performed. The plated EB was monitored for 72 hours, subsequently fixed and stained for p75NTR (Fig. 11). The resulting video shows that initially after plating, cells with a flat, fibroblast-like morphology started to grow out of the EB. In subsequently performed immunostainings, those cells were found to be negative for p75NTR. Following the flat cells, elongated cells appear at the outer edges of the EB, which were identified by post-movie immunostaining as p75NTR-positive, leading to the conclusion that p75NTR-positive cells start to leave the EB around day 3 after plating. Six days after plating p75NTR-positive cells were found augmented in the crescent-shaped aggregates in the periphery of the plated EBs (Fig 10). The movie can be found in the appendix of this thesis, Fig. 11 shows the development of the plated EB in 10-hour-intervals.

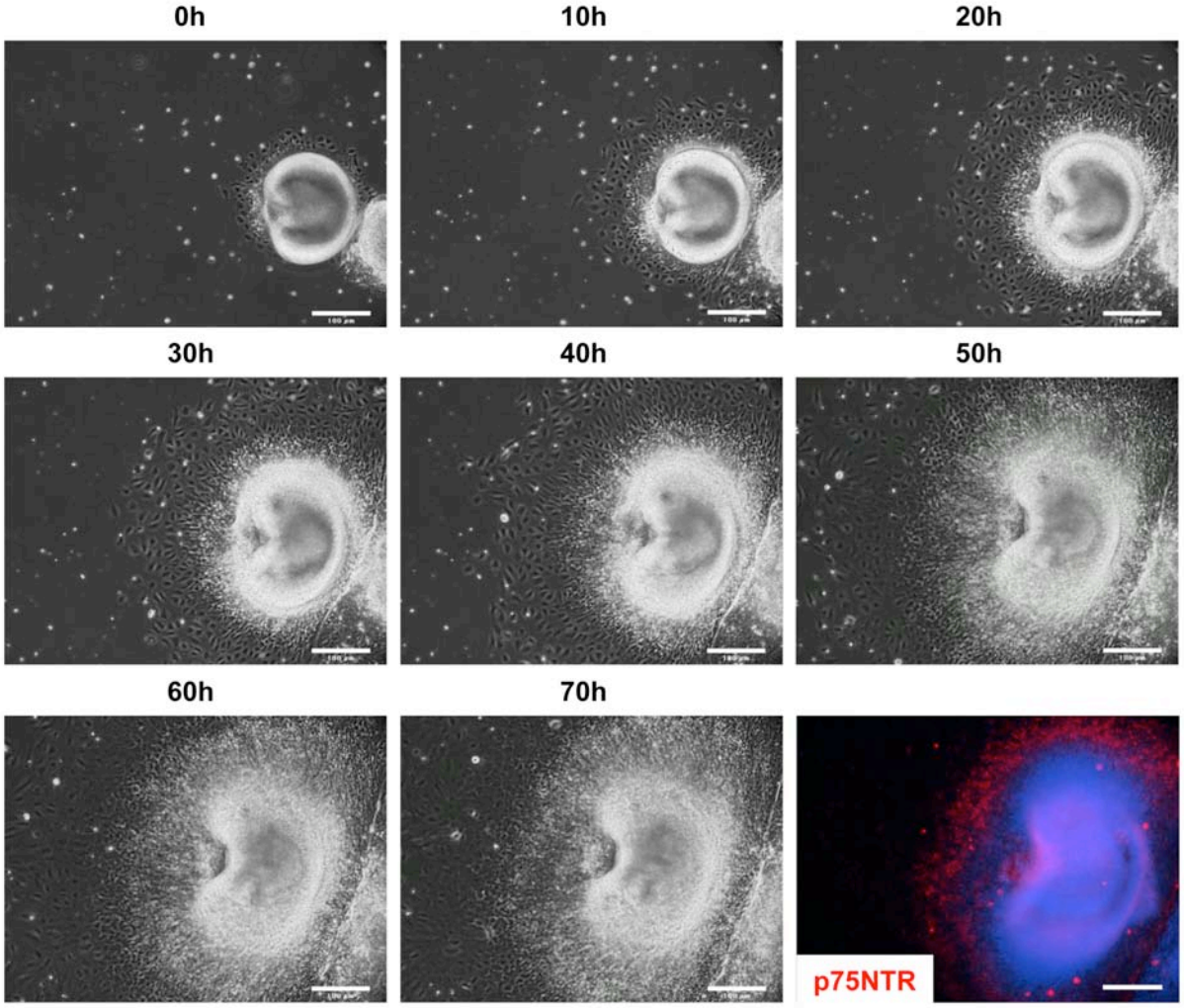

Figure 11: Plated EB monitored by time-lapse imaging for 72 hours. Associated illustrations to time-lapse video, the plated EB is shown in 10-hour intervals. The last figure shows the subsequent p75NTR staining of the fixed EB. Nuclei are counterstained with DAPI (blue). Scale bar: 100μm.

3.4 Crescent-shaped aggregates form in the periphery of isolated neural tube-like structures

In order to elucidate whether neural crest cells continue to migrate also from isolated and replated neural tube-like structures, hES cell-derived neural tube-like structures were isolated from 8-day-old plated EB cultures, showing typical self-organization (Fig. 12A), with neural tube-like structures in the center of the plated EB and the crescent-shaped aggregates containing of neural crest cells in the periphery. Neural tube-like structures were isolated using a sterile cannula, replated on PO/Fn/Ln-coated cell culture dishes and cultivated for 4 days in N2 medium supplemented with FGF2 and Fn. After this additional cultivation time, again neural crest cells migrated from the plated neural tube-like structures and formed aggregates in the periphery of the plated neural tube-like structures (Fig. 12B). Subsequent staining for p75NTR showed that those aggregates were positive for the neural crest marker p75NTR (Fig. 12C).

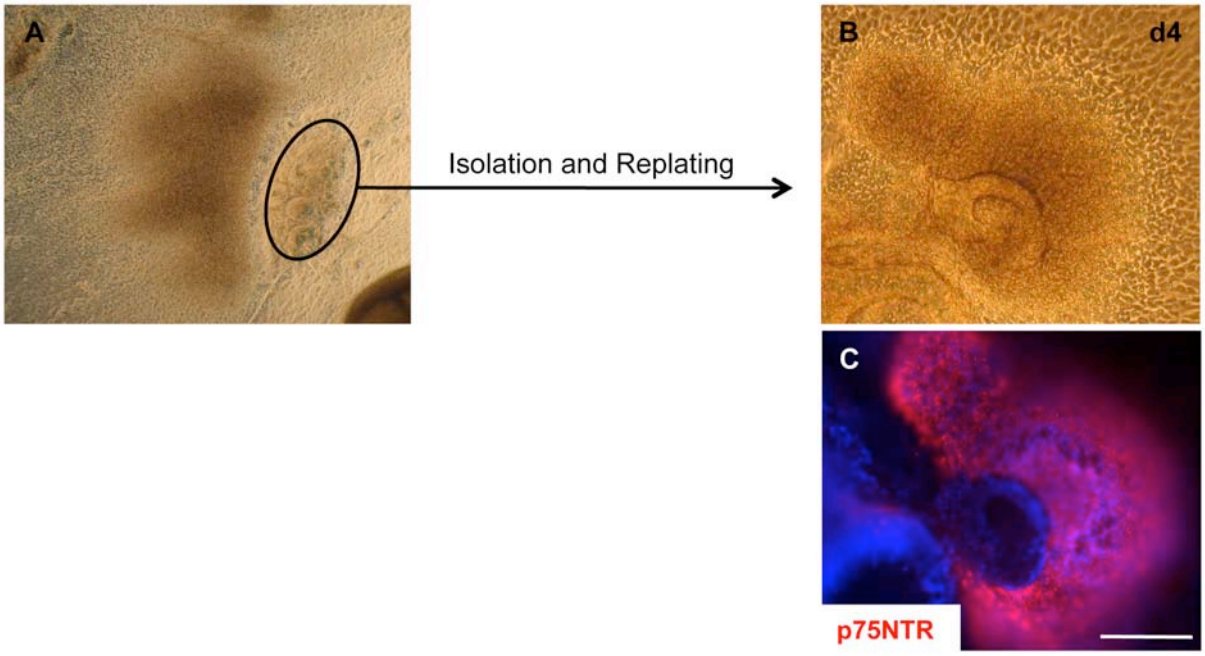

Figure 12: Isolated neural tube-like structures giving rise to p75NTR-positive cells. Neural tube-like structures were isolated from 8-days-old plated EB cultures (**A**), replated on PO/Fn/Ln-coated cell culture dishes and cultivated for 4 days in the presence of FGF2 and Fn. After 4 days of culture, crescent-shaped aggregates formed in the periphery of the isolated rosettes, which stained positive for p75NTR (**B**+**C**). C: Nuclei were counterstained with DAPI (blue). Scale bar: F: 100 μm.

3.5 Switching Cadherin expression patterns in human embryonic stem cell-derived neural crest cells mimic *in vivo* Cadherin distribution

Having identified neural crest cells in the periphery of hES cell-derived neural tube-like structures, it should be investigated whether this cell culture model can be exploited to study events of human neural crest development *in vitro*.

As neural crest cells leave the neural tube and start their migration they undergo an epithelial-to-mesenchymal transition (EMT; Duband et al., 1995). In doing so, they have to go through massive cellular changes. These changes are accompanied by alterations in cadherin expressions (Taneyhill, 2008). Cells in the neural plate express E-cadherin, which is switched to N-cadherin in the rising neural folds (Hatta et al., 1987; Thiery et al., 1984). N-cadherin aids the meeting folds to recognize themselves as tissue of the same kind and therefore facilitates their fusion. While the cells in the densely packed epithelial structure of the neural tube express N-cadherin, delaminating neural crest cells downregulate N-cadherin and express cadherin-7 and -11 instead. This type II cadherins prompt neural crest cells to gain a mesenchymal morphology, which they require to start their migration (Nakagawa and Takeichi, 1995; Nakagawa and Takeichi, 1998). As neural crest cell migration ceases and the cells cluster to form the ganglia, N-cadherin expression is upregulated again (Akitaya and Bronner-Fraser, 1992; Kasemeier-Kulesa et al., 2006). All this understanding of neural crest development comes from studies on several animal models, including mouse, frog and chicken, but so far EMT of neural crest cells has not been studied in primates. Here, it was investigated whether switches in cadherin expressions can be detected in developing neural crest cultures. Therefore different compartments of the whole plated EB culture were analyzed. The crescent-shaped delaminate and the neural tube-like structures were isolated by manual picking and compared to the whole plated EB culture at day 3 and 8 by immunoblot analysis (Fig. 13A). As a loading control beta-actin expression was assessed. E-cadherin expression was found in the whole plated EB culture at day 3 and 8, faintly in isolated neural tube-like structures and absent in the isolated crescent-shaped delaminate. N-cadherin was expressed at day 3 and 8 of the whole plated EB culture and persisted in the isolated neural tube-like structures, but was absent in the isolated delaminate. On the other hand, the isolated delaminate showed strong expression of cadherin-7 and -11, which was not expressed in neural tube-like structures and was detected to a lesser extend in the whole plated EB cultures. N-cadherin was also visual-

ized on different stages of the whole plated EB culture using immunocytochemistry. In 8-days-old plated EB cultures, SOX*E* expression was detected in cells in the periphery of the neural tube-like structures, leaving the neural tube-like structures with N-cadherin expression only (Fig. 13B). In spontaneously differentiating neurons, N-cadherin expression was strongly expressed in the neurites (Fig. 13C). This is explained by the observed upregulation of N-cadherin expression during dorsal root and sympathetic ganglia formation. N-cadherin causes neural crest cells to cease migration at ganglia sites by mediating adhesive cell-to-cell contacts (Akitaya and Bronner-Fraser, 1992; Kasemeier-Kulesa et al., 2006).

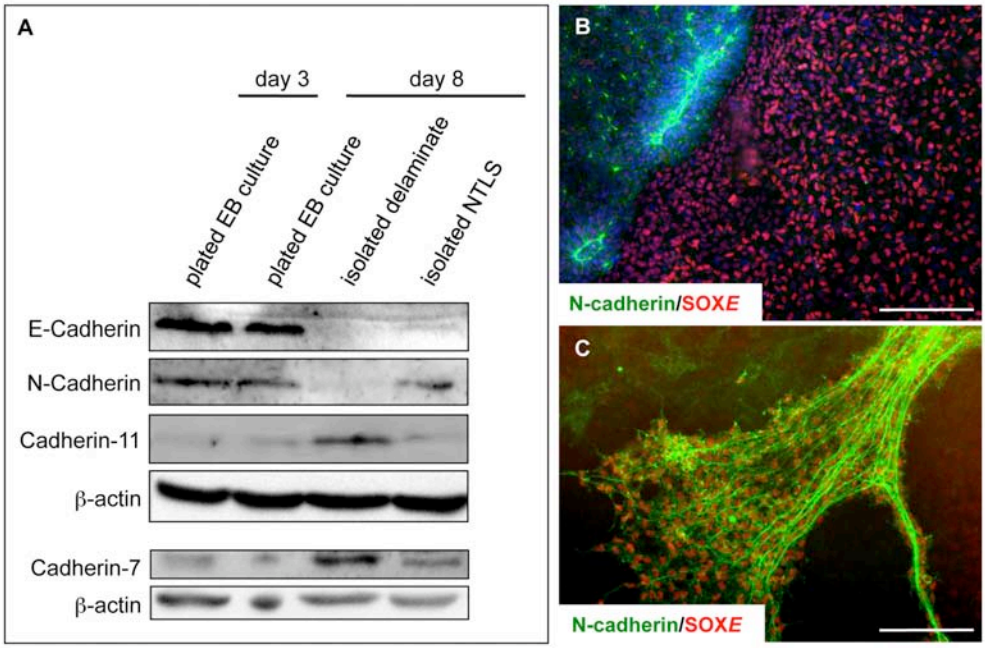

Figure 13: Developing hES cell-derived neural crest cells show a switch in cadherin expression. Western blot analysis showed expression of E-cadherin in the whole cultures of plated EBs, but is just faintly expressed in NTLS and absent in isolated neural crest delaminates. N-cadherin was expressed in the whole culture of plated EBs and in isolated NTLS, but was absent in the isolated aggregates. Expression of Cadherin-7 and -11 on the other hand was upregulated in the isolated aggregates in comparison to the whole plated EB culture and NTLS (**A**). Immunocytochemistry of N-cadherin in whole plated EB culture (d6-7) showed expression of N-cadherin exclusively in the neural tube-like structures, namely in the lumen. Migrating SOX*E* positive cells were negative for N-cadherin (**B**). In differentiating cells, N-cadherin was upregulated again (**C**). B+C: Nuclei are counterstained with DAPI (blue). Scale bars: 100 μm. NTLS: Neural tube-like structures.

Altogether these results indicate that switching cadherin expression can be detected in human neural crest cell development *in vitro*, in a pattern similar to what is observed *in vivo* in various animal models.

3.6 Spontaneous differentiation of peripheral neurons in the periphery of plated embryoid bodies

In addition to proliferating undifferentiated neural crest cells, a significant number of mature neurons were found in the periphery of the plated EBs. Occasionally, in the periphery of plated EBs the formation of ganglion-like clusters was observed, from where the neurites extended (Fig. 14A+B). Remarkably, those neurons developed in the absence of any neuronal supporting factors except for FGF2 and Fn and appeared in the cultures already six days after plating of the EBs.

The neurons exhibited long axons, showed strong expression of Peripherin and co-expressed BRN3A (Fig. 14C+D). The typical long axons, as well as the double staining of Peripherin and BRN3A is a strong indication for peripheral neurons of a sensory phenotype.

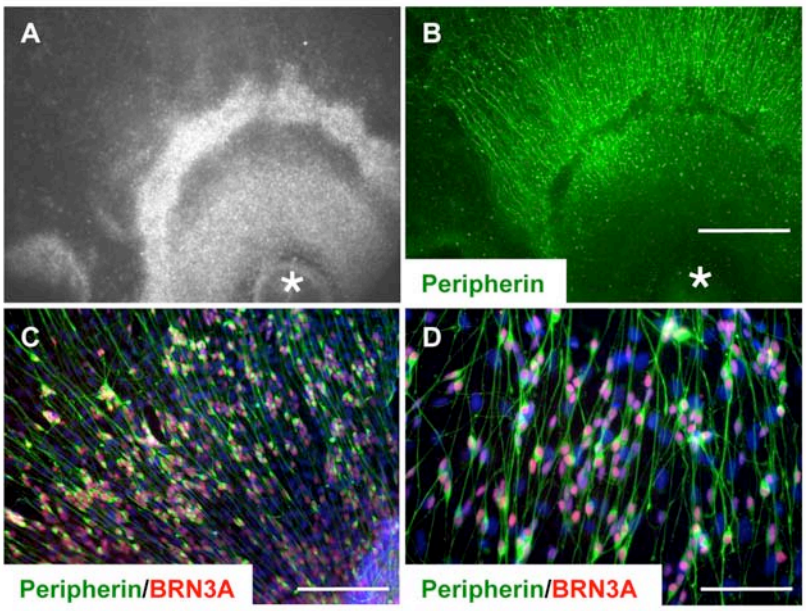

Figure 14: Sensory neurons are found during early differentiation. Peripherin-positive neurons emerged in the periphery of neural rosettes (**A**+**B**). Peripherin-positive neurons exhibited bipolar morphology with long axons and co-expressed BRN3A (**C**+**D**). Nuclei are counter-stained with DAPI (blue). Scale bars: B: 500 µm, C: 200µm, D: 100µm

3.7 Isolation of neural crest cells by manual picking

As a next step, a highly purified population of proliferating, undifferentiated neural crest cells should be established. The distinct crescent-shaped aggregates in which the neural crest cells assembled could easily be detected with the binocular microscope and therewith allowed for an efficient morphology-based isolation (Fig. 15A). The characteristic aggregates were circled with a sterile cannula and transferred into medium filled, Fn-coated cell culture dishes, where they could readily be replated. Upon replating of the isolated crescent-shaped aggregates cells

migrated from them. The cells exhibited a bipolar, spindle-shaped morphology. So as to clarify the cellular identity of the migrating cells, immunocytochemical analysis was performed. The expression of neural crest specific markers was assessed. The cells, as well as the cells residing in the cluster expressed the neural crest-associated markers p75NTR, AP2α, as well as SOX*E* (Fig. 15B-D).

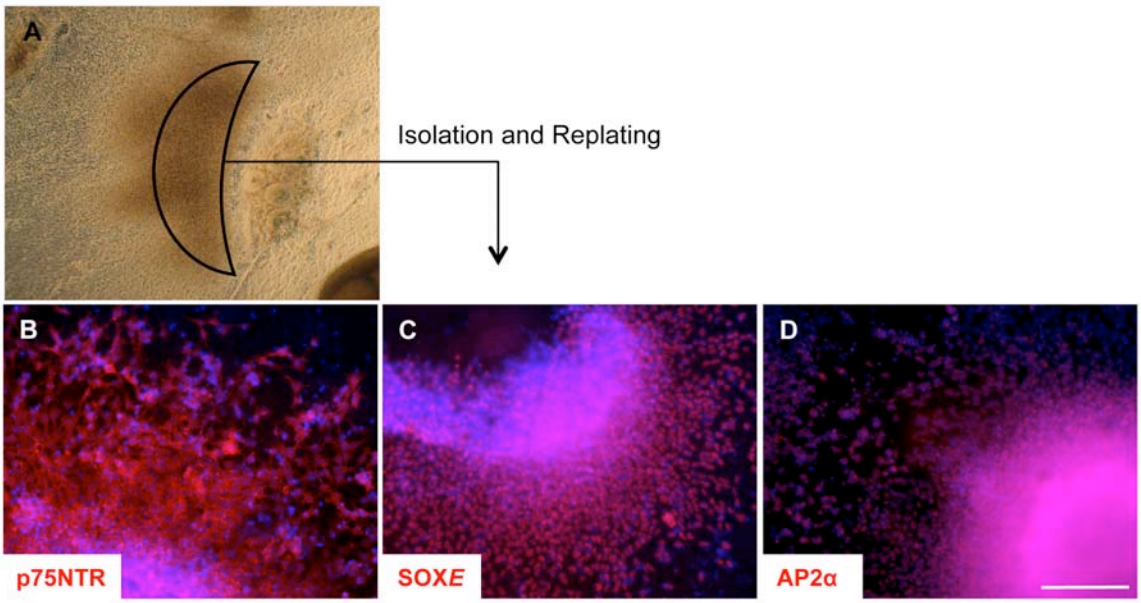

Figure 15: hES cell-derived NC cells can be isolated manually as they form evidently recognizable aggregates. Crescent-shaped aggregates can be manually isolated by picking with a sterile canula (**A**). Upon replating of aggregates, cells migrate out of the clusters over the fibronectin-coated dish. Those cells expressed p75NTR (**B**), as well as SOX*E* (**C**). Scale bars: 200 μm.

In order to investigate the behavior of the cells within the isolated aggregates, time-lapse imaging of isolated aggregates was performed. Upon plating of the aggregate, the strong migrating behavior of the cells could be observed. Cells were monitored for 72 hours. Already after 10 hours the first cells started migrating. Migrating cells populated approximately half of the lens coverage after 20 to 30 hours. The bipolar, spindle-shaped cells migrating out of the plated aggregates covered up to 90% of the field of view after 50 to 60 hours. Complete confluence of the cell culture dish was achieved after 70 hours. The movie can be found in the appendix of this thesis. Figure 16 shows the migrating cells in 10 hour-intervals. After light microscopy analysis the cells were analyzed for neural crest specific key molecule expression, e.g. p75NTR and others in order to confirm initial findings (see Fig. 15). Cells that migrated out of the plated aggregates readily stained positive for neural crest specific markers (data not shown).

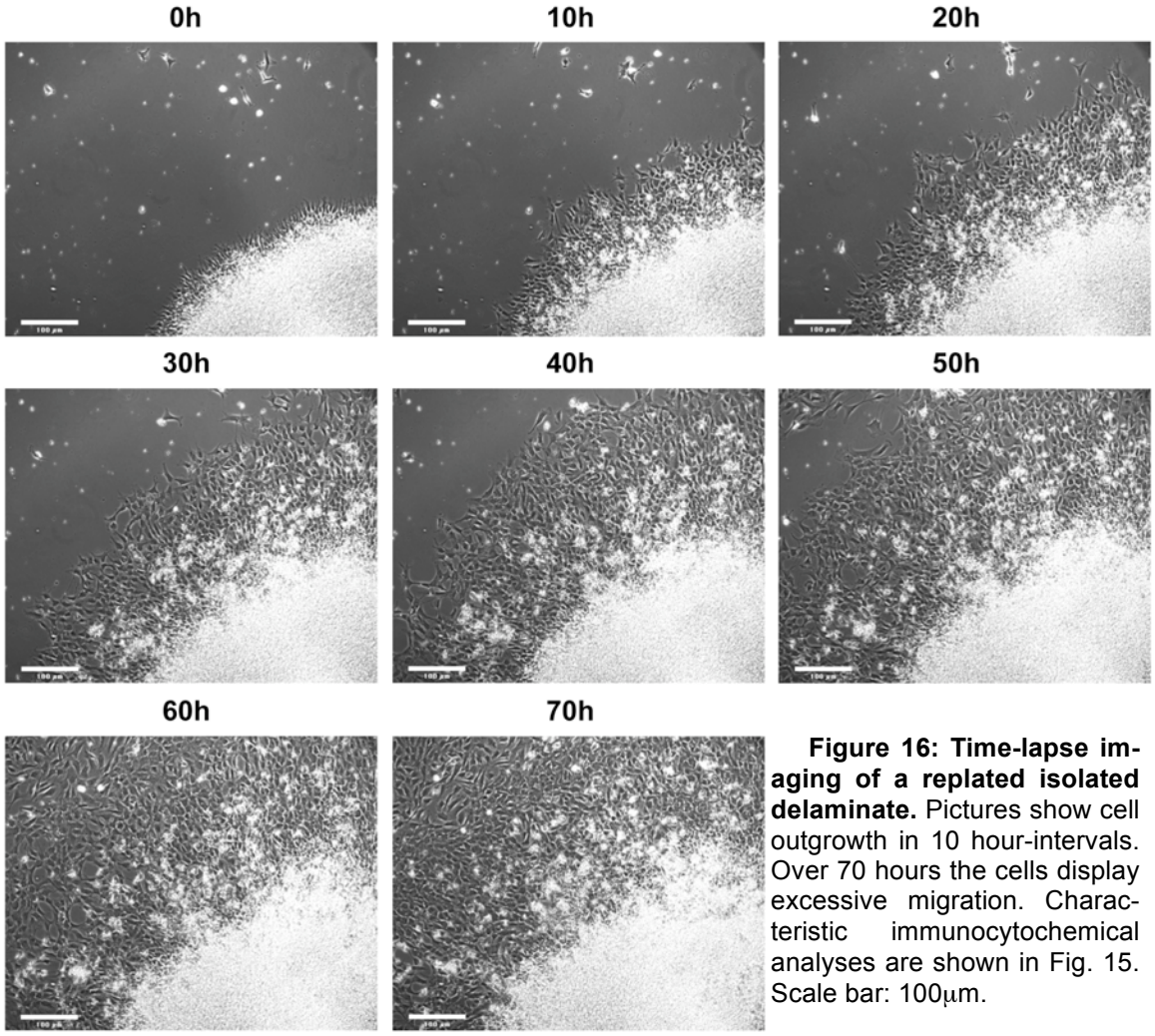

Figure 16: Time-lapse imaging of a replated isolated delaminate. Pictures show cell outgrowth in 10 hour-intervals. Over 70 hours the cells display excessive migration. Characteristic immunocytochemical analyses are shown in Fig. 15. Scale bar: 100μm.

Western blot analysis confirmed the strong enrichment of neural crest cells upon this simple manual enrichment procedure. Using p75NTR- and SOX10-specific antibodies, different compartments of the plated EB culture were analyzed. For this purpose, delaminates and neural tube-like structures were isolated separately by manual picking and as control, protein lysate from the initial heterogeneous population of the whole plated EB culture, was used. The expression of beta actin was analyzed in order to function as loading control. The isolated delaminate clearly showed an elevated level in the expression of p75NTR and SOX10 protein (Fig. 17A).

To further characterize the isolated delaminate, RT-PCR was performed to analyze the expression of more neural crest-associated genes (Fig. 17B). The expression of the transcripts *NGFR*, *SOX10*, *B3GAT1* (*HNK-1*), *SNAI2*, *SNAI1* and *TFAP2A* (*AP2α*) was elevated, further underlining the results of immunocytochemical analysis shown above.

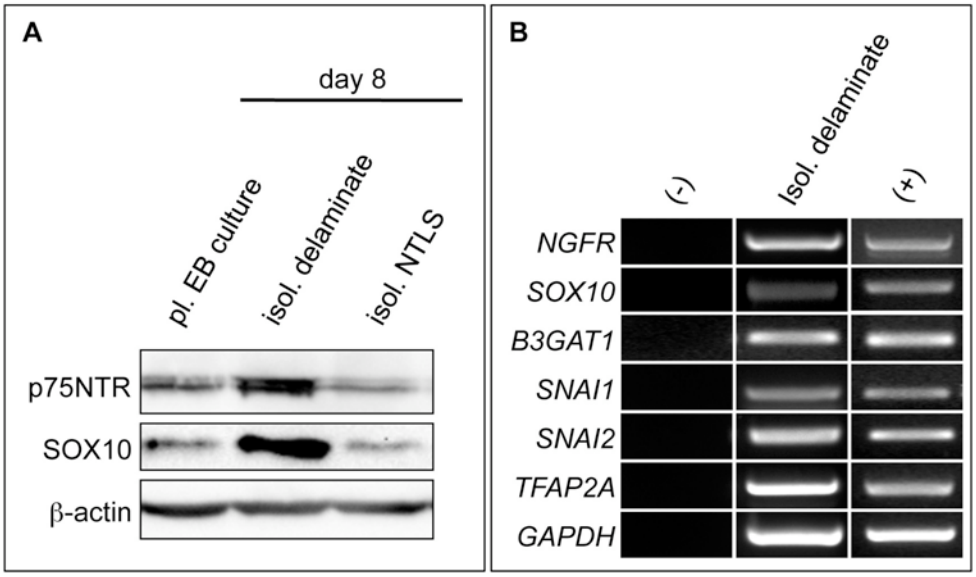

Figure 17: Analysis of manually isolated aggregates. The neural crest identity was also confirmed by immunoblot analysis, here a SOX10 specific antibody was used. In comparison with isolated neural tube-like structures, cells in the isolated delaminate upregulated p75NTR as well as SOX10 (**A)**. The isolated cell population was tested for several neural crest-associated markers via RT-PCR. Expression of *NGFR* and *SOX10* was confirmed; additionally expression of *B3GAT1* (*HNK-1*), *SNAI1*, *SNAI2* and *TFAP2A* was detected (**B**). B: Positive control: Human Schwannoma biopsy.

Upon enzymatic detachment and trituation a homogenous cell population was obtained that efficiently plated on Fn-coated cell culture dishes. The population displayed p75NTR expression at a purity of 95.3±3.6% (Fig. 18A). Virtually all p75NTR-positive cells co-expressed SOX*E* (Fig. 18B). The cell population proliferated in the presence of growth factors FGF2 and EGF and could be passaged every three days at a 1:3 ratio. For differentiation paradigms cells not older than passage 3 were used, as with increasing passage number the cell proliferation, as well as the capacity for neuronal differentiation, declined (data not shown).

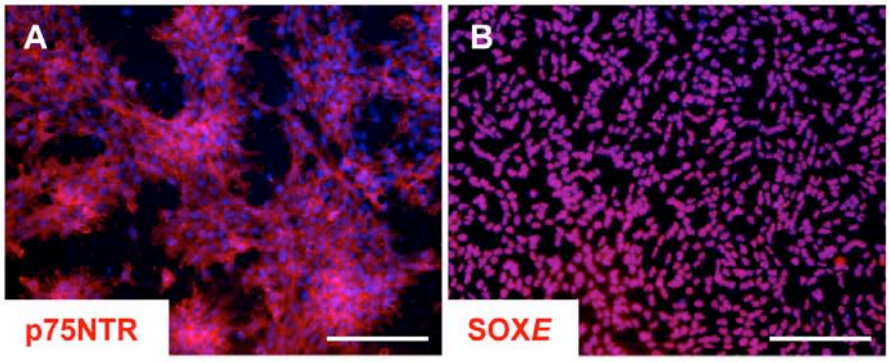

Figure 18: Trituation of manually isolated crescent-shaped aggregates led to a homogenous cell population. Upon trituation of clusters a homogenous cell population was yielded, expressing p75NTR (**A**), as well as SOX*E* (**B**). Nuclei counterstained with DAPI. Scale bars: 200 μm.

In order to demonstrate the efficiency of the manual isolation procedure, the result was compared with a purified population obtained by FACSorting for p75NTR expression. For that purpose plated EB cultures were enzymatically detached from the dish, singularized and subjected to live immunostaining for p75NTR. Cell sorting was performed in cooperation with the Flow Cytometry Core Facility situated at the Institute of Molecular Medicine, Medical Center, University of Bonn.

The p75NTR positive population was evidently distinguishable from negative cells, and made up 15.2±5.2 % of the whole culture (Fig. 19A). The sorted cells could be expanded to form a homogenous monolayer expressing p75NTR (Fig. 19B). Virtually all cells showed expression of SOX*E* (Fig. 20C). Sorted cells expressed p75NTR at a purity of 94.2±2.2%, resembling the purity that was achieved by manual picking (95.3±3.6%; Fig. 19D).

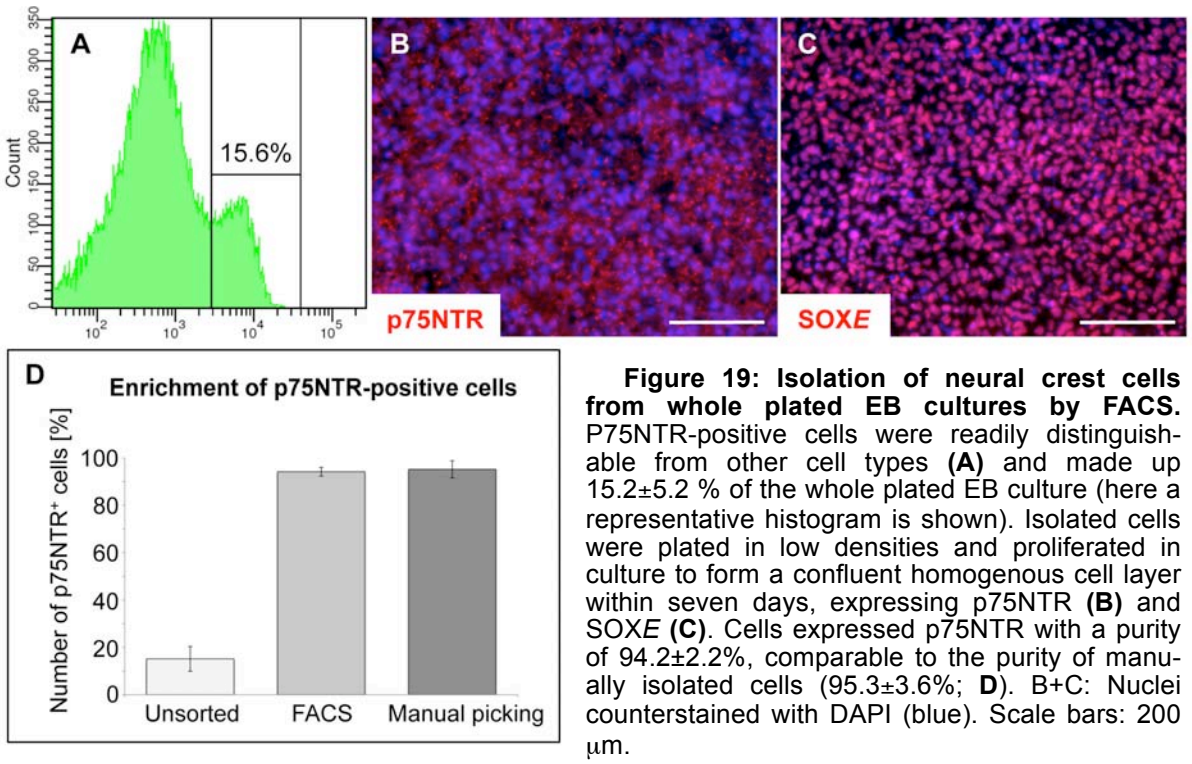

Figure 19: Isolation of neural crest cells from whole plated EB cultures by FACS. P75NTR-positive cells were readily distinguishable from other cell types **(A)** and made up 15.2±5.2 % of the whole plated EB culture (here a representative histogram is shown). Isolated cells were plated in low densities and proliferated in culture to form a confluent homogenous cell layer within seven days, expressing p75NTR **(B)** and SOX*E* **(C)**. Cells expressed p75NTR with a purity of 94.2±2.2%, comparable to the purity of manually isolated cells (95.3±3.6%; **D**). B+C: Nuclei counterstained with DAPI (blue). Scale bars: 200 μm.

Manual picking offers an attractive alternative to FACSorting due to various reasons. It causes less stress to the cells, is also less susceptive to contamination and a fast method of isolation. Furthermore, the yield of positive cells is considerably higher. In addition, as no antibody staining and expensive equipment are needed it is cheaper compared to FACSorting. As for these reasons, all further experiments aiming at the further characterization and differ-

entiation of human ES cell-derived neural crest cells were carried out on manually isolated cell populations.

3.8 Microarray analysis shows substantial gene expression differences between neural crest cells and a human embryonic stem cell-derived neural stem cell population

Considering ease and efficiency of the manual isolation technique, delaminate-derived cells were used for all further studies. To further characterize the isolated cell population, a microarray analysis using Illumina array technology was performed in collaboration with Dr. Michael Alexander (Department of Genomics, Life&Brain Center, University of Bonn). Here, a long term-proliferating, rosette-type neural stem cell population (lt-hESNSCs), which was initially obtained from hES cell-derived neural tube-like structures established from the same parental hES cell line was used as comparison (Koch et al., 2009).

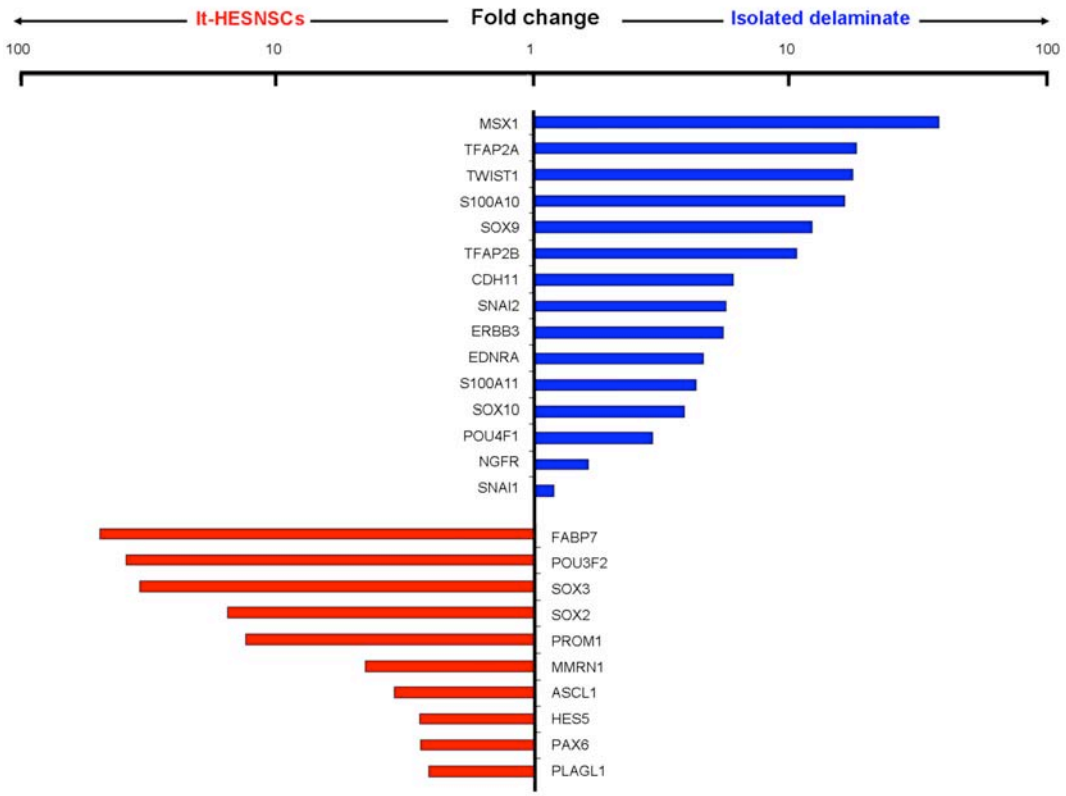

Figure 20: Comparison of isolated delaminates vs. lt-hESNSCs by microarray analysis. The figure represents the gene expression levels of several top marker genes from lt-hESNSCs and isolated delaminates assessed by microarray analyses (Illumina human HT-12 Expression BeadChips v3). Fluorescence intensity of marker genes from duplicate analyses was average normalized and compared (lt-hESNSCs versus isolated delaminates and isolated delaminates versus lt-hESNSCs) to create a fold-change of gene expression levels. Expressed genes with high expression levels in isolated delaminates compared to lt-hESNSCs are shown in blue and expressed genes with high expression levels in lt-hESNSCs compared to isolated delaminates are shown in red.

The differential expression of a selected neural crest and neural stem cell marker set was investigated. Fold change differences were found for the neural crest-associated markers: *MSX1*, *TFAP2A* (*AP2α*), *TWIST1*, *S100A10*, *SOX9*, *TFAP2B* (*AP2β*), *CDH11* (*cadherin-11*), *SNAI2*, *ERBB3*, *EDNRA*, *S100A11*, *SOX10*, *POU4F1* (*BRN3A*), *NGFR* (*p75NTR*) and *SNAI1*, showing an upregulation of these genes in the isolated delaminates. In contrast, typical neural rosette markers such as *FABP7*, *POU3F2*, *SOX3*, *SOX2*, *PROM1*, *MMRN1*, *ASCL1*, *PAX6*, *HES5*, *PLAGL1* were found downregulated in the delaminate-derived cells (Fig. 20) compared to hESC-derived neural stem cells.

3.9 Isolated neural crest cells can readily be differentiated into different types of peripheral neurons

Neural crest cells give rise to sensory neurons of the cranial nerves and the dorsal root ganglia and autonomic neurons of the sympathetic and enteric ganglia. In order to assess the neuronal differentiation potential of the isolated hES cell-derived neural crest cells, cells were cultivated in neuronal differentiation medium supplemented with the neurotrophins BDNF and NGF. Both are known to support the survival and differentiation of sensory neuron precursors; BDNF by binding to the receptors TrkB and p75NTR, and NGF by binding to TrkA and p75NTR (Patapoutian and Reichardt, 2001).

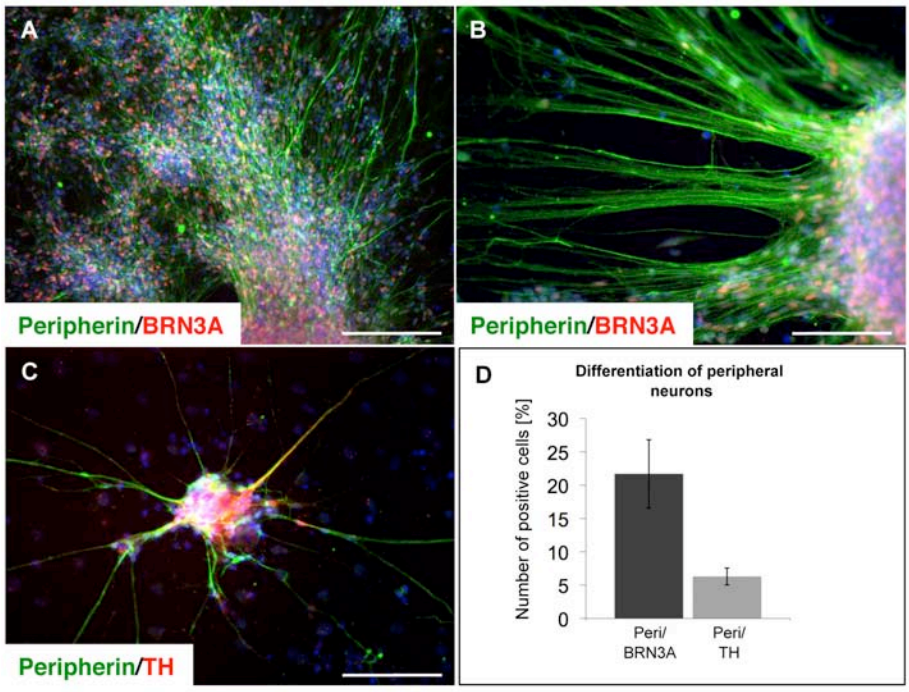

Figure 21: hES cell-derived neural crest cells differentiate into different types of peripheral neurons. Differentiation in neuronal medium containing NGF and BDNF yielded 21.7±5.1% of Peripherin/BRN3a positive neurons, which are considered as sensory neurons due to the expression of this marker combination (**A**+**B**, **D**). Furthermore 6.3±1.3% of Peripherin/TH positive cells are obtained, which are considered as autonomic neurons (**C**+**D**). Scale bars: A: 200 µm, B, C: 100 µm.

During the differentiation paradigm the formation of ganglion-like neuronal clusters could be observed (Fig. 21A-C). Double labeling with antibodies to Peripherin and BRN3A, a marker combination typically used to identify sensory neurons (Fedtsova and Turner, 1995), revealed 21.7±5.1% immunopositive cells (Fig. 21A+B, D). Peripherin and TH, a marker combination indicating autonomic lineages (Mizuseki et al., 2003) was found in 6.3±1.3% of the cells (Fig. 21C+D).

In order to characterize the neuronal population, a more detailed RT-PCR analysis of proliferating neural crest cells and neuronal differentiated cells thereof were performed (Fig. 22).

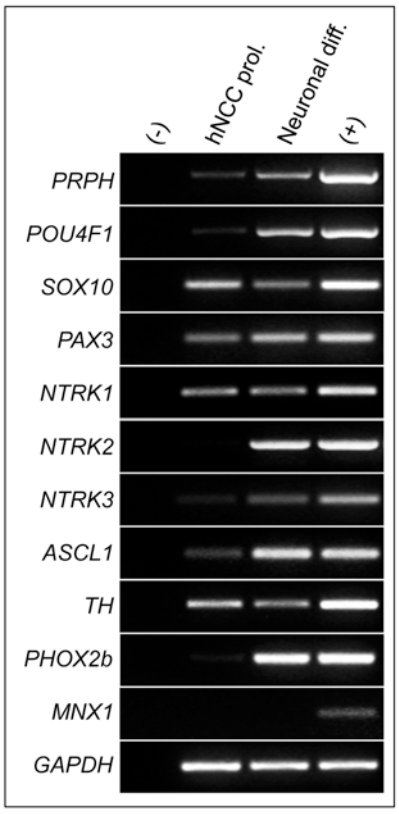

Figure 22: RT-PCR profile of neuronal differentiated isolated neural crest cells. RT-PCR confirmed expression of *PRPH* (*PERIPHERIN*), *POU4F1* (*BRN3A*) and *TH*, which also have been assessed by immunocytochemical analysis. Additionally expression of *SOX10* and *PAX3* but also *ASCL1*, *PHOX2B*, and *NTRK1* (*TrkA), NTRK2* (*TrkB),* and *NTRK3* (*TrkC)* was revealed. No expression of the central motoneuron marker *MNX1* was detected (**E**) Positive controls: *POU4F1, SOX10*, *PAX3*, *ASCL1*, *NTRK1*, *NTRK2, NTRK3, TH, MNX1*: Human fetal spinal cord; *PRPH*, *PHOX2B*: Human fetal colon tissue. *GAPDH* is representatively shown for human fetal spinal cord. hNCCs: Human neural crest cells.

RT-PCR further confirmed the expression of *PRPH (Peripherin), POU4F1 (BRN3A)*, and *TH*, which have also been assessed by immunocytochemical analysis. While for *PRPH* and *POU4F1* an upregulation could be observed after differentiation, *TH* was also strongly expressed in proliferating cells. This observation is compatible with data of Young et al. suggesting that some undifferentiated neural crest precursors show a transient expression of this hydroxylase (Young et al., 1999). In addition, expression of *SOX10*, which is transiently expressed in sensory neurons (Carney et al., 2006) and the neuronal marker *PAX3* (Koblar et al., 1999) was detected. Not surprisingly, those markers were also expressed in proliferating

neural crest cells. Furthermore the expression of markers indicative for peripheral neuronal subtypes, for which no antibodies were available, was investigated. The expression of *NTRK1* (*TrkA*), expressed by peptidergic small diameter neurons mediating pain sensation, and *NTRK2* and *-3* (*TrkB and TrkC*), which is found in large diameter mechanoreceptive and proprioceptive neurons (Mu et al., 1993; Wright and Snider, 1995) was detected. Moreover the expression of *ASCL1* and *PHOX2B* was identified, genes, which play an essential role in the development of the sympathetic, parasympathetic, and enteric ganglia within the peripheral autonomic nervous system (Pattyn et al., 1999). On the other hand, *MNX1* (*HB9*), a marker for CNS motoneurons (Vult von Steyern et al., 1999), could not be detected in the differentiated cells.

In order to verify the functionality of the obtained neurons, their electrophysiological properties were assessed. All electrophysiological measurements were performed in collaboration with Dr. Jaideep Kesavan (Institute of Reconstructive Neurobiology, Medical Center, University of Bonn). For long-time differentiation, isolated neural crest cells were plated on mitotically inactivated astrocytes and cultivated in neuronal differentiation medium for 6-8 weeks.

Current-clamp measurements were performed to elicit action potentials. All of the neurons tested generated multiple action potentials during current injection (Fig. 23A). Voltage-dependent membrane currents were also observed in these neurons (Fig. 23B). The fast and transient inward current was sensitive to the application of 300 nM TTx (a selective Na^+ channel blocker). One of the hallmarks of neurons is their ability to form synapses. Therefore, whole-cell voltage-clamp recordings were performed in these neurons to monitor spontaneous synaptic currents. Spontaneous postsynaptic currents were observed in whole-cell voltage-clamp recordings indicating functional synapses in these neurons (Fig. 23D). Thus, neurons derived from neural crest cells exhibited functional characteristics *in vitro*. After patch-clamp recordings, post-hoc immunostaining of the recorded neurons revealed co-localization of biocytin (diffused from the patch pipette to the cell) and peripherin (Fig. 23E). However, occasionally neurons detached from the culture dish after patch-clamp measurements, thus making post-hoc immunostainings impossible. No obvious differences in the electrophysiological properties of any of the neurons measured could be observed.

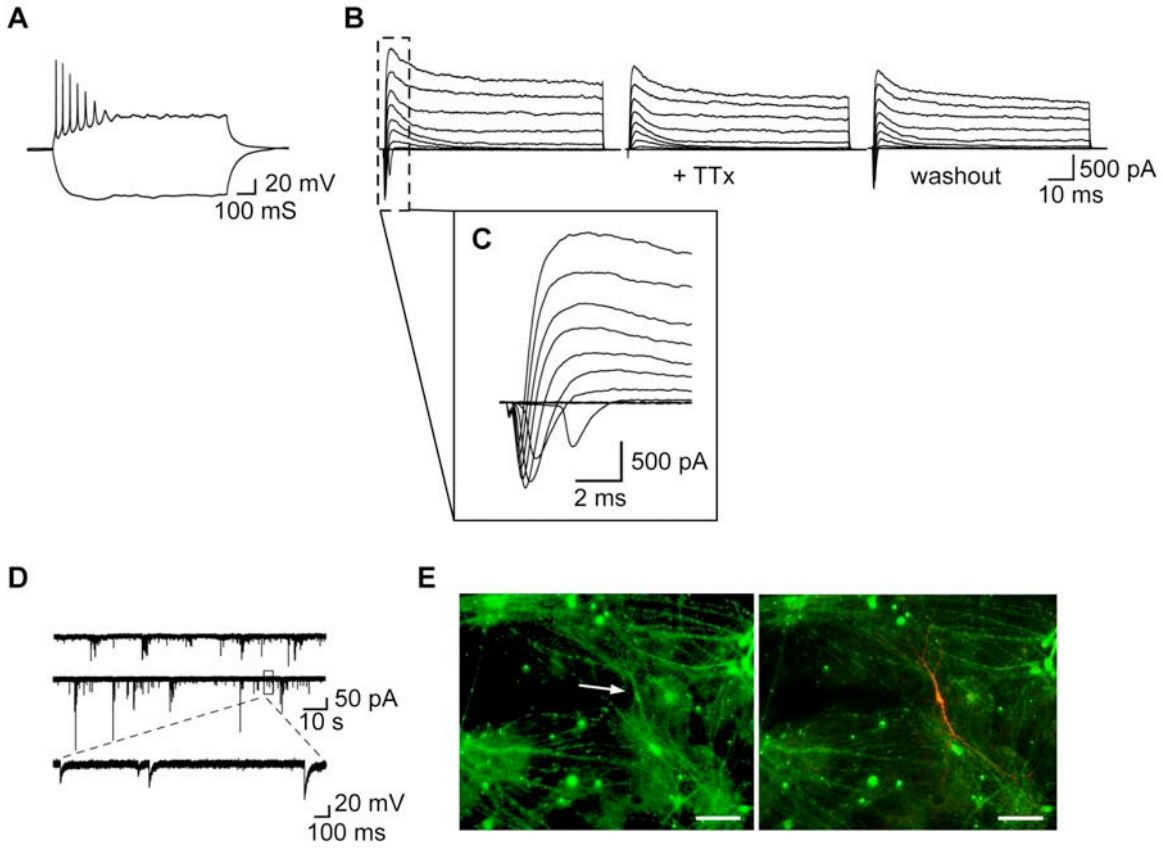

Figure 23: Electrophysiological analysis of the neural crest cell-derived neuronal population. Neural crest-derived neurons fired action potentials in response to step depolarization by current injection (**A**). Depolarizing voltage steps elicited voltage-dependent fast inactivating inward and sustained outward currents. The fast inward currents were blocked by bath application of 300 nM TTx (**B**). The boxed region in B is shown at a higher magnification (**C**). Representative traces of spontaneous synaptic currents from neural crest-derived neurons (**D**). Post-hoc staining of the recorded cells reveals co-localization of Peripherin and biocytin (diffused from the path pipette into the recorded cell) (**E**). Scale bars: 100 µm.

3.10 Isolated neural crest cells give rise to putative Schwann cells

In vivo, Schwann cells need the contact to neurons to proliferate and differentiate. *In vitro*, these environmental cues can be mimicked by the application of certain factors. In order to differentiate isolated neural crest cells into Schwann cells, a powerful glial instructor, NRG-1, was used. NRG-1 is secreted from peripheral neurons and plays the central role in Schwann cell growth and differentiation. It also regulates the thickness of myelin (Michailov et al., 2004). Isolated hES cell-derived neural crest cells were initially cultivated in the additional presence of FGF2, as it is known to promote Schwann cell proliferation after nerve injury (Jungnickel et al., 2006). In addition, cell culture medium was supplemented with Forskolin, which increases the intracellular level of cAMP. This in turn, enhances the NRG-dependent

proliferation of Schwann cells and also promotes the maturation and myelination of Schwann cells (Sobue et al., 1986).

After three weeks of proliferation in Schwann cell supporting medium, FGF2 was withdrawn from the medium to initiate terminal differentiation. Upon differentiation the cells showed a spindle-like morphology, typical for Schwann cells. 40.4±17.4% expressed the marker combination p75NTR/L1CAM, 30.1±16.0% expressed p75NTR/GFAP (Fig. 24A+B). The expression of markers associated with mature Schwann cells was analyzed by RT-PCR (Fig. 24C). In addition to *NGFR* (*p75NTR*), *L1CAM* and *GFAP*, expression of *SOX10*, *CNP* and *EGR2* (*Krox20*) was detected. *L1CAM*, *SOX10* and *p75NTR* are expressed in proliferating neural crest cells, as well as in differentiated cultures. *SOX10* and *p75NTR* are, as described above, markers for undifferentiated neural crest cells and persist during glial differentiation. *L1CAM* has also been shown in proliferating neural crest cells. Surprisingly, proliferating cells also show a high level of *CNP*, a marker for Schwann cells and Oligodendrocytes. This is compatible with data by Chandross and colleagues, who showed that the CNP promoter is active in neural crest progenitors, i.e. specifies early Schwann cell precursors (Chandross et al., 1999). In the case of *GFAP* and *EGR2* an upregulation in the differentiated cultures could be observed.

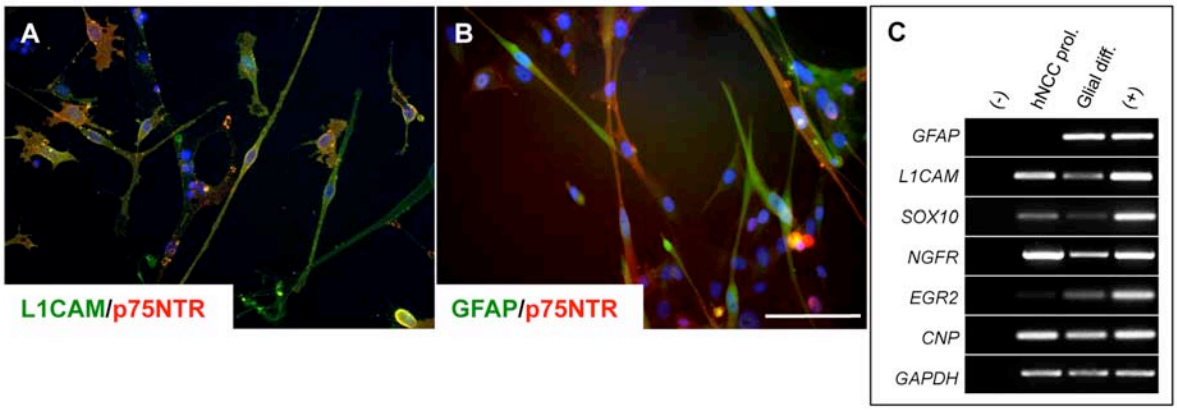

Figure 24: hES cell-derived NC cells differentiate into Schwann-like cells. Upon cultivation in FGF, Forskolin and NRG-1 followed by terminal differentiation induced by FGF2 withdrawal, 40.4±17.4% of cells expressed L1CAM/p75NTR (**A**) and 30.1±16.0% p75NTR/GFAP (**B**) were obtained. Positive cells adopted a spindle-like morphology. RT-PCR additionally confirmed expression of mature Schwann cell markers, namely *GFAP*, *L1CAM*, *SOX10*, *NGFR* (*p75NTR*), EGR2 (*Krox20*), and *CNP* (**C**). A+B: Nuclei were counterstained with DAPI. Scale bars: 100 µm. C: Positive control: Human Schwannoma biopsy.

3.11 Isolated neural crest cells give rise to mesenchymal derivatives

Neural crest cells are able to differentiate into several mesenchymal cell types, including smooth muscle cells, bone and cartilage of the head, as well as adipocytes. Neural crest-derived smooth muscle cells are found in the heart and in the gastrointestinal tract. In order to induce differentiation of the isolated human neural crest cell population into mesenchymal cell types, they were cultivated in the presence of 10% FCS, culture conditions known to promote mesenchymal differentiation. The cultivation in DMEM+10% FCS for three weeks yielded 82.7±3.3% SMA-positive cells (Fig. 25A). RT-PCR revealed in addition to *ACTA2* (*SMAα*) an upregulation of *ACTG2* (*SMAγ*) gene expression, an actin isoform present in enteric smooth muscle cells (Fig. 25B).

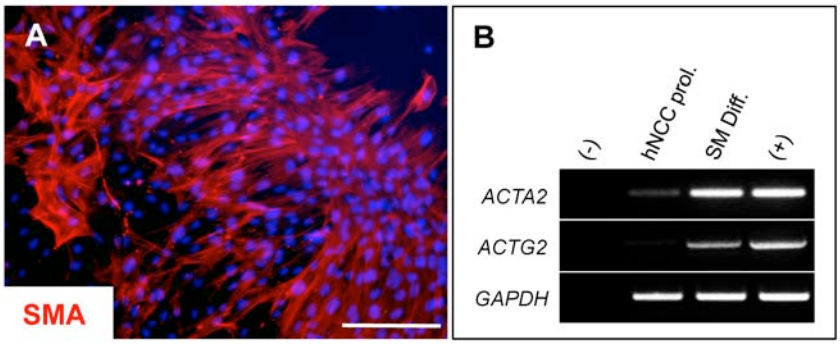

Figure 25: hES cell-derived NC cells differentiate into smooth muscle cells. Treatment of isolated NC cells with FCS led to formation of 82.7±3.3% SMA positive cells (**A**). RT-PCR revealed beneath the expression of *ACTA2* (*SMAα*) as well as the expression of *ACTG2* (*SMAγ*), which is found in enteric smooth muscle cells (**B**). A: Nuclei were counterstained with DAPI. Scale bar: 100 µm. B: Positive control: Human fetal colon.

In order to facilitate the differentiation and survival of chondrocytes, ascorbic acid, forskolin and FGF2 were added to the mesenchymal basic medium, as these factors are known to have a promoting effect on chondrogenic differentiation (Ido and Ito, 2006; Sarkar et al., 2001). After 4 weeks in this medium, clusters of chondrocytes that stained positive for alcian blue were detected (Fig. 26A+B). Alcian blue stains accumulations of mucopolysaccharides associated with chondrocyte differentiation (Schofield et al., 1975). Additionally, the clusters expressed S100β (Fig. 26C), which is associated with chondrogenesis as well (Stefansson et al., 1982; Vega et al., 1990).

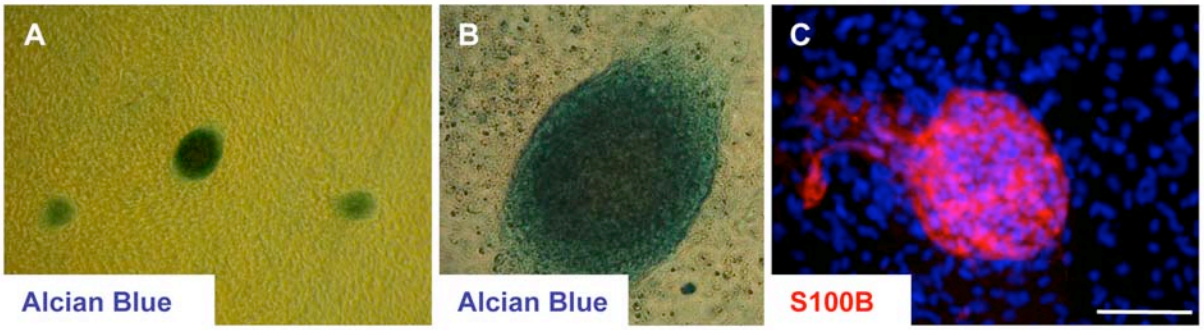

Figure 26: hES cell-derived neural crest cells differentiate into chondrocyte nodules. Upon differentiation of isolated neural crest cells in high density in chondrocyte promoting medium, chondrocyte nodules formed, which stained positive for Alcian Blue (**A**+**B**), as well as S100β (**C**). Scale bar: C: 100 µm.

To explore the potential of hES cell-derived neural crest cells for adipocyte differentiation, cells were cultivated in the presence of hydrocortisone, isobutylmethylxanthine and indomethacine, which are reagents used for the promotion of adipocyte differentiation (Fang et al., 2005; Hauner et al., 1989). Upon three weeks of differentiation, numerous cells developed intracytoplasmic lipid droplets positive for oil red staining (Fig. 27A). This is a typical staining pattern used to identify adipocytes. (Ramirez-Zacarias et al., 1992).

For osteoblast differentiaton, cells were cultured 3 weeks in the presence of Dexamethasone, L-ascorbic acid and β-glycerolphosphate (Fang et al., 2005; Jaiswal et al., 1997). Identification of osteoblasts was done by Alizarin red staining (Fig. 27B), which visualizes calcium-rich deposits (Bodine et al., 1997).

Pronounced variability in the formation of lipid droplets within adipocytes and cluster formation of chondrocytes and osteoblasts precluded a precise quantification of these cell types.

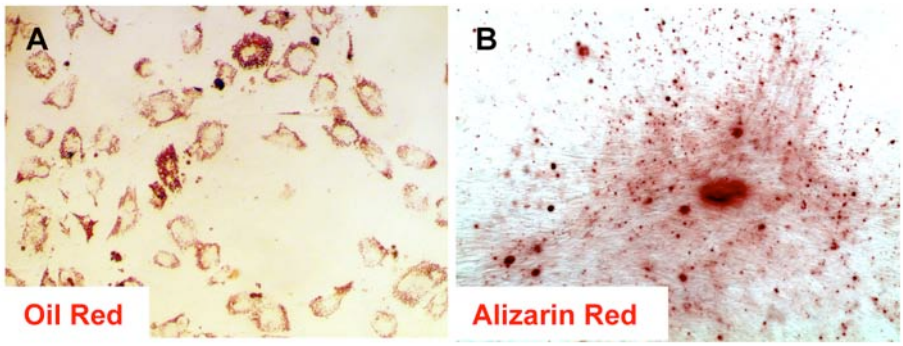

Figure 27: hES cell-derived neural crest cells readily differentiate into adipocytes and osteoblasts. Upon cultivation of isolated neural crest cells in appropriate conditions, adipocytes, identified by the inclusion of lipid droplets stained by oil red (**A**), as well as osteoblasts, identified by the staining of calcium rich areas by alizarin red (**B**), were obtained.

Mesenchymal derivatives are mainly derived from cranial neural crest cells. As the isolated hES cell-derived neural crest population readily differentiated into the mesenchymal derivatives, their expression of transcription factors associated with neural crest cells from the head region was investigated by RT-PCR (Fig. 28).

The HOX genes of the second homologue were found highly expressed in the isolated population, namely *HOXA2* and *HOXB2*. Expression of those genes was shown in the migrating streams of cranial neural crest (Hunt et al., 1991). Furthermore, cells showed expression of *GBX2* and *OTX2*, which are involved in the formation and pattering of the head. *GBX2* was shown to be expressed in migrating cranial neural crest cells and the pharyngeal arches (Kikuta et al., 2003). *OTX2* expression has also been observed in cranial neural crest cells (Kimura et al., 1997).

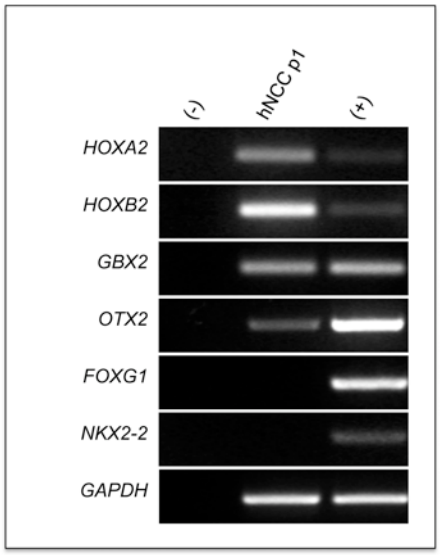

Figure 28: Isolated neural crest cells express markers associated with cranial neural crest cells. Isolated neural crest cells show high expression of *HOXA2* and *HOXB2*, as well as *GBX2* and *OTX2,* which are associated with migrating cranial neural crest cells. In contrast, they do not show expression of *FOXG1* or *NKX2-2*, connected to ventral organization of the head. Positive control: Human fetal brain.

FOXG1, expressed in the ventral telencephalon and placode cells (Duggan et al., 2008; Pratt et al., 2002), was not detected in the isolated cells. The same is true for *NKX2-2*, likewise associated with ventral organization (Briscoe et al., 1999). As a positive control, cDNA of human fetal brain was used in the RT-PCR. The expression of the housekeeping gene GAPDH was assessed in order to be able to compare the expression of the hES cell-derived neural crest population with the positive control.

4 Discussion

The hES cell-based model system presented here allows for the recapitulation of neural crest development *in vitro*. Remarkably, it could be observed that differentiating hES cells mimic early neurulation and patterning events occurring *in vivo*. Mature neural rosettes display a dorsal-ventral marker expression pattern, further strengthening the idea of a neural tube-like character. Neural crest cells emerge in parallel to neural tube-like structures, delaminate and re-aggregate in their periphery. This dynamic process not only provides experimental access to the early events of human neural crest formation including migration cues but also facilitates the *in vitro* generation of various neural crest cell types, which can be directly differentiated from isolated delaminated aggregates. In the following the two key aspects of the hES cell-based model system, the recapitulation of neural crest development *in vitro* and the methodical benefits in terms of efficiency of the protocol and differentiation potential of hES cell-derived neural crest cells, will be elaborated.

4.1 Neural crest development can be recapitulated *in vitro*

HES cell-derived neural tube-like structures acquire a dorsal-ventral organization

HES cell-derived neural rosettes have previously been shown to exhibit characteristics similar to the developing neural tube, as they exhibit a primitive dorsal-ventral patterning (Li et al., 2005). However, as cultivation occurs in an artificial 2D cell culture model, neural rosettes lack the organization present *in vivo*. During embryonic development neuroepithelial cells face the basal lamina at their basal side, and the amniotic fluid at their apical side. As the neural plate forms the neural tube, the apical side faces the lumen of the neural tube. This apical-basal orientation of the cells is also observed in hES cell-derived neural rosettes. In the presented study the expression of dorsal transcription factors PAX3 and PAX7 was found concentrated and elevated at the outer edges of hES cell-derived neural rosettes, while the ventral marker SHH was detected in the lumen, suggesting a dorsal-ventral patterning of the mature neural rosettes. This data add up to the previous published work regarding similarity of mature neural rosettes to the embryonic neural tube (Colleoni et al., 2010; Elkabetz et al., 2008; Li et al., 2005). It was shown in this thesis that early neural rosettes (day 3 after plating of EBs) display a diffuse staining of the ventral markers PAX3 and PAX7. These results suggest that neural rosettes acquire a dorsal-ventral patterning during prolonged time in culture.

Therefore, in the thesis presented here, mature neural rosettes have been termed neural tube-like structures.

Neural crest cells migrate from neural tube-like structures

When setting out to discover neural crest cells in differentiating hES cells, one obviously will explore the periphery of neural tube-like structures. Thereby it was found that plated EB cultures show a remarkable self-organization. During their cultivation, neural tube-like structures arise in their centers. In the periphery, a homogenous cell population builds clusters that are arranged in a centrifugal manner around the centered neural tube-like structures. The extensive characterization of the isolated clusters identified this early arising population as neural crest cells. So where does the neural crest population come from?

One theory is that the neural crest cells delaminate from the developing neural tube-like structures. The neural tube-like organization and the expression of dorsal-ventral markers point at this direction. Furthermore, in chapter 3.4 of this thesis it was shown that isolated, separately plated neural tube-like structures (from 8-day-old plated EB cultures) gave rise for a second time to neural crest cells. Those neural tube-like structures have been isolated from plated EB cultures at a time point when neural crest cells already left the neural rosette zone and crescent-shaped aggregates again formed around them. In order to study their migration from neural tube-like structures, neural crest cells were investigated for expression of several cadherins. The observed expression patterns correspond to the published data of cadherin-switching, as shown in several animal models during the emergence of neural crest cells from the neural tube; i.e. early expression of E- and N-cadherin, downregulation of these cadherins in migrating neural crest cells and upregulation of cadherin-7 and -11 instead (Duband et al., 1995; Taneyhill, 2008). So far, switching in cadherin expression during neural crest development has only been identified in animal models. Cadherin-7 has been identified in migrating neural crest cells of the chicken and in a subpopulation of migrating neural crest cells in the rat (Dufour et al., 1999; Nakagawa and Takeichi, 1998; Takahashi and Osumi, 2008). Cadherin-11 has been identified as crucial adhesion molecule in migrating neural crest cells in *Xenopus* and in cranial neural crest cells with mesenchymal differentiation potential in the mouse (Borchers et al., 2001; Kimura et al., 1995). Furthermore, Cadherin-11 has been used to isolate hES cell-derived cranial neural crest cells (Zhou and Snead, 2008). This is the first study to describe the sequential expression of cadherins in human cells.

The other hypothesis is that neural crest cells develop in parallel to neural tube-like structures instead of actually delaminating from them and reside in-between them before they start to proliferate and migrate. This hypothesis is underlined by findings made by Basch and colleagues (2006). In this study it was found that the neural crest is induced independently from neural tissue and that the medial epiblast is sufficient for neural crest specification. The authors conclude that neural crest induction occurs just before or at the time of gastrulation and that other observations may be due to cell culture artifacts. The controversial discussions in the literature show that neural crest development is still largely unknown; especially onto the human system little light has been shed.

It is striking that in the hES cell-based model appearance and migration of neural crest cells occurred without specific external stimulation by BMPs, which have been shown to stimulate delamination of neural crest cells from explanted neural tubes (Sela-Donenfeld and Kalcheim, 2002) or members of the Wnt family, which play a key role in neural crest induction. A study by ten Berge and colleagues showed that EBs undergo a process similar to gastrulation and even form a primitive streak-like region depending on the activation of the Wnt pathway. Wnt signaling is activated spontaneously in the EBs, which is possibly due to the growth factor cocktail applied through the cultivation in the presence of serum or serum replacement (ten Berge et al., 2008). This shows that EBs possess the capability of self-organization and this may also explain the formation of neural tube-like structures, as well as the emergence of neural crest cells. In the cell culture system presented here, EBs are cultivated in the presence of serum replacement, before they are plated and transferred into N2-based medium containing FGF2 and fibronectin only. FGFs are, besides BMPs and Wnts, also involved in the induction of the neural crest (Monsoro-Burq et al., 2003). FGF2, in combination with BMP2, has been shown to be required for the conversion of CNS precursor cells towards neural crest cells (Sailer et al., 2005). The supplemented FGF2 might stimulate the neural crest cells to leave the neural rosette zone: It is known to promote the proliferation of neural crest cells, so that the excessive proliferation and migration of the hES cell-derived neural crest cells may be directly linked to the presence of FGF2 in the medium (Kalcheim, 1989; Murphy et al., 1994). Fibronectin on the other hand is known to promote neural crest adhesion and migration via integrins in an indirect manner (Strachan and Condic, 2008).

Another factor that might play a role in neural crest migration from the neural rosette zone are the flat, fibroblast-like cells that were observed in the time lapse imaging of the plated EB.

These cells leave the EB first, before the p75NTR-positive cells appear at the border. Possibly they are secreting chemokines that attract newborn neural crest cells to migrate. Moreover, the neural tube-like structures may provide cues that cause neural crest cells to delaminate and migrate, as also suggested in other publications (Lazzari et al., 2006; Colleoni et al., 2010). In future experiments it will be of great interest to investigate whether the presence of neural tube-like structures causes activation of signaling pathways in the neural crest cells. Possibly, the amount of neural crest cells migrating from neural tube-like structures could be enhanced by additional external stimuli such as the application of BMPs or members of the Wnt family.

Another interesting aspect of the segregation phenomenon of the plated EB culture is, beside the origin and migration of neural crest cells, the cease of cell migration, which leads to formation of the characteristic cell aggregates. At a defined distance from the neural tube-like structures neural crest cells stop to migrate and aggregate to form crescent-shaped clusters. The crescent-like shape is possible due to the centrifugal migration of neural crest cells from the plated EB. From these clusters cells sporadically continue to migrate. As the clusters were isolated, cells extensively grew out of these clusters, as analyzed by time-lapse imaging. The heterogeneous culture with the centered neural tube-like structures and the circumjacent crescent-shaped aggregates seems to exhibit a sophisticated balance, which is de-restricted as the clusters are isolated and re-plated. During neural crest migration *in vivo*, some cells also stop along the way to start differentiation while others continue migration to other destinations as seen with dorsal root ganglia and sympathetic ganglia generation (Duband, 2006; Marmigere and Ernfors, 2007). Possibly, the observed pattern of migration points at a mixed pool of already restricted neural crest precursor cells instead of a homogenous neural crest *stem* cell population. Although isolated neural crest cell populations seem to exhibit multipotency, meaning a true neural crest *stem* cell character, they may still be pre-specified, as it has been shown that trunk neural crest cells are able to adapt a cranial cell fate when they are exposed to appropriate culture conditions (McGonnell and Graham, 2002). The topic of neural crest plasticity is discussed below.

Future studies may use this interesting model to investigate the cues and signaling pathways that are involved in neural crest migration and what causes some cells to stop and others to continue migration. The signals from the centered neural tube-like structures may range to a certain distance and thereby build a gradient, which may lead to cell aggregation as signals decrease. Another possibility is that not the distance from the cells to the neural tube-like

structures is determining the cease of migration, but time. The signals from the neural tube-like structures might change during their further maturation. During normal development, timing of neural crest emigration from the neural tube is crucial to determine migration pathways and later terminal differentiation. Also, if the described flat fibroblast-like cells, which leave the plated EB at first, are causing newborn neural crest cells to migrate, they may stop the release of chemokines or even undergo apoptosis, as the culture conditions are not appropriate for their maintenance. Another reason may be the substrate used. *In vivo*, neural crest cells are guided into the pharyngeal arches or along the somites. Here, the neural crest cells migrate on fibronectin-coated cell culture dishes and this artificial environment may cause specific behavior of the adherent cells. Transplantation into the chicken at different developmental stages would be meaningful in order to investigate the migration pathways of the neural crest cells.

Peripheral neurons emerge early in human embryonic stem cell differentiation

It is striking that large numbers of cells in the aggregated delaminates already adopted a sensory neuron fate at the plated EB stage. This shows that some cells in the aggregates are already restricted in their developmental fate. It has been shown from studies in the mouse that the presence of the neural tube is essential for the differentiation of the dorsal root ganglion (Kalcheim and Le Douarin, 1986). The presence of the neural tube-like structures in the plated EB cultures could have a similar effect on the delaminated neural crest cells. This is most likely, as usually the differentiation of neural crest cells into sensory neurons requires the application of a growth factor cocktail. As sensory neurogenesis *in vivo* is conducted in three waves (for review see Marmigere and Ernfors, 2007), with the first wave differentiating predominantly into large mechanoreceptive and proprioceptive sensory neurons, the second wave leading to differentiation in all subtypes of sensory neurons and the third wave causing differentiation into small neurons, it will be interesting to investigate whether these early emerging sensory neurons represent the large mechanoreceptive and proprioceptive sensory neurons of the first developmental wave.

4.2 The human embryonic stem cell-based model as source for multipotent neural crest cells

Derivation of human embryonic stem cell-derived neural crest cells is fast and efficient

The research on human neural crest cells is still in the fledging stages but of high significance, considering the number of diseases related with neural crest malformation. In recent studies, hES cells have been discovered as potential source for neural crest cells and their progeny. The published protocols differ in the manner of neural crest induction, length of the culture periods, method of isolation of neural crest cells, and differentiation paradigms as well as obtained neural crest phenotypes. Several protocols use co-cultivation with stromal cells for neural induction (Lee et al., 2007; Pomp et al., 2005). Hotta and colleagues used a combination of co-cultivation with feeder or stromal cells and treatment with the small-molecule ROCK1/2 inhibitor Y27632 (Hotta et al., 2009). However, stromal cells are ill-defined, and co-cultivations are difficult to standardize. Chambers and colleagues detected an interesting population of early neural crest cells in neural rosette cultures derived by treatment with two inhibitors of the SMAD signaling pathway. Future studies will have to show the potential of this cell population and the differences compared to other hES cell-derived neural crest cells (Chambers et al., 2009). Another group isolated Cadherin-11-positive putative cranial neural crest cells from embryoid bodies and focused on the osteogenic potential of the cells (Jiang et al., 2009). Also, the generation of neural crest cells from hES cell-derived neural spheres has been shown (Curchoe et al., 2010). The most recent published study shows that the activation of Wnt signaling and suppression of the ActivinA/Nodal pathway led to direct differentiation from pluripotent stem cells to neural crest cells (Menendez et al., 2011). Each protocol for itself provides different interesting aspects for the research on hES cell-derived neural crest cells, however, they all face some drawbacks and many aspects regarding human neural crest development further remain unknown.

The here presented cell culture model offers a different perspective on neural crest development and presents some major advantages upon other *in vitro* settings. Additionally to the above-described capture of early neural crest development, it also offers practical benefits according to time, efficiency and span of applications. The segregation and aggregation of newly generated immature neural crest cells is exploited to efficiently purify a neural crest cell population. Already 6-8 days after EB plating, the crescent-shaped delaminates could be easily discerned and isolated with a canula or pipette tip. Manual isolation is a more efficient

method than FACS, as the same purity is achieved but additionally a higher quantity of cells is yielded. It is considerable faster and cheaper than FACSorting and less amenable to contamination. The isolated homogeneous cell population expressed typical neural crest markers such as p75NTR and SOX*E* with a purity of >95% and proliferated in culture. However, after prolonged culture the proliferation rate decreases and for differentiation experiments populations maintained for no longer than three passages were used. It is likely that FGF2 and EGF are not sufficient to keep the cells proliferating. Furthermore it has been observed that neuronal differentiation potential of the cells decreased over prolonged time in culture. This goes in line with published findings showing that over prolonged culture of neural crest cells the differentiation potential is shifted towards skeletogenic and osteogenic fates (Colleoni et al., 2010). The presence of the growth factor FGF2 may be one cause of this, as FGF2 is known to favor the mesenchymal differentiation of cranial neural crest cells (Sarkar et al., 2001). In this thesis, the chondrogenic effect of FGF2 has been used in the chondrocyte differentiation paradigm.

Further studies are required to find specific culture conditions that support proliferation and prolonged multipotency of the isolated hES cell-derived neural crest cells. It was shown by Sommer group that the combination of BMP and WNT keeps primary mouse neural crest cells in a proliferating state, while the sole application of BMP alone yields differentiation towards autonomic neurons and smooth muscle, whereas the sole application of WNT promotes the differentiation towards sensory neurons (Kleber et al., 2005). The protocol in its published form could not be successfully transferred to hES cell-derived neural crest cells (data not shown). Culture conditions may need to be adjusted to human neural crest cells in terms of application of other proliferation-inducing cues or additional factor combinations.

Another reason for the declining proliferation and differentiation capacity may be that probably the obtained neural crest population is rather a pool of fate-restricted progenitors than true multipotent neural crest stem cells. So the question comes up: Are neural crest cells specified at the time they are born or are they multipotent at first and then fate restricted by the environment they migrate into? This subject has been addressed by many neural crest researchers and extensively discussed in the literature. However, some studies point at contradictory results and there also seem to be specie specific differences, so that up to date the issue is not clarified (for review see Ruhrberg and Schwarz, 2010 and Sandell and Trainor, 2006).

One argument for the hypothesis of pre-specification of neural crest cells are the results of the lineage tracing studies of Krispin and colleagues, which suggest that avian neural crest derivatives follow a spatiotemporal fate map. The diversion of prospective neuronal precursors into the melanocytic pathway did not cause a change in their neuronal fate (Krispin et al., 2010). As neural crest migration routes change during development, with the first wave migrating medio-ventral and the second wave migrating dorso-lateral, another study examined whether early migrating neural crest cells will change their migration route when transplanted into older hosts and vice versa. Here it was found that neural crest cells did not change their migration route when transplanted into hosts at different stages of development, indicating that neural crest cells are pre-specified by the time of delamination and that their fate is not determined by environmental cues (Erickson and Goins, 1995). Another research result emphasizing the hypothesis of pre-specified neural crest cells is that prospective melanoblasts, which migrate as last wave from the neural tube, express melanogenic markers from their very emergence on (Thomas and Erickson, 2008).

Contradictory to these findings, studies on zebrafish and mice aiming at the transplantation of neural crest cells to different positions showed that plasticity of migrating neural crest cells depends on the size of the graft as well as on the developmental stage. The cell fate of transplanted individual cells was determined by the new environment, while grafts consisting of small groups of cells kept the fate determined by their origin. Also, adaption to the new environment was more efficient when transplantation was done during early development (Schilling et al., 2001; Trainor and Krumlauf, 2000) These studies point out that in addition to the impact of environmental cues, also cellular interactions between neural crest cells contribute to neural crest cell fate. Additionally, it was shown that apparently fate-restricted trunk neural crest cells, which during development do not give rise to cranial derivatives, could be differentiated towards mesenchymal derivatives by cultivating them in appropriate conditions or transplanting them in the cranial region (McGonnell and Graham, 2002; Real et al., 2005).

Isolated neural crest cells show upregulation of typical neural crest markers when compared to neural stem cells by microarray analysis

The conducted microarray analysis shows a significant upregulation of various neural crest-associated genes in the isolated neural crest aggregates in comparison to a stable proliferating neural stem cell line generated from the same parental hES cell line (lt-hESNSCs, Koch et al.,

2009). Among these are *NGFR* (*p75NTR*) and *SOX10*, genes typically used to identify neural crest cells. The expression of those markers could also be observed in the isolated population by RT-PCR, immunocytochemistry, as well as Western blot analysis. Two of the most upregulated genes in the isolated neural crest aggregates are *MSX1* and *TFAP2A*. Both genes have been shown to be important for cranial neural crest development (Ishii et al., 2005; Schorle et al., 1996). Mutations in these genes are also related with cleft lip or palate in humans (Milunsky et al., 2008; van den Boogaard et al., 2000). Dysregulation of *SOX9*, which is also strongly upregulated in the isolated neural crest cells, is also connected with orofacial disorders, such as Pierre Robin syndrome (Benko et al., 2009; Jakobsen et al., 2007). *TWIST* has been shown to be important for proper neural crest delamination and migration of mouse cranial neural crest cells (Vincentz et al., 2008). S100 proteins are widely expressed throughout many tissues and are also present in the neural crest and in its derivatives Schwann cells, melanocytes, chondrocytes and adipocytes. hES cell-derived neural crest cells show an upregulation of *S100A10* and *S100A11* (Kahn et al., 1984). *TFAP2B*, expressed in neural crest cells, has been shown to be involved in Char syndrome, which involves facial dysmorphism, patent ductus ateriosus and hand anomalies (Satoda et al., 2000).

The important role of Cadherins in neural crest delamination and migration has been described above. Microarray analysis showed an upregulation of *CDH11* (*Cadherin-11*) in the isolated neural crest aggregate in comparison to neural stem cells. Cadherin-11 is also known as osteoblast cadherin and is involved in skeletal development (Di Benedetto et al., 2010). This relates to the presented potential of hES cell-derived neural crest cells to differentiate into osteoblasts. *SNAI1* and *SNAI2*, both early neural crest determinants are also highly expressed in the isolated population. Members of the Snail family play an important role in neural crest specification. Furthermore, depletions of members of the Snail family led to severe craniofacial defects including cleft palate in mice (Murray et al., 2007). *ERBB3* encodes for receptor tyrosine-proetine kinase erbB-3, a member of the EGF receptor family, which binds to NRG-1. The NRG-1/ERbB system fulfils several functions in neural crest development. For instance, it promotes the development of Schwann cells, and was therefore used in the presented Schwann cell differentiation paradigm (Syroid et al., 1996). *EDNRA*, encoding for the endothelin receptor type A, is also upregulated in the isolated population. It binds to endothelin-1 (edn1) and supposedly is downstream of the early neural crest specifier *MSX1*, but upstream of *SOX9* and *SOX10 (Bonano et al., 2008)*. It has been shown to inhibit apoptosis

and is required for neural crest migration. Furthermore, mice depleted for Ednra/Edn1 die shortly after birth due to severe neural crest malformations, associated with cranial and cardiac neural crest cells. *POU4F1*, also known as *BRN3A,* is a transcription factor that plays a central role in the development of sensory neurons (Abe et al., 2007). The expression of this transcription factor has also been detected in the sensory neurons derived in this thesis by immunocytochemical analysis, as well as by RT-PCR. Although many upregulated genes detected in the microarray analysis point towards the mesenchymal differentiation potential, the upregulation of this gene demonstrates the neuronal differentiation potential of the hES cell-derived neural crest cells.

In addition to the upregulated neural crest associated genes in the isolated population, several genes linked to CNS development were found downregulated. These include *FABP7*, encoding for a brain fatty acid protein involved in neurogenesis in CNS development, the transcription factors *SOX3*, *SOX2*, as well as *PAX6*. *SOX2* and *PAX6* are, additionally to their expression in the developing CNS, also involved in the development of the lens and olfactory placode. *POU3F2* (*BRN2*), as well as *ASCL1* (*MASH1*), have recently been discovered as two of the three factors capable to directly convert murine fibroblasts into functional neurons *in vitro*. *PROM1*, also known as *CD133*, is a marker typical used to identify neural stem cells, which is also associated with several types of tumorigenic cells. *MMRN1* has been described as marker expressed in neural tube-like structures. *HES5*, a target gene of the Notch pathway, is involved in the maintenance of neural stem cells, in which it is highly expressed. Neural stem cells overexpressing HES5 fail to differentiate (Ohtsuka et al., 2001). Another gene upregulated in the lt-hESNSCs compared to the isolated neural crest population is *PLAGL1* (*ZAC1*). *PLAGL1* has been identified in the highly proliferating areas of the embryonic brain, as well as neural retina and neural tube. To sum up, the microarray analysis underlined the marker profile of the isolated hES cell-derived neural crest cells. Furthermore it can be excluded that the population harbors neural stem cells or are rather of placode identity. Placode cells also form cranial ganglia, but express a different marker profile. Additionally, they do not give rise to autonomic neurons, cartilage, or smooth muscle (Baker and Bronner-Fraser, 2001).

As other laboratories also published findings about pluripotent stem cell-derived neural crest cells, an interesting approach would be to compare the human neural crest cells derived in this work with other lines. Differences in differentiation potential and marker expression already

give a hint on different neural crest identities. The comparison could offer valuable cues regarding the characteristics of pluripotent stem cell-derived neural crest cells.

Implications for the derivation of neural stem cell lines from neural tube-like structures

The closely related development of neural crest cells and neural tube-like structures furthermore explains the often-observed contamination of neural stem cell populations with neural crest cells (Philipp Koch, personal communication). This contamination problem of neural rosette-derived neural stem cells might be avoided by application of agents inhibiting neural crest development. The BMP antagonist Noggin controls neural crest emergence *in vivo* by inhibiting BMP4, which is needed for neural crest delamination (Sela-Donenfeld and Kalcheim, 2000). Application of BMP antagonists, such as Noggin, in a neural crest differentiation protocol has been shown to reduce the number of obtained neural crest cells (Lee et al., 2007). Another candidate for neural crest abrogation is the anti-inflammatory drug leflunomide, which inhibits dihydroorotate dehydrogenase and has been shown to completely prevent neural crest development (White et al., 2011). Obviously, the inhibition of neural crest development does not only play a role in protocols aiming at the derivation of pure cultures of neural stem cells, it is also of high importance in the study of neural crest-derived tumours, such as melanoma and schwannoma. The here described cell culture model offers the possibility to study effects of neural crest inhibitors in an *in vitro* setting.

Manually isolated neural crest cells differentiate into peripheral neurons and glia

Upon manual isolation and singularizing of neural crest aggregates, differentiation of neural crest cells into 21.7±5.1% Peripherin/BRN3A positive cells, a marker combination commonly used for sensory neurons, was feasible. The application of recombinant WNT1 was not required for differentiation of hES cell-derived neural crest cells into sensory neurons. However, it has been shown that neural crest cells that can be efficiently differentiated into sensory neurons in the presence of WNT (Lee et al., 2004). It has also been reported that neural crest cells lose their responsiveness to WNT when cultured for a prolonged period of time (Kléber et al., 2005). In our hands, addition of WNT yielded only a minor increase in the amount of Peripherin/BRN3A positive sensory neurons, but increased the survival of differentiated neurons (data not shown). According to Zirlinger and colleagues, neural crest cells acquire a de-

velopmental bias towards neuronal fate early in their development (Zirlinger et al., 2002), as also discussed above. In agreement with this finding stands the observation made in this work that neural crest cells cultivated for prolonged periods of time were less accessible to the neuronal differentiation paradigm (data not shown). This has also been reported for hES cell-derived neural crest cells from other groups and for neural stem cells (Colleoni et al., 2010; Elkabetz et al., 2008).

The RT-PCR profile offered valuable cues to the identity of differentiated neurons. On the one hand, the sensory neuronal fate was confirmed, as cells showed expression of *POU4F1* (*BRN3A*), as well as *SOX10*, and *PAX3*, which also play a role in sensory neurogenesis (Carney et al., 2006; Koblar et al., 1999). The expression of *PAX3* and *SOX10* in sensory neurogenesis and in undifferentiated neural crest cells is a good example for the complex gene regulatory network of neural crest cells. Many of the described genes are of recurrent importance during the life of neural crest cells. Some genes that play key roles in delamination or maintenance of neural crest stemness are again present in differentiated lineages.

For the more detailed apportionment of the obtained neuronal population, the expression of NTRKs was investigated. While the detected *NTRK1 (TrkA)* marks small diameter neurons, *NTRK2* (*TrkB*) and *NTRK3* (*TrkC)* are expressed in large diameter neurons of the dorsal root ganglion (Mu et al., 1993). Consequently it can be recorded that the isolated neural crest cell population gives rise to different subtypes of sensory neurons. Further investigation of sensory neurogenesis will greatly contribute to the understanding of diseases associated with the loss of sensory neurons and consequently for the development of therapeutic approaches.

In addition to sensory neurons a small percentage of Peripherin/TH positive cells could be obtained, indicating peripheral neurons of the autonomic type. RT-PCR also showed expression of *TH* on molecular level. Surprisingly, *TH* could also be detected in proliferating neural crest cells. This observation is coherent with published data from Young and colleagues, showing that *TH* is already expressed in a subset of proliferating neural crest cells (Young et al., 1999). The expression of *ASCL1* and *PHOX2B* mRNA in differentiated cultures could be detected as well. Both genes are essential for the development of the peripheral autonomic nervous system, which main components are the sympathetic, parasympathetic and enteric ganglia (Guillemot et al., 1993; Pattyn et al., 1999). No *HB9* expression was detected in the cultures, so that it can be excluded that the expression of those markers originates from CNS motorneurons derived from possibly contaminating neural stem cells. Importantly, those cells

were generated without external stimulation with BMPs. It has been shown that BMP enhances autonomic neurogenesis by causing an upregulation of the transcription factor *ASCL1* (Gossrau et al., 2007; Kleber et al., 2005; Mizuseki et al., 2003; Shah et al., 1996) suggesting that additional application of BMPs could be used to further increase the numbers of peripheral autonomic neurons in the differentiated culture.

Additionally to the expression of specific antigens assessed by immunocytochemical analysis and the expression of neuronal-associated genes assessed by RT-PCR, the functionality of the differentiated neurons was shown by electrophysiological measurements. All neurons tested fired action potentials during current injection. Also, the peripheral neurons formed functional synapses, as spontaneous postsynaptic currents were observed in whole-cell voltage-clamp recordings.

In addition to neurons of the peripheral nervous system, hES cell-derived neural crest cells give rise to putative Schwann cells, which express combinations of Schwann cell markers as assessed by immunocytochemical analysis and RT-PCR. Cells showed expression of L1CAM, GFAP, p75NTR, CNP, SOX10, and EGR2 (for review see Jessen and Mirsky, 2005). SOX10 and p75NTR are expressed in proliferating neural crest cells as well as in Schwann cells derived thereof. The same is true for L1CAM. The neuronal cell adhesion molecule has been shown to be important for the migration of neural crest cells and is also retained in Schwann cells (Anderson et al., 2006b; Jessen and Mirsky, 2005).

The surprisingly high expression of *CNP* already in proliferating cells is compatible with published data showing the early activation of the *CNP* promoter in neural crest progenitors (Chandross et al., 1999). It will be interesting to further investigate whether the hES cell-derived Schwann cells are able to form myelin. This could be either achieved *in vitro* by co-cultivation with dorsal root ganglion cultures or by transplanting them into nerve-injured animal models.

Schwann cells derived from pluripotent cells could gain intensive attention in terms of cell replacement therapies, especially with progressing iPS technology. Not only could they be used for remyelination in the injured or diseased PNS, they also provoke promises for CNS repair, in terms of trauma or demyelination disorders (Lavdas et al., 2008). Additionally they could be used as vehicles to secrete active agents facilitating spinal cord repair. In general, for

enrichment of peripheral glia one could think of an intermediate purification step of precursor cells. Prior to the terminal differentiation step, FACSorting for early Schwann cell markers, like e.g. L1CAM could be applied to enrich the cultures. Thereby it could be possible to generate Schwann cell cultures of high purities.

Manually isolated neural crest cells have the potential to differentiate into cranial neural crest phenotypes

In addition to neural phenotypes manually isolated neural crest cells could be successfully differentiated into smooth muscle, osteoblasts, chondrocytes and adipocytes. For smooth muscle differentiation it was sufficient to add 10% FCS to the culture medium. This has also been described in other hES cell-derived neural crest cells (Colleoni et al., 2010). As RT-PCR revealed expression of *ACTG2* (*γSMA*), the hES cell-derived neural crest cells exhibit potential to differentiate into enteric smooth muscle. This is in line with the detected enteric neuron marker *PHOX2B* expression after neuronal differentiation. Enteric neural crest derivatives can either have a vagal or sacral origin (Anderson et al., 2006a), the identity of the cells differentiated by this paradigm could not be determined.

Distinct culture conditions promoted the formation of chondocytes, osteoblasts, and adipocytes. For chondrogenesis, FGF2 as well as FGF8 have been identified as inducer (Ido and Ito, 2006; Trainor et al., 2002). In the presented cell culture paradigm, FGF2 in combination with Forskolin and the presence of FCS, led to the formation of cartilage-like clusters. For the osteogenic and adipogenic differentiation, published medium conditions were applied (Fang et al., 2005). For the differentiation of osteoblasts, Dexamethasone was used, a synthetic steroid hormone of the glucocorticoid class. Medically prescribed as anti-inflammatory drug, it is known to have a positive effect on osteoblast proliferation and differentiation (Cheng et al., 1994). Relatively little is known about the differentiation of adipocytes from the neural crest in comparison to other neural crest-derived mesenchymal cells, although Le Lievre and Le Douarin already suggested in their pioneer work of 1975 that some facial adipocytes are neural crest derived. Back then it was discovered that the adipocytes around the trachea and parasympathetic enteric ganglia, as well as the adipocytes in the skin under the skullcap and in the ventral part of the neck are of neural crest origin (Le Lievre and Le Douarin, 1975). Recent work has shown that mouse ES cell-derived neural crest cells give rise to adipocytes *in vitro*. In the same publication it was suggested that the adipocytes in the ear region and salivary

gland are also neural crest derived (Billon et al., 2007). In this thesis for the *in vitro* differentiation of human neural crest cells, hydrocortisone, another steroid hormone of the same class as Dexamethasone but naturally occurring and produced by the adrenal gland, was applied for adipocyte differentiation. Hydrocortisone causes adipocytes to store fat, explaining why adiposity is a common side effect of long-term medication with hydrocortisone. Hydrocortisone is widely used in differentiation paradigms of mesenchymal cells (Eshel et al., 1990). Isobutylmethylxanthine is another adipogenic agent, which was used in the presented differentiation paradigm. Isobutylmethylxanthine increases the intracellular level of cAMP and additionally acts on the upregulation of adipocyte transcripition factors (Elks and Manganiello, 1985). Staining of intracellular lipid droplets with oil red could demonstratively identify the fat cells differentiated by this treatment from the isolated hES cell-derived neural crest population. The observation that the hES cell-derived neural crest cells give rise to chondrocytes, osteoblasts and adipocytes indicate that the derived cell population displays a cranial identity. This hypothesis is supported by the expression of *HOXA2* and *–B2*, *OTX2* and *GBX2*. *In vivo*, *HOXA2* and *–B2* mark neural crest cells migrating in the second brachial arch (Hunt et al., 1991). Additionally expression of *GBX2* and *OTX2*, both expressed in cranial migrating neural crest cells (Kikuta et al., 2003; Kimura et al., 1997) was detected. The expression profile, as well as the mesenchymal derivatives, suggests that cells exhibit a cranial identity. However, as neural crest cells from different regions have been shown to exhibit plasticity (Trainor and Krumlauf, 2000), it cannot be excluded that the applied culture conditions caused committed neural crest cells to regain multipotency, as it has been shown for trunk neural crest cells in the mouse (McGonnell and Graham, 2002). Therefore the possibility exists that the isolated cell population is a mixed pool of neural crest cells of different regional identities instead of a neural crest cell population with true stem cell characteristic.

While hES cell-derived neural crest cells could be successfully differentiated into peripheral neurons and glia as well as to mesenchymal derivatives, differentiation towards melanocytes could not be achieved in this thesis. Future studies will show whether improved culture conditions will lead to melanocyte differentiation or whether the melanocyte lineage arises from another already restricted neural crest ancestor cell, which is not accessible at this time point and using this type of isolation. Although some published protocols show the differentiation of pigment cells from hES cell-derived neural crest cells, it remains to be clarified whether the obtained cells are truly melanocytes or retina pigmented epithelial cells derived from placode

cells. Even though both cell types display a pigmented phenotype, they differ in their morphology. Retina pigmented epithelial cells exhibit a small roundish cell shape, while melanocytes have widely branched dendrites.

Although it could be shown that isolated neural crest cells give rise to several neural crest phenotypes, analysis of isolated cells at a clonal density will help understanding whether these cells exhibit true fate plasticity. It will be interesting to investigate whether the isolated cell population is a pool of already committed neural crest precursor cells or a neural crest *stem* cell population, for which the ideal propagating culture conditions have not been found yet.

4.3 Outlook

Due to the fact that the *in vivo* situation of neural crest cells development can be mimicked and followed *in vitro*, the hES cell-based cell culture model presented here provides important insights regarding emergence, migration, re-aggregation and differentiation of human neural crest cells. It can serve as a useful tool for the investigation of signaling pathways involved in human neural crest development. Another interesting approach is transplantation of isolated hES cell-derived neural crest cells into embryonic chicken in order to investigate their migration pathways and differentiation behavior. As described above, several protocols show different approaches for the derivation of neural crest cells from hES and iPS cells (for review see Chimge and Bayarsaihan, 2009 and Achilleos and Trainor, 2012). It will be interesting to compare those alternatively derived neural crest cells, e.g. by microarray analysis and to investigate whether differences exist regarding their transcriptional profile. Possibly they exhibit a different regional identity and therefore also display a distinctive differentiation potential.

The knowledge that can be gained by using this hES cell-based model may lead to a better understanding of diseases related with neural crest abnormalities, including neural crest related cancers like neuroblastomas and schwannomas, but also of diseases associated with neural crest malformations. As the hES cell-derived neural crest cells presented in this thesis express several markers of cranial neural crest cells, diseases especially caused by abnormal development of those cells will be interesting targets, such as cleft lip and palate, Bardet-Biedl syndrome, CHARGE syndrome or DiGeorge syndrome. The fast growing field of iPS cell technology offers a broad range of new possibilities regarding this matter in this area. A

recent study shows the use of patient-specific cell lines as disease model for familial dysautonomia (Lee et al. 2009). Due to its quoted advantages the model system described here could also be adapted and efficiently used in iPS cell research for disease modeling of neurocristopathies.

5 References

Aasen, T., Raya, A., Barrero, M. J., Garreta, E., Consiglio, A., Gonzalez, F., Vassena, R., Bilic, J., Pekarik, V., Tiscornia, G. et al. (2008). Efficient and rapid generation of induced pluripotent stem cells from human keratinocytes. *Nat Biotechnol* **26**, 1276-84.

Abe, M., Ruest, L. B. and Clouthier, D. E. (2007). Fate of cranial neural crest cells during craniofacial development in endothelin-A receptor-deficient mice. *Int J Dev Biol* **51**, 97-105.

Achilleos, A. and Trainor, P. A. (2012). Neural crest stem cells: discovery, properties and potential for therapy. *Cell Res*.

Akitaya, T. and Bronner-Fraser, M. (1992). Expression of cell adhesion molecules during initiation and cessation of neural crest cell migration. *Dev Dyn* **194**, 12-20.

Amit, M., Carpenter, M. K., Inokuma, M. S., Chiu, C. P., Harris, C. P., Waknitz, M. A., Itskovitz-Eldor, J. and Thomson, J. A. (2000). Clonally derived human embryonic stem cell lines maintain pluripotency and proliferative potential for prolonged periods of culture. *Dev Biol* **227**, 271-8.

Amit, M., Shariki, C., Margulets, V. and Itskovitz-Eldor, J. (2004). Feeder layer- and serum-free culture of human embryonic stem cells. *Biol Reprod* **70**, 837-45.

Anderson, R. B., Stewart, A. L. and Young, H. M. (2006a). Phenotypes of neural-crest-derived cells in vagal and sacral pathways. *Cell Tissue Res* **323**, 11-25.

Anderson, R. B., Turner, K. N., Nikonenko, A. G., Hemperly, J., Schachner, M. and Young, H. M. (2006b). The cell adhesion molecule l1 is required for chain migration of neural crest cells in the developing mouse gut. *Gastroenterology* **130**, 1221-32.

Anokye-Danso, F., Trivedi, C. M., Juhr, D., Gupta, M., Cui, Z., Tian, Y., Zhang, Y., Yang, W., Gruber, P. J., Epstein, J. A. et al. (2011). Highly efficient miRNA-mediated reprogramming of mouse and human somatic cells to pluripotency. *Cell Stem Cell* **8**, 376-88.

Avilion, A. A., Nicolis, S. K., Pevny, L. H., Perez, L., Vivian, N. and Lovell-Badge, R. (2003). Multipotent cell lineages in early mouse development depend on SOX2 function. *Genes Dev* **17**, 126-40.

Baker, C. V. and Bronner-Fraser, M. (2001). Vertebrate cranial placodes I. Embryonic induction. *Dev Biol* **232**, 1-61.

Belmadani, A., Tran, P. B., Ren, D., Assimacopoulos, S., Grove, E. A. and Miller, R. J. (2005). The chemokine stromal cell-derived factor-1 regulates the migration of sensory neuron progenitors. *J Neurosci* **25**, 3995-4003.

Benko, S., Fantes, J. A., Amiel, J., Kleinjan, D. J., Thomas, S., Ramsay, J., Jamshidi, N., Essafi, A., Heaney, S., Gordon, C. T. et al. (2009). Highly conserved non-coding elements on either side of SOX9 associated with Pierre Robin sequence. *Nat Genet* **41**, 359-64.

Betters, E., Liu, Y., Kjaeldgaard, A., Sundstrom, E. and Garcia-Castro, M. I. (2010). Analysis of early human neural crest development. *Dev Biol* **344**, 578-92.

Billon, N., Iannarelli, P., Monteiro, M. C., Glavieux-Pardanaud, C., Richardson, W. D., Kessaris, N., Dani, C. and Dupin, E. (2007). The generation of adipocytes by the neural crest. *Development* **134**, 2283-92.

Bodine, P. V., Green, J., Harris, H. A., Bhat, R. A., Stein, G. S., Lian, J. B. and Komm, B. S. (1997). Functional properties of a conditionally phenotypic, estrogen-responsive, human osteoblast cell line. *J Cell Biochem* **65**, 368-87.

Bonano, M., Tribulo, C., De Calisto, J., Marchant, L., Sanchez, S. S., Mayor, R. and Aybar, M. J. (2008). A new role for the Endothelin-1/Endothelin-A receptor signaling during early neural crest specification. *Dev Biol* **323**, 114-29.

Borchers, A., David, R. and Wedlich, D. (2001). Xenopus cadherin-11 restrains cranial neural crest migration and influences neural crest specification. *Development* **128**, 3049-60.

Briscoe, J., Sussel, L., Serup, P., Hartigan-O'Connor, D., Jessell, T. M., Rubenstein, J. L. and Ericson, J. (1999). Homeobox gene Nkx2.2 and specification of neuronal identity by graded Sonic hedgehog signalling. *Nature* **398**, 622-7.

Britsch, S., Li, L., Kirchhoff, S., Theuring, F., Brinkmann, V., Birchmeier, C. and Riethmacher, D. (1998). The ErbB2 and ErbB3 receptors and their ligand, neuregulin-1, are essential for development of the sympathetic nervous system. *Genes Dev* **12**, 1825-36.

Burns, A. J. and Douarin, N. M. (1998). The sacral neural crest contributes neurons and glia to the post-umbilical gut: spatiotemporal analysis of the development of the enteric nervous system. *Development* **125**, 4335-47.

Carmona-Fontaine, C., Matthews, H. K., Kuriyama, S., Moreno, M., Dunn, G. A., Parsons, M., Stern, C. D. and Mayor, R. (2008). Contact inhibition of locomotion in vivo controls neural crest directional migration. *Nature* **456**, 957-61.

Carney, T. J., Dutton, K. A., Greenhill, E., Delfino-Machin, M., Dufourcq, P., Blader, P. and Kelsh, R. N. (2006). A direct role for Sox10 in specification of neural crest-derived sensory neurons. *Development* **133**, 4619-30.

Chambers, I., Colby, D., Robertson, M., Nichols, J., Lee, S., Tweedie, S. and Smith, A. (2003). Functional expression cloning of Nanog, a pluripotency sustaining factor in embryonic stem cells. *Cell* **113**, 643-55.

Chambers, S. M., Fasano, C. A., Papapetrou, E. P., Tomishima, M., Sadelain, M. and Studer, L. (2009). Highly efficient neural conversion of human ES and iPS cells by dual inhibition of SMAD signaling. *Nat Biotechnol* **27**, 275-80.

Chandross, K. J., Cohen, R. I., Paras, P., Jr., Gravel, M., Braun, P. E. and Hudson, L. D. (1999). Identification and characterization of early glial progenitors using a transgenic selection strategy. *J Neurosci* **19**, 759-74.

Cheng, S. L., Yang, J. W., Rifas, L., Zhang, S. F. and Avioli, L. V. (1994). Differentiation of human bone marrow osteogenic stromal cells in vitro: induction of the osteoblast phenotype by dexamethasone. *Endocrinology* **134**, 277-86.

Chimge, N. O. and Bayarsaihan, D. (2009). Generation of neural crest progenitors from human embryonic stem cells. *J Exp Zoolog B Mol Dev Evol*.

Clarke, D. L., Johansson, C. B., Wilbertz, J., Veress, B., Nilsson, E., Karlstrom, H., Lendahl, U. and Frisen, J. (2000). Generalized potential of adult neural stem cells. *Science* **288**, 1660-3.

Coffman, C. R., Skoglund, P., Harris, W. A. and Kintner, C. R. (1993). Expression of an extracellular deletion of Xotch diverts cell fate in Xenopus embryos. *Cell* **73**, 659-71.

Colleoni, S., Galli, C., Giannelli, S. G., Armentero, M. T., Blandini, F., Broccoli, V. and Lazzari, G. (2010). Long-term culture and differentiation of CNS precursors derived from anterior human neural rosettes following exposure to ventralizing factors. *Exp Cell Res* **316**, 1148-58.

Curchoe, C. L., Maurer, J., McKeown, S. J., Cattarossi, G., Cimadamore, F., Nilbratt, M., Snyder, E. Y., Bronner-Fraser, M. and Terskikh, A. V. (2010). Early Acquisition of Neural Crest Competence During hESCs Neuralization. *PLoS One* **5**, e13890.

Debby-Brafman, A., Burstyn-Cohen, T., Klar, A. and Kalcheim, C. (1999). F-Spondin, expressed in somite regions avoided by neural crest cells, mediates inhibition of distinct somite domains to neural crest migration. *Neuron* **22**, 475-88.

Di Benedetto, A., Watkins, M., Grimston, S., Salazar, V., Donsante, C., Mbalaviele, G., Radice, G. L. and Civitelli, R. (2010). N-cadherin and cadherin 11 modulate postnatal bone growth and osteoblast differentiation by distinct mechanisms. *J Cell Sci* **123**, 2640-8.

Dickinson, M. E., Selleck, M. A., McMahon, A. P. and Bronner-Fraser, M. (1995). Dorsalization of the neural tube by the non-neural ectoderm. *Development* **121**, 2099-106.

Dickman, E. D., Thaller, C. and Smith, S. M. (1997). Temporally-regulated retinoic acid depletion produces specific neural crest, ocular and nervous system defects. *Development* **124**, 3111-21.

Dimos, J. T., Rodolfa, K. T., Niakan, K. K., Weisenthal, L. M., Mitsumoto, H., Chung, W., Croft, G. F., Saphier, G., Leibel, R., Goland, R. et al. (2008). Induced pluripotent stem cells generated from patients with ALS can be differentiated into motor neurons. *Science* **321**, 1218-21.

Duband, J. L. (2006). Neural crest delamination and migration: integrating regulations of cell interactions, locomotion, survival and fate. *Adv Exp Med Biol* **589**, 45-77.

Duband, J. L., Monier, F., Delannet, M. and Newgreen, D. (1995). Epithelium-mesenchyme transition during neural crest development. *Acta Anat (Basel)* **154**, 63-78.

Duband, J. L. and Thiery, J. P. (1987). Distribution of laminin and collagens during avian neural crest development. *Development* **101**, 461-78.

Dufour, S., Beauvais-Jouneau, A., Delouvee, A. and Thiery, J. P. (1999). Differential function of N-cadherin and cadherin-7 in the control of embryonic cell motility. *J Cell Biol* **146**, 501-16.

Duggan, C. D., DeMaria, S., Baudhuin, A., Stafford, D. and Ngai, J. (2008). Foxg1 is required for development of the vertebrate olfactory system. *J Neurosci* **28**, 5229-39.

Ebert, A. D., Yu, J., Rose, F. F., Jr., Mattis, V. B., Lorson, C. L., Thomson, J. A. and Svendsen, C. N. (2009). Induced pluripotent stem cells from a spinal muscular atrophy patient. *Nature* **457**, 277-80.

Elkabetz, Y., Panagiotakos, G., Al Shamy, G., Socci, N. D., Tabar, V. and Studer, L. (2008). Human ES cell-derived neural rosettes reveal a functionally distinct early neural stem cell stage. *Genes Dev* **22**, 152-65.

Elks, M. L. and Manganiello, V. C. (1985). A role for soluble cAMP phosphodiesterases in differentiation of 3T3-L1 adipocytes. *J Cell Physiol* **124**, 191-8.

Endo, Y., Osumi, N. and Wakamatsu, Y. (2002). Bimodal functions of Notch-mediated signaling are involved in neural crest formation during avian ectoderm development. *Development* **129**, 863-73.

Erickson, C. A. and Goins, T. L. (1995). Avian neural crest cells can migrate in the dorsolateral path only if they are specified as melanocytes. *Development* **121**, 915-24.

Eshel, I., Savion, N. and Shoham, J. (1990). Analysis of thymic stromal cell subpopulations grown in vitro on extracellular matrix in defined medium. I. Growth conditions and morphology of murine thymic epithelial and mesenchymal cells. *J Immunol* **144**, 1554-62.

Evans, M. J. and Kaufman, M. H. (1981). Establishment in culture of pluripotential cells from mouse embryos. *Nature* **292**, 154-6.

Fang, D., Leishear, K., Nguyen, T. K., Finko, R., Cai, K., Fukunaga, M., Li, L., Brafford, P. A., Kulp, A. N., Xu, X. et al. (2006). Defining the conditions for the generation of melanocytes from human embryonic stem cells. *Stem Cells* **24**, 1668-77.

Fang, D., Nguyen, T. K., Leishear, K., Finko, R., Kulp, A. N., Hotz, S., Van Belle, P. A., Xu, X., Elder, D. E. and Herlyn, M. (2005). A tumorigenic subpopulation with stem cell properties in melanomas. *Cancer Res* **65**, 9328-37.

Fedtsova, N. G. and Turner, E. E. (1995). Brn-3.0 expression identifies early post-mitotic CNS neurons and sensory neural precursors. *Mech Dev* **53**, 291-304.

Gammill, L. S., Gonzalez, C., Gu, C. and Bronner-Fraser, M. (2006). Guidance of trunk neural crest migration requires neuropilin 2/semaphorin 3F signaling. *Development* **133**, 99-106.

Gossrau, G., Thiele, J., Konang, R., Schmandt, T. and Brustle, O. (2007). Bone morphogenetic protein-mediated modulation of lineage diversification during neural differentiation of embryonic stem cells. *Stem Cells* **25**, 939-49.

Guillemot, F., Lo, L. C., Johnson, J. E., Auerbach, A., Anderson, D. J. and Joyner, A. L. (1993). Mammalian achaete-scute homolog 1 is required for the early development of olfactory and autonomic neurons. *Cell* **75**, 463-76.

Guthrie, S. (2007). Patterning and axon guidance of cranial motor neurons. *Nat Rev Neurosci* **8**, 859-71.

Haase, A., Olmer, R., Schwanke, K., Wunderlich, S., Merkert, S., Hess, C., Zweigerdt, R., Gruh, I., Meyer, J., Wagner, S. et al. (2009). Generation of induced pluripotent stem cells from human cord blood. *Cell Stem Cell* **5**, 434-41.

Hatta, K., Takagi, S., Fujisawa, H. and Takeichi, M. (1987). Spatial and temporal expression pattern of N-cadherin cell adhesion molecules correlated with morphogenetic processes of chicken embryos. *Dev Biol* **120**, 215-27.

Hauner, H., Entenmann, G., Wabitsch, M., Gaillard, D., Ailhaud, G., Negrel, R. and Pfeiffer, E. F. (1989). Promoting effect of glucocorticoids on the differentiation of human adipocyte precursor cells cultured in a chemically defined medium. *J Clin Invest* **84**, 1663-70.

Heanue, T. A. and Pachnis, V. (2007). Enteric nervous system development and Hirschsprung's disease: advances in genetic and stem cell studies. *Nat Rev Neurosci* **8**, 466-79.

Honma, Y., Araki, T., Gianino, S., Bruce, A., Heuckeroth, R., Johnson, E. and Milbrandt, J. (2002). Artemin is a vascular-derived neurotropic factor for developing sympathetic neurons. *Neuron* **35**, 267-82.

Hotta, R., Pepdjonovic, L., Anderson, R. B., Zhang, D., Bergner, A. J., Leung, J., Pebay, A., Young, H. M., Newgreen, D. F. and Dottori, M. (2009). Small-molecule induction of neural crest-like cells derived from human neural progenitors. *Stem Cells* **27**, 2896-905.

Hunt, P., Wilkinson, D. and Krumlauf, R. (1991). Patterning the vertebrate head: murine Hox 2 genes mark distinct subpopulations of premigratory and migrating cranial neural crest. *Development* **112**, 43-50.

Ido, A. and Ito, K. (2006). Expression of chondrogenic potential of mouse trunk neural crest cells by FGF2 treatment. *Dev Dyn* **235**, 361-7.

Ikenouchi, J., Matsuda, M., Furuse, M. and Tsukita, S. (2003). Regulation of tight junctions during the epithelium-mesenchyme transition: direct repression of the gene expression of claudins/occludin by Snail. *J Cell Sci* **116**, 1959-67.

Ikeya, M., Lee, S. M., Johnson, J. E., McMahon, A. P. and Takada, S. (1997). Wnt signalling required for expansion of neural crest and CNS progenitors. *Nature* **389**, 966-70.

Inzunza, J., Gertow, K., Stromberg, M. A., Matilainen, E., Blennow, E., Skottman, H., Wolbank, S., Ahrlund-Richter, L. and Hovatta, O. (2005). Derivation of human embryonic stem cell lines in serum replacement medium using postnatal human fibroblasts as feeder cells. *Stem Cells* **23**, 544-9.

Ishii, M., Han, J., Yen, H. Y., Sucov, H. M., Chai, Y. and Maxson, R. E., Jr. (2005). Combined deficiencies of Msx1 and Msx2 cause impaired patterning and survival of the cranial neural crest. *Development* **132**, 4937-50.

Jaiswal, N., Haynesworth, S. E., Caplan, A. I. and Bruder, S. P. (1997). Osteogenic differentiation of purified, culture-expanded human mesenchymal stem cells in vitro. *J Cell Biochem* **64**, 295-312.

Jakobsen, L. P., Ullmann, R., Christensen, S. B., Jensen, K. E., Molsted, K., Henriksen, K. F., Hansen, C., Knudsen, M. A., Larsen, L. A., Tommerup, N. et al. (2007). Pierre Robin sequence may be caused by dysregulation of SOX9 and KCNJ2. *J Med Genet* **44**, 381-6.

Jessen, K. R. and Mirsky, R. (2005). The origin and development of glial cells in peripheral nerves. *Nat Rev Neurosci* **6**, 671-82.

Jesuthasan, S. (1996). Contact inhibition/collapse and pathfinding of neural crest cells in the zebrafish trunk. *Development* **122**, 381-9.

Jia, L., Cheng, L. and Raper, J. (2005). Slit/Robo signaling is necessary to confine early neural crest cells to the ventral migratory pathway in the trunk. *Dev Biol* **282**, 411-21.

Jiang, X., Gwye, Y., McKeown, S. J., Bronner-Fraser, M., Lutzko, C. and Lawlor, E. R. (2009). Isolation and characterization of neural crest stem cells derived from in vitro-differentiated human embryonic stem cells. *Stem Cells Dev* **18**, 1059-70.

Jiang, X., Iseki, S., Maxson, R. E., Sucov, H. M. and Morriss-Kay, G. M. (2002). Tissue origins and interactions in the mammalian skull vault. *Dev Biol* **241**, 106-16.

Johnston, M. C. (1966). A radioautographic study of the migration and fate of cranial neural crest cells in the chick embryo. *Anat Rec* **156**, 143-55.

Jungnickel, J., Haase, K., Konitzer, J., Timmer, M. and Grothe, C. (2006). Faster nerve regeneration after sciatic nerve injury in mice over-expressing basic fibroblast growth factor. *J Neurobiol* **66**, 940-8.

Kahn, H. J., Baumal, R. and Marks, A. (1984). The value of immunohistochemical studies using antibody to S100 protein in dermatopathology. *Int J Dermatol* **23**, 38-44.

Kalcheim, C. (1989). Basic fibroblast growth factor stimulates survival of nonneuronal cells developing from trunk neural crest. *Dev Biol* **134**, 1-10.

Kalcheim, C. and Le Douarin, N. M. (1986). Requirement of a neural tube signal for the differentiation of neural crest cells into dorsal root ganglia. *Dev Biol* **116**, 451-66.

Kasemeier-Kulesa, J. C., Bradley, R., Pasquale, E. B., Lefcort, F. and Kulesa, P. M. (2006). Eph/ephrins and N-cadherin coordinate to control the pattern of sympathetic ganglia. *Development* **133**, 4839-47.

Kaufman, D. S., Hanson, E. T., Lewis, R. L., Auerbach, R. and Thomson, J. A. (2001). Hematopoietic colony-forming cells derived from human embryonic stem cells. *Proc Natl Acad Sci U S A* **98**, 10716-21.

Kawasaki, H., Mizuseki, K., Nishikawa, S., Kaneko, S., Kuwana, Y., Nakanishi, S., Nishikawa, S. I. and Sasai, Y. (2000). Induction of midbrain dopaminergic neurons from ES cells by stromal cell-derived inducing activity. *Neuron* **28**, 31-40.

Kawasaki, T., Bekku, Y., Suto, F., Kitsukawa, T., Taniguchi, M., Nagatsu, I., Nagatsu, T., Itoh, K., Yagi, T. and Fujisawa, H. (2002). Requirement of neuropilin 1-mediated Sema3A signals in patterning of the sympathetic nervous system. *Development* **129**, 671-80.

Kehat, I., Kenyagin-Karsenti, D., Snir, M., Segev, H., Amit, M., Gepstein, A., Livne, E., Binah, O., Itskovitz-Eldor, J. and Gepstein, L. (2001). Human embryonic stem cells can differentiate into myocytes with structural and functional properties of cardiomyocytes. *J Clin Invest* **108**, 407-14.

Kikuta, H., Kanai, M., Ito, Y. and Yamasu, K. (2003). gbx2 Homeobox gene is required for the maintenance of the isthmic region in the zebrafish embryonic brain. *Dev Dyn* **228**, 433-50.

Kil, S. H., Krull, C. E., Cann, G., Clegg, D. and Bronner-Fraser, M. (1998). The alpha4 subunit of integrin is important for neural crest cell migration. *Dev Biol* **202**, 29-42.

Kim, J. B., Greber, B., Arauzo-Bravo, M. J., Meyer, J., Park, K. I., Zaehres, H. and Scholer, H. R. (2009). Direct reprogramming of human neural stem cells by OCT4. *Nature* **461**, 649-3.

Kimura, C., Takeda, N., Suzuki, M., Oshimura, M., Aizawa, S. and Matsuo, I. (1997). Cis-acting elements conserved between mouse and pufferfish Otx2 genes govern the expression in mesencephalic neural crest cells. *Development* **124**, 3929-41.

Kimura, Y., Matsunami, H., Inoue, T., Shimamura, K., Uchida, N., Ueno, T., Miyazaki, T. and Takeichi, M. (1995). Cadherin-11 expressed in association with mesenchymal morphogenesis in the head, somite, and limb bud of early mouse embryos. *Dev Biol* **169**, 347-58.

Kirby, M. L., Gale, T. F. and Stewart, D. E. (1983). Neural crest cells contribute to normal aorticopulmonary septation. *Science* **220**, 1059-61.

Kleber, M., Lee, H. Y., Wurdak, H., Buchstaller, J., Riccomagno, M. M., Ittner, L. M., Suter, U., Epstein, D. J. and Sommer, L. (2005). Neural crest stem cell maintenance by combinatorial Wnt and BMP signaling. *J Cell Biol* **169**, 309-20.

Kléber, M., Lee, H. Y., Wurdak, H., Buchstaller, J., Riccomagno, M. M., Ittner, L. M., Suter, U., Epstein, D. J. and Sommer, L. (2005). Neural crest stem cell maintenance by combinatorial Wnt and BMP signaling. In *J Cell Biol*, vol. 169 (ed., pp. 309-20.

Koblar, S. A., Murphy, M., Barrett, G. L., Underhill, A., Gros, P. and Bartlett, P. F. (1999). Pax-3 regulates neurogenesis in neural crest-derived precursor cells. *J Neurosci Res* **56**, 518-30.

Koch, P., Breuer, P., Peitz, M., Jungverdorben, J., Kesavan, J., Poppe, D., Doerr, J., Ladewig, J., Mertens, J., Tuting, T. et al. (2011). Excitation-induced ataxin-3 aggregation in neurons from patients with Machado-Joseph disease. *Nature* **480**, 543-6.

Koch, P., Opitz, T., Steinbeck, J. A., Ladewig, J. and Brustle, O. (2009). A rosette-type, self-renewing human ES cell-derived neural stem cell with potential for in vitro instruction and synaptic integration. *Proc Natl Acad Sci U S A* **106**, 3225-30.

Krause, D. S., Theise, N. D., Collector, M. I., Henegariu, O., Hwang, S., Gardner, R., Neutzel, S. and Sharkis, S. J. (2001). Multi-organ, multi-lineage engraftment by a single bone marrow-derived stem cell. *Cell* **105**, 369-77.

Krispin, S., Nitzan, E., Kassem, Y. and Kalcheim, C. (2010). Evidence for a dynamic spatiotemporal fate map and early fate restrictions of premigratory avian neural crest. *Development* **137**, 585-95.

Krull, C. E., Lansford, R., Gale, N. W., Collazo, A., Marcelle, C., Yancopoulos, G. D., Fraser, S. E. and Bronner-Fraser, M. (1997). Interactions of Eph-related receptors and ligands confer rostrocaudal pattern to trunk neural crest migration. *Curr Biol* **7**, 571-80.

Kulesa, P., Bronner-Fraser, M. and Fraser, S. (2000). In ovo time-lapse analysis after dorsal neural tube ablation shows rerouting of chick hindbrain neural crest. *Development* **127**, 2843-52.

Kulesa, P. M., Bailey, C. M., Kasemeier-Kulesa, J. C. and McLennan, R. (2010). Cranial neural crest migration: new rules for an old road. *Dev Biol* **344**, 543-54.

Kulesa, P. M., Lu, C. C. and Fraser, S. E. (2005). Time-lapse analysis reveals a series of events by which cranial neural crest cells reroute around physical barriers. *Brain Behav Evol* **66**, 255-65.

Kunisada, T., Yoshida, H., Yamazaki, H., Miyamoto, A., Hemmi, H., Nishimura, E., Shultz, L. D., Nishikawa, S. and Hayashi, S. (1998). Transgene expression of steel factor in the basal layer of epidermis promotes survival, proliferation, differentiation and migration of melanocyte precursors. *Development* **125**, 2915-23.

Lallier, T. and Bronner-Fraser, M. (1993). Inhibition of neural crest cell attachment by integrin antisense oligonucleotides. *Science* **259**, 692-5.

Lavdas, A. A., Papastefanaki, F., Thomaidou, D. and Matsas, R. (2008). Schwann cell transplantation for CNS repair. *Curr Med Chem* **15**, 151-60.

Lavon, N., Yanuka, O. and Benvenisty, N. (2004). Differentiation and isolation of hepatic-like cells from human embryonic stem cells. *Differentiation* **72**, 230-8.

Lazzari, G., Colleoni, S., Giannelli, S. G., Brunetti, D., Colombo, E., Lagutina, I., Galli, C. and Broccoli, V. (2006). Direct derivation of neural rosettes from cloned bovine blastocysts: a model of early neurulation events and neural crest specification in vitro. *Stem Cells* **24**, 2514-21.

Le Douarin, N. M., Creuzet, S., Couly, G. and Dupin, E. (2004). Neural crest cell plasticity and its limits. *Development* **131**, 4637-50.

Le Douarin, N. M. and Kalcheim, C. (1999). The Neural Crest. U.K.: Cambridge University Press.

Le Lievre, C. S. and Le Douarin, N. M. (1975). Mesenchymal derivatives of the neural crest: analysis of chimaeric quail and chick embryos. *J Embryol Exp Morphol* **34**, 125-54.

Lee, G., Kim, H., Elkabetz, Y., Al Shamy, G., Panagiotakos, G., Barberi, T., Tabar, V. and Studer, L. (2007). Isolation and directed differentiation of neural crest stem cells derived from human embryonic stem cells. *Nat Biotechnol* **25**, 1468-75.

Lee, G., Papapetrou, E. P., Kim, H., Chambers, S. M., Tomishima, M. J., Fasano, C. A., Ganat, Y. M., Menon, J., Shimizu, F., Viale, A. et al. (2009). Modelling pathogenesis and treatment of familial dysautonomia using patient-specific iPSCs. *Nature* **461**, 402-6.

Lee, H. Y., Kléber, M., Hari, L., Brault, V., Suter, U., Taketo, M. M., Kemler, R. and Sommer, L. (2004). Instructive role of Wnt/beta-catenin in sensory fate specification in neural crest stem cells. In *Science*, vol. 303 (ed., pp. 1020-3.

Leimeroth, R., Lobsiger, C., Lussi, A., Taylor, V., Suter, U. and Sommer, L. (2002). Membrane-bound neuregulin1 type III actively promotes Schwann cell differentiation of multipotent Progenitor cells. *Dev Biol* **246**, 245-58.

Li, X. J., Du, Z. W., Zarnowska, E. D., Pankratz, M., Hansen, L. O., Pearce, R. A. and Zhang, S. C. (2005). Specification of motoneurons from human embryonic stem cells. *Nat Biotechnol* **23**, 215-21.

Liu, A. and Niswander, L. A. (2005). Bone morphogenetic protein signalling and vertebrate nervous system development. *Nat Rev Neurosci* **6**, 945-54.

Lo, C. W., Cohen, M. F., Huang, G. Y., Lazatin, B. O., Patel, N., Sullivan, R., Pauken, C. and Park, S. M. (1997). Cx43 gap junction gene expression and gap junctional communication in mouse neural crest cells. *Dev Genet* **20**, 119-32.

Lohle, M., Hermann, A., Glass, H., Kempe, A., Schwarz, S. C., Kim, J. B., Poulet, C., Ravens, U., Schwarz, J., Scholer, H. R. et al. (2011). Differentiation Efficiency of Induced Pluripotent Stem Cells Depends on the Number of Reprogramming Factors. *Stem Cells*.

Lumsden, A., Sprawson, N. and Graham, A. (1991). Segmental origin and migration of neural crest cells in the hindbrain region of the chick embryo. *Development* **113**, 1281-91.

Marmigere, F. and Ernfors, P. (2007). Specification and connectivity of neuronal subtypes in the sensory lineage. *Nat Rev Neurosci* **8**, 114-27.

Martin, G. R. (1981). Isolation of a pluripotent cell line from early mouse embryos cultured in medium conditioned by teratocarcinoma stem cells. *Proc Natl Acad Sci U S A* **78**, 7634-8.

McGonnell, I. M. and Graham, A. (2002). Trunk neural crest has skeletogenic potential. *Curr Biol* **12**, 767-71.

McLennan, R. and Kulesa, P. M. (2007). In vivo analysis reveals a critical role for neuropilin-1 in cranial neural crest cell migration in chick. *Dev Biol* **301**, 227-39.

McLennan, R., Teddy, J. M., Kasemeier-Kulesa, J. C., Romine, M. H. and Kulesa, P. M. (2010). Vascular endothelial growth factor (VEGF) regulates cranial neural crest migration in vivo. *Dev Biol* **339**, 114-25.

Menendez, L., Yatskievych, T. A., Antin, P. B. and Dalton, S. (2011). Wnt signaling and a Smad pathway blockade direct the differentiation of human pluripotent stem cells to multipotent neural crest cells. *Proc Natl Acad Sci U S A* **108**, 19240-5.

Meyer, D., Yamaai, T., Garratt, A., Riethmacher-Sonnenberg, E., Kane, D., Theill, L. E. and Birchmeier, C. (1997). Isoform-specific expression and function of neuregulin. *Development* **124**, 3575-86.

Michailov, G. V., Sereda, M. W., Brinkmann, B. G., Fischer, T. M., Haug, B., Birchmeier, C., Role, L., Lai, C., Schwab, M. H. and Nave, K. A. (2004). Axonal neuregulin-1 regulates myelin sheath thickness. *Science* **304**, 700-3.

Milunsky, J. M., Maher, T. A., Zhao, G., Roberts, A. E., Stalker, H. J., Zori, R. T., Burch, M. N., Clemens, M., Mulliken, J. B., Smith, R. et al. (2008). TFAP2A mutations result in branchio-oculo-facial syndrome. *Am J Hum Genet* **82**, 1171-7.

Ming, G. L., Brustle, O., Muotri, A., Studer, L., Wernig, M. and Christian, K. M. (2011). Cellular reprogramming: recent advances in modeling neurological diseases. *J Neurosci* **31**, 16070-5.

Mitsui, K., Tokuzawa, Y., Itoh, H., Segawa, K., Murakami, M., Takahashi, K., Maruyama, M., Maeda, M. and Yamanaka, S. (2003). The homeoprotein Nanog is required for maintenance of pluripotency in mouse epiblast and ES cells. *Cell* **113**, 631-42.

Miyoshi, N., Ishii, H., Nagano, H., Haraguchi, N., Dewi, D. L., Kano, Y., Nishikawa, S., Tanemura, M., Mimori, K., Tanaka, F. et al. (2011). Reprogramming of mouse and human cells to pluripotency using mature microRNAs. *Cell Stem Cell* **8**, 633-8.

Mizuseki, K., Sakamoto, T., Watanabe, K., Muguruma, K., Ikeya, M., Nishiyama, A., Arakawa, A., Suemori, H., Nakatsuji, N., Kawasaki, H. et al. (2003). Generation of neural crest-derived peripheral neurons and floor plate cells from mouse and primate embryonic stem cells. *Proc Natl Acad Sci U S A* **100**, 5828-33.

Monier-Gavelle, F. and Duband, J. L. (1997). Cross talk between adhesion molecules: control of N-cadherin activity by intracellular signals elicited by beta1 and beta3 integrins in migrating neural crest cells. *J Cell Biol* **137**, 1663-81.

Monsoro-Burq, A. H., Fletcher, R. B. and Harland, R. M. (2003). Neural crest induction by paraxial mesoderm in Xenopus embryos requires FGF signals. *Development* **130**, 3111-24.

Motohashi, T., Aoki, H., Chiba, K., Yoshimura, N. and Kunisada, T. (2007). Multipotent cell fate of neural crest-like cells derived from embryonic stem cells. *Stem Cells* **25**, 402-10.

Mu, X., Silos-Santiago, I., Carroll, S. L. and Snider, W. D. (1993). Neurotrophin receptor genes are expressed in distinct patterns in developing dorsal root ganglia. *J Neurosci* **13**, 4029-41.

Murphy, M., Reid, K., Ford, M., Furness, J. B. and Bartlett, P. F. (1994). FGF2 regulates proliferation of neural crest cells, with subsequent neuronal differentiation regulated by LIF or related factors. *Development* **120**, 3519-28.

Murray, S. A., Oram, K. F. and Gridley, T. (2007). Multiple functions of Snail family genes during palate development in mice. *Development* **134**, 1789-97.

Nakagawa, S. and Takeichi, M. (1995). Neural crest cell-cell adhesion controlled by sequential and subpopulation-specific expression of novel cadherins. *Development* **121**, 1321-32.

Nakagawa, S. and Takeichi, M. (1998). Neural crest emigration from the neural tube depends on regulated cadherin expression. *Development* **125**, 2963-71.

Newgreen, D. and Thiery, J. P. (1980). Fibronectin in early avian embryos: synthesis and distribution along the migration pathways of neural crest cells. *Cell Tissue Res* **211**, 269-91.

Nichols, J., Zevnik, B., Anastassiadis, K., Niwa, H., Klewe-Nebenius, D., Chambers, I., Scholer, H. and Smith, A. (1998). Formation of pluripotent stem cells in the mammalian embryo depends on the POU transcription factor Oct4. *Cell* **95**, 379-91.

O'Rahilly, R. and Muller, F. (2007). The development of the neural crest in the human. *J Anat* **211**, 335-51.

Ohtsuka, T., Sakamoto, M., Guillemot, F. and Kageyama, R. (2001). Roles of the basic helix-loop-helix genes Hes1 and Hes5 in expansion of neural stem cells of the developing brain. *J Biol Chem* **276**, 30467-74.

Olesnicky Killian, E. C., Birkholz, D. A. and Artinger, K. B. (2009). A role for chemokine signaling in neural crest cell migration and craniofacial development. *Dev Biol* **333**, 161-72.

Osumi-Yamashita, N., Ninomiya, Y., Doi, H. and Eto, K. (1994). The contribution of both forebrain and midbrain crest cells to the mesenchyme in the frontonasal mass of mouse embryos. *Dev Biol* **164**, 409-19.

Park, I. H., Zhao, R., West, J. A., Yabuuchi, A., Huo, H., Ince, T. A., Lerou, P. H., Lensch, M. W. and Daley, G. Q. (2008). Reprogramming of human somatic cells to pluripotency with defined factors. *Nature* **451**, 141-6.

Patapoutian, A. and Reichardt, L. F. (2001). Trk receptors: mediators of neurotrophin action. *Curr Opin Neurobiol* **11**, 272-80.

Pattyn, A., Morin, X., Cremer, H., Goridis, C. and Brunet, J. F. (1999). The homeobox gene Phox2b is essential for the development of autonomic neural crest derivatives. *Nature* **399**, 366-70.

Pomp, O., Brokhman, I., Ben-Dor, I., Reubinoff, B. and Goldstein, R. S. (2005a). Generation of peripheral sensory and sympathetic neurons and neural crest cells from human embryonic stem cells. In *Stem Cells*, vol. 23 (ed., pp. 923-930.

Pomp, O., Brokhman, I., Ben-Dor, I., Reubinoff, B. and Goldstein, R. S. (2005b). Generation of peripheral sensory and sympathetic neurons and neural crest cells from human embryonic stem cells. *Stem Cells* **23**, 923-30.

Pratt, T., Quinn, J. C., Simpson, T. I., West, J. D., Mason, J. O. and Price, D. J. (2002). Disruption of early events in thalamocortical tract formation in mice lacking the transcription factors Pax6 or Foxg1. *J Neurosci* **22**, 8523-31.

Ramirez-Zacarias, J. L., Castro-Munozledo, F. and Kuri-Harcuch, W. (1992). Quantitation of adipose conversion and triglycerides by staining intracytoplasmic lipids with Oil red O. *Histochemistry* **97**, 493-7.

Real, C., Glavieux-Pardanaud, C., Vaigot, P., Le-Douarin, N. and Dupin, E. (2005). The instability of the neural crest phenotypes: Schwann cells can differentiate into myofibroblasts. *Int J Dev Biol* **49**, 151-9.

Reissmann, E., Ernsberger, U., Francis-West, P. H., Rueger, D., Brickell, P. M. and Rohrer, H. (1996). Involvement of bone morphogenetic protein-4 and bone morphogenetic protein-7 in the differentiation of the adrenergic phenotype in developing sympathetic neurons. *Development* **122**, 2079-88.

Reubinoff, B. E., Itsykson, P., Turetsky, T., Pera, M. F., Reinhartz, E., Itzik, A. and Ben-Hur, T. (2001). Neural progenitors from human embryonic stem cells. *Nat Biotechnol* **19**, 1134-40.

Reubinoff, B. E., Pera, M. F., Fong, C. Y., Trounson, A. and Bongso, A. (2000). Embryonic stem cell lines from human blastocysts: somatic differentiation in vitro. *Nat Biotechnol* **18**, 399-404.

Rizzino, A. (2008). Transcription factors that behave as master regulators during mammalian embryogenesis function as molecular rheostats. *Biochem J* **411**, e5-7.

Roffers-Agarwal, J. and Gammill, L. S. (2009). Neuropilin receptors guide distinct phases of sensory and motor neuronal segmentation. *Development* **136**, 1879-88.

Ruhrberg, C. and Schwarz, Q. (2010). In the beginning: Generating neural crest cell diversity. *Cell Adh Migr* **4**, 622-30.

Sailer, M. H., Hazel, T. G., Panchision, D. M., Hoeppner, D. J., Schwab, M. E. and McKay, R. D. (2005). BMP2 and FGF2 cooperate to induce neural-crest-like fates from fetal and adult CNS stem cells. *J Cell Sci* **118**, 5849-60.

Sandell, L. L. and Trainor, P. A. (2006). Neural crest cell plasticity. size matters. *Adv Exp Med Biol* **589**, 78-95.

Santagati, F. and Rijli, F. M. (2003). Cranial neural crest and the building of the vertebrate head. *Nat Rev Neurosci* **4**, 806-18.

Santiago, A. and Erickson, C. A. (2002). Ephrin-B ligands play a dual role in the control of neural crest cell migration. *Development* **129**, 3621-32.

Sarkar, S., Petiot, A., Copp, A., Ferretti, P. and Thorogood, P. (2001). FGF2 promotes skeletogenic differentiation of cranial neural crest cells. *Development* **128**, 2143-52.

Satoda, M., Zhao, F., Diaz, G. A., Burn, J., Goodship, J., Davidson, H. R., Pierpont, M. E. and Gelb, B. D. (2000). Mutations in TFAP2B cause Char syndrome, a familial form of patent ductus arteriosus. *Nat Genet* **25**, 42-6.

Sauka-Spengler, T. and Bronner-Fraser, M. (2008). Evolution of the neural crest viewed from a gene regulatory perspective. *Genesis* **46**, 673-82.

Schilling, T. F. and Kimmel, C. B. (1994). Segment and cell type lineage restrictions during pharyngeal arch development in the zebrafish embryo. *Development* **120**, 483-94.

Schilling, T. F., Prince, V. and Ingham, P. W. (2001). Plasticity in zebrafish hox expression in the hindbrain and cranial neural crest. *Dev Biol* **231**, 201-16.

Schmidt, K., Glaser, G., Wernig, A., Wegner, M. and Rosorius, O. (2003). Sox8 is a specific marker for muscle satellite cells and inhibits myogenesis. *J Biol Chem* **278**, 29769-75.

Schneider, C., Wicht, H., Enderich, J., Wegner, M. and Rohrer, H. (1999). Bone morphogenetic proteins are required in vivo for the generation of sympathetic neurons. *Neuron* **24**, 861-70.

Schofield, B. H., Williams, B. R. and Doty, S. B. (1975). Alcian Blue staining of cartilage for electron microscopy. Application of the critical electrolyte concentation principle. *Histochem J* **7**, 139-49.

Schorle, H., Meier, P., Buchert, M., Jaenisch, R. and Mitchell, P. J. (1996). Transcription factor AP-2 essential for cranial closure and craniofacial development. *Nature* **381**, 235-8.

Schwarz, Q., Maden, C. H., Davidson, K. and Ruhrberg, C. (2009). Neuropilin-mediated neural crest cell guidance is essential to organise sensory neurons into segmented dorsal root ganglia. *Development* **136**, 1785-9.

Sechrist, J., Serbedzija, G. N., Scherson, T., Fraser, S. E. and Bronner-Fraser, M. (1993). Segmental migration of the hindbrain neural crest does not arise from its segmental generation. *Development* **118**, 691-703.

Sela-Donenfeld, D. and Kalcheim, C. (2000). Inhibition of noggin expression in the dorsal neural tube by somitogenesis: a mechanism for coordinating the timing of neural crest emigration. *Development* **127**, 4845-54.

Sela-Donenfeld, D. and Kalcheim, C. (2002). Localized BMP4-noggin interactions generate the dynamic patterning of noggin expression in somites. *Dev Biol* **246**, 311-28.

Shah, N. M., Groves, A. K. and Anderson, D. J. (1996). Alternative neural crest cell fates are instructively promoted by TGFbeta superfamily members. *Cell* **85**, 331-43.

Shah, N. M., Marchionni, M. A., Isaacs, I., Stroobant, P. and Anderson, D. J. (1994). Glial growth factor restricts mammalian neural crest stem cells to a glial fate. *Cell* **77**, 349-60.

Shakhova, O. and Sommer, L. (2010). Neural crest-derived stem cells. In *StemBook*, (ed. L. Girard). Cambridge.

Sobue, G., Shuman, S. and Pleasure, D. (1986). Schwann cell responses to cyclic AMP: proliferation, change in shape, and appearance of surface galactocerebroside. *Brain Res* **362**, 23-32.

Soldner, F., Hockemeyer, D., Beard, C., Gao, Q., Bell, G. W., Cook, E. G., Hargus, G., Blak, A., Cooper, O., Mitalipova, M. et al. (2009). Parkinson's disease patient-derived induced pluripotent stem cells free of viral reprogramming factors. *Cell* **136**, 964-77.

Stefansson, K., Wollmann, R. L., Moore, B. W. and Arnason, B. G. (1982). S-100 protein in human chondrocytes. *Nature* **295**, 63-4.

Strachan, L. R. and Condic, M. L. (2008). Neural crest motility on fibronectin is regulated by integrin activation. *Exp Cell Res* **314**, 441-52.

Sun, N., Panetta, N. J., Gupta, D. M., Wilson, K. D., Lee, A., Jia, F., Hu, S., Cherry, A. M., Robbins, R. C., Longaker, M. T. et al. (2009). Feeder-free derivation of induced pluripotent stem cells from adult human adipose stem cells. *Proc Natl Acad Sci U S A* **106**, 15720-5.

Syroid, D. E., Maycox, P. R., Burrola, P. G., Liu, N., Wen, D., Lee, K. F., Lemke, G. and Kilpatrick, T. J. (1996). Cell death in the Schwann cell lineage and its regulation by neuregulin. *Proc Natl Acad Sci U S A* **93**, 9229-34.

Takahashi, K., Tanabe, K., Ohnuki, M., Narita, M., Ichisaka, T., Tomoda, K. and Yamanaka, S. (2007). Induction of pluripotent stem cells from adult human fibroblasts by defined factors. *Cell* **131**, 861-72.

Takahashi, K. and Yamanaka, S. (2006). Induction of pluripotent stem cells from mouse embryonic and adult fibroblast cultures by defined factors. *Cell* **126**, 663-76.

Takahashi, M. and Osumi, N. (2008). Expression study of cadherin7 and cadherin20 in the embryonic and adult rat central nervous system. *BMC Dev Biol* **8**, 87.

Taneyhill, L. A. (2008). To adhere or not to adhere: the role of Cadherins in neural crest development. *Cell Adh Migr* **2**, 223-30.

ten Berge, D., Koole, W., Fuerer, C., Fish, M., Eroglu, E. and Nusse, R. (2008). Wnt signaling mediates self-organization and axis formation in embryoid bodies. *Cell Stem Cell* **3**, 508-18.

Thiery, J. P., Delouvee, A., Gallin, W. J., Cunningham, B. A. and Edelman, G. M. (1984). Ontogenetic expression of cell adhesion molecules: L-CAM is found in epithelia derived from the three primary germ layers. *Dev Biol* **102**, 61-78.

Thomas, A. J. and Erickson, C. A. (2008). The making of a melanocyte: the specification of melanoblasts from the neural crest. *Pigment Cell Melanoma Res* **21**, 598-610.

Thomas, S., Thomas, M., Wincker, P., Babarit, C., Xu, P., Speer, M. C., Munnich, A., Lyonnet, S., Vekemans, M. and Etchevers, H. C. (2008). Human neural crest cells display molecular and phenotypic hallmarks of stem cells. *Hum Mol Genet* **17**, 3411-25.

Thomson, J. A., Itskovitz-Eldor, J., Shapiro, S. S., Waknitz, M. A., Swiergiel, J. J., Marshall, V. S. and Jones, J. M. (1998). Embryonic stem cell lines derived from human blastocysts. *Science* **282**, 1145-7.

Tickle, C. and Trinkaus, J. P. (1976). Observations on nudging cells in culture. *Nature* **261**, 413.

Trainor, P. and Krumlauf, R. (2000). Plasticity in mouse neural crest cells reveals a new patterning role for cranial mesoderm. *Nat Cell Biol* **2**, 96-102.

Trainor, P. A. (2003). Making headway: the roles of Hox genes and neural crest cells in craniofacial development. *ScientificWorldJournal* **3**, 240-64.

Trainor, P. A., Ariza-McNaughton, L. and Krumlauf, R. (2002). Role of the isthmus and FGFs in resolving the paradox of neural crest plasticity and prepatterning. *Science* **295**, 1288-91.

Tucker, R. P., Hagios, C., Chiquet-Ehrismann, R., Lawler, J., Hall, R. J. and Erickson, C. A. (1999). Thrombospondin-1 and neural crest cell migration. *Dev Dyn* **214**, 312-22.

van den Boogaard, M. J., Dorland, M., Beemer, F. A. and van Amstel, H. K. (2000). MSX1 mutation is associated with orofacial clefting and tooth agenesis in humans. *Nat Genet* **24**, 342-3.

Vazin, T., Chen, J., Lee, C. T., Amable, R. and Freed, W. J. (2008). Assessment of stromal-derived inducing activity in the generation of dopaminergic neurons from human embryonic stem cells. *Stem Cells* **26**, 1517-25.

Vega, J. A., Del Valle, M. E., Alvarez-Mendez, J. C., Hernandez, L. C., Zubizarreta, J. J. and Calzada, B. (1990). Expression of glial fibrillary acidic protein-like and S-100 protein like immunoreactivities on cartilages of the rat vestibulum nasi. Post-natal development changes. *Arch Anat Histol Embryol* **73**, 59-66.

Vierbuchen, T., Ostermeier, A., Pang, Z. P., Kokubu, Y., Sudhof, T. C. and Wernig, M. (2010). Direct conversion of fibroblasts to functional neurons by defined factors. *Nature* **463**, 1035-41.

Vincentz, J. W., Barnes, R. M., Rodgers, R., Firulli, B. A., Conway, S. J. and Firulli, A. B. (2008). An absence of Twist1 results in aberrant cardiac neural crest morphogenesis. *Dev Biol* **320**, 131-9.

Vult von Steyern, F., Martinov, V., Rabben, I., Nja, A., de Lapeyriere, O. and Lomo, T. (1999). The homeodomain transcription factors Islet 1 and HB9 are expressed in adult alpha and gamma motoneurons identified by selective retrograde tracing. *Eur J Neurosci* **11**, 2093-102.

Warren, L., Manos, P. D., Ahfeldt, T., Loh, Y. H., Li, H., Lau, F., Ebina, W., Mandal, P. K., Smith, Z. D., Meissner, A. et al. (2010). Highly efficient reprogramming to pluripotency and directed differentiation of human cells with synthetic modified mRNA. *Cell Stem Cell* **7**, 618-30.

Wernig, M., Meissner, A., Cassady, J. P. and Jaenisch, R. (2008). c-Myc is dispensable for direct reprogramming of mouse fibroblasts. *Cell Stem Cell* **2**, 10-2.

White, R. M., Cech, J., Ratanasirintrawoot, S., Lin, C. Y., Rahl, P. B., Burke, C. J., Langdon, E., Tomlinson, M. L., Mosher, J., Kaufman, C. et al. (2011). DHODH modulates transcriptional elongation in the neural crest and melanoma. *Nature* **471**, 518-22.

Wright, D. E. and Snider, W. D. (1995). Neurotrophin receptor mRNA expression defines distinct populations of neurons in rat dorsal root ganglia. *J Comp Neurol* **351**, 329-38.

Xu, C., Inokuma, M. S., Denham, J., Golds, K., Kundu, P., Gold, J. D. and Carpenter, M. K. (2001). Feeder-free growth of undifferentiated human embryonic stem cells. *Nat Biotechnol* **19**, 971-4.

Yamane, T., Hayashi, S., Mizoguchi, M., Yamazaki, H. and Kunisada, T. (1999). Derivation of melanocytes from embryonic stem cells in culture. *Dev Dyn* **216**, 450-8.

Young, H. M., Ciampoli, D., Hsuan, J. and Canty, A. J. (1999). Expression of Ret-, p75(NTR)-, Phox2a-, Phox2b-, and tyrosine hydroxylase-immunoreactivity by undifferenti-

ated neural crest-derived cells and different classes of enteric neurons in the embryonic mouse gut. *Dev Dyn* **216**, 137-52.

Yu, J., Vodyanik, M. A., Smuga-Otto, K., Antosiewicz-Bourget, J., Frane, J. L., Tian, S., Nie, J., Jonsdottir, G. A., Ruotti, V., Stewart, R. et al. (2007). Induced pluripotent stem cell lines derived from human somatic cells. *Science* **318**, 1917-20.

Zhang, S. C., Wernig, M., Duncan, I. D., Brustle, O. and Thomson, J. A. (2001). In vitro differentiation of transplantable neural precursors from human embryonic stem cells. *Nat Biotechnol* **19**, 1129-33.

Zhou, Y. and Snead, M. L. (2008). Derivation of cranial neural crest-like cells from human embryonic stem cells. *Biochem Biophys Res Commun* **376**, 542-7.

Zirlinger, M., Lo, L. C., McMahon, J., McMahon, A. P. and Anderson, D. J. (2002). Transient expression of the bHLH factor neurogenin-2 marks a subpopulation of neural crest cells biased for a sensory but not a neuronal fate. In *P Natl Acad Sci Usa*, vol. 99 (ed., pp. 8084-8089.

6 Acknowledgement

After completing my dissertation I would like to take the opportunity to look back on my time as Ph.D. student and to express my gratitude to the people who supported me. They made it possible for me to do my research and to write this thesis.

I would like to sincerely thank my supervisor Prof. Dr. Oliver Brüstle for giving me the opportunity to do my research on this fascinating scientific project. I am deeply grateful for his guidance throughout the years as well as for his commitment to discuss and correct this thesis. I earnestly thank Prof. Dr. Michael Hoch for being the second assessor of my thesis. Also, I'm indebted to Prof. Dr. Hubert Schorle and PD Dr. Frank Edenhofer for agreeing to act as third and fourth reviewer.

Dr. Michael Alexander from the Department of Genomics, Life&Brain Center helped me with genome expression analysis and I would like to thank him for the excellent collaboration. Also, I would like to thank Elmar Endl and the team of the flow cytometry core facility for providing their knowledge and flow cytometry instrumentation.

I thank all current and former members of the Institute of Reconstructive Neurobiology for creating an inspiring scientific environment and for lending a helping hand whenever possible. Especially, I thank Dr. Philipp Koch for scientific discussions and sharing his knowledge on neural differentiation. In addition, I am thankful to Dr. Jaideep Kesavan for cooperating with me on electrophysiological studies. I also would like to thank Roman Reinartz for his help with mesenchymal differentiation. Dr. Lodovica Borghese always supported me throughout my Ph.D. studies. She also proofread this thesis and I'm deeply thankful for that. Furthermore I thank Karin Frangenberg for her kindness and support throughout the years.

I especially thank Raphaela Gorris, bench neighbor, fellow sufferer and friend for scientific and non-scientific discussions and for proofreading this thesis as well. Moreover, I would like to thank Claudia Schreiner for support and fun in and beyond the lab. Kim Erwes, Jule Fischer, Melanie Bloschies, and Jos Burgert always helped me during daily lab life. Thanks for adopting the AG Schenk and for the fun times we had! Furthermore, I would like to thank Dr. Daniel Trageser for valuable discussions and coffee delivery.

Additionally, I would like to thank my friends outside the lab for helpful advices and for keeping my spirits up. I especially thank Dr. Bettina Mavrommatis, who accompanies me since 1997. She also proofread this thesis. Mrs. Scherer would be proud of us.

I wholeheartedly thank my parents Annegret and Heinz Schenk for encouraging, supporting and advising me no matter what. Also, I thank my brothers Christian and Jochen Schenk with their families for standing by my side. It's time to go for a sail.

Last but not least I thank my husband Dr. Bernhard Münst for being awesome.

7 Appendix

Time-lapse microscopy: supplementary movies

Movie 01: Time-lapse microscopy of plated EB

5-day-old EB was plated on a fibronectin-coated cell culture dish. Cell migration was monitored 72 hours. Scale bar: 100 µm.

Movie 02: Time-lapse microscopy of re-plated crescent-shaped aggregate

Crescent-shaped aggregate containing neural crest cells was isolated from an 8-day-old EB outgrowth and re-plated on a fibronectin-coated cell culture dish. Cell migration was monitored for 72 hours. Scale bar: 100 µm.

8 Declaration

I hereby declare that the work in this thesis is original and has been carried out by myself at the Institute of Reconstructive Neurobiology, Medical Center, University of Bonn. This thesis was prepared under the supervision of Prof. Dr. Oliver Brüstle in fulfillment of the requirements of the doctoral degree of natural sciences of the University of Bonn. I further declare that this work has not been the basis for the awarding of any degree, diploma, fellowship, associateship or similar title at any university or institution.

Bonn, February 2012

Sabine Münst